THE UNIVERSITY OF MICHIGAN

INDUSTRY PROGRAM OF THE COLLEGE OF ENGINEERING

MOMENTUM EXCHANGE IN A CONFINED CIRCULAR JET WITH TURBULENT SOURCE

John M. Dealy

A dissertation submitted in partial fulfillment
of the requirements for the degree of
Doctor of Philosophy in the
University of Michigan
Department of Chemical and Metallurgical Engineering
1964

January, 1964

IP-657

engn

UMRC762

Doctoral Committee:

Professor J. Louis York, Chairman
Professor Arthur G. Hansen
Professor Joseph J. Martin
Professor Richard B. Morrison
Professor Victor L. Streeter
Associate Professor M. Rasin Tek

ACKNOWLEDGEMENTS

The author wishes to express his thanks to:

Professor J. L. York, Chairman of the Doctoral Committee, for his friendly encouragement and advice, and his suggestion of a research area, which provided the initial impetus for this study;

The other members of the Doctoral Committee for their guidance and assistance during the course of the research;

Roger Curtet, of the Fluid Mechanics Laboratory at the University of Grenoble, whose correspondence was a valuable source of information and stimulus;

The Research Corporation for financial support of the experimental program;

The Standard Oil Company of California, the Eastman Kodak Company and the National Science Foundation for their generous fellowship aid.

ABSTRACT

The few studies to date of circular confined jets have dealt with a jet source, the flow from which was uniform and irrotational, and the radius of which was small compared to the mixing tube radius. In this study, the effects of turbulence in the jet source and larger ratios of jet source to mixing tube diameters, on the mixing process, were examined both experimentally and by the application of turbulent flow theories.

Previous work on turbulent, incompressible jets was critically reviewed. A straightforward mathematical model for recirculation in confined jets was developed without recourse to a detailed analysis of the equations of motion. Based on several hypotheses concerning the fundamental characteristics of the flow, a mathematical model for the flow in the mixing field was established.

Velocity profiles and wall static pressures were measured at various points downstream of turbulent jet sources having Reynolds numbers between 10^4 and 10^5. It was observed that, in the case of the larger jet tube, the flow did not develop a self-preserving structure before the jet expanded to the mixing tube wall. Recirculation was observed in all flows having Craya-Curtet numbers below 0.78, and the jet tube Reynolds number was found to have little effect on recirculation and other features of the downstream development of the flow. A negative axial pressure gradient was observed near the jet entrance in agreement with the result predicted on the basis of the mathematical model.

It was concluded that turbulence in the jet source has an important effect on the behavior of a jet near the source. For the particular case of a source consisting of the efflux from a long circular conduit, the pressure falls and the structure of the turbulence in the center portion of the flow is self-preserving for a distance of from 2 to 5 jet tube radii from the source. The jet tube Reynolds number probably has an important influence on the development of the wall boundary layer although a detailed study of the flow near the wall was not carried out. In spite of several significant differences between the flow considered here and that of previous studies, the concepts of R. Curtet regarding similarity and recirculation were found to have a definite value in characterizing the general behavior of the system.

TABLE OF CONTENTS

TABLE OF CONTENTS (CONT'D)

LIST OF TABLES

LIST OF FIGURES

LIST OF FIGURES (CONT'D)

CHAPTER I

INTRODUCTION

The confined jet, considered in detail, is a very complex flow involving free turbulent shear as well as a boundary layer and significant pressure gradients. It is of practical interest in the theoretical analysis of jet pump performance and jet flame behavior.

Considerable research has been conducted in the area of free jets, and many of the principles established in the course of this work have been applied with some success to the analysis of confined jets. The main difference, hydrodynamically, between the free and confined jets is that in the free jet it is usually assumed that the pressure everywhere is the same and that axial momentum is conserved from one cross section to another, whereas in the confined jet, the axial mass flux is constant while the pressure and total momentum vary axially.

Research on confined jets to date has involved jet sources with uniform velocity and very low turbulent intensity, and mixing tubes which were much larger than the source nozzle. To study the effects of deviations from these conditions on the flow behavior, an experimental and theoretical analysis of a somewhat different system were undertaken. First the source consisted of the efflux from a long circular conduit. Thus, for sufficiently high jet tube Reynolds numbers, the structure of the flow in the source is that of the much studied and well documented fully developed turbulent pipe flow. Furthermore, ratios of jet tube to mixing tube diameter were 0.25 and 0.5, so that the confinement of the flow was more severe than that in previous studies.

In the following pages, previous research on round turbulent jets of incompressible fluid is reviewed, theoretical and experimental analyses are described, and the important features of the flow are discussed.

The object of this study was to learn something about the details of the flow in a confined circular jet. Of particular interest were the effects of turbulence in the source and a relatively small ratio of mixing tube to source diameters, on the applicability of the models developed for simpler jets by previous researchers.

In the following pages, previous research on round turbulent jets of incompressible fluid is reviewed, theoretical and experimental analyses are described, and the important features of the flow are discussed.

The validity of the application of principles of free jet flows to the analysis of confined jets are examined. The integral analysis of R. Curtet, and his criterion for the occurrence of recirculation are discussed with regard to their general applicability.

The effect of turbulence in the source is discussed, and some interesting features of the fully developed turbulent source are presented. The manner in which the severe confinement resulting from the small mixing tube diameter influences the validity of the usual assumptions made in jet analyses is pointed out.

CHAPTER II

ROUND TURBULENT JETS OF INCOMPRESSIBLE FLUID -- AN ANALYSIS OF DEVELOPMENTS TO DATE

There is presented in this section an analysis of work to date on turbulent jets of incompressible fluids. Free jets with and without motion of the ambient fluid are discussed, as well as the more recent studies of confined jets.

A. Fundamental Equations

The equations governing the turbulent mixing of incompressible fluids are the Reynolds equations which are derived from the Navier-Stokes equations by the use of time-averaging techniques. These are, in cylindrical coordinates

$$\rho\left(\frac{dv}{dt} - \frac{\omega^2}{r}\right) = -\frac{\partial p}{\partial r} + \mu\left(\nabla^2 v - \frac{v}{r^2} - \frac{2}{r^2}\frac{\partial w}{\partial \phi}\right)$$

$$- \frac{\rho}{r}\frac{\partial}{\partial r}\left(r\overline{v'^2}\right) - \frac{\rho}{r}\frac{\partial\left(\overline{v'w'}\right)}{\partial \phi} - \rho\frac{\partial}{\partial x}\left(\overline{v'u'}\right)$$

$$+ \rho\frac{\overline{w'^2}}{r} + F_r \tag{2.1}$$

$$\rho\left(\frac{dw}{dt} + \frac{vw}{r}\right) = -\frac{1}{r}\frac{\partial p}{\partial \phi} + \mu\left(\nabla^2 w - \frac{w}{r^2} + \frac{2}{r^2}\frac{\partial v}{\partial \phi}\right) - \frac{\rho}{r}\frac{\partial \overline{w'^2}}{\partial \phi}$$

$$- \frac{\partial\left(\overline{w'v'}\right)}{\partial r} - \rho\frac{\partial}{\partial x}\left(\overline{w'u'}\right) - 2\rho\frac{\overline{w'v'}}{r} + F_\phi \tag{2.2}$$

$$\rho \frac{du}{dt} = -\frac{\partial p}{\partial z} + \mu \nabla^2 u - \rho \frac{\partial \overline{u'^2}}{\partial x}$$

$$-\frac{\rho}{r}\frac{\partial}{\partial r}\left(r\overline{v'u'}\right) - \frac{\rho}{r}\frac{\partial}{\partial \phi}\left(\overline{w'u'}\right) + F_x \tag{2.3}$$

For an axi-symmetric steady flow, we have:

$$u\frac{\partial u}{\partial x} + v\frac{\partial u}{\partial r} = -\frac{1}{\rho}\frac{\partial p}{\partial x} - \frac{\partial}{\partial x}\left(\overline{u'^2}\right)$$

$$-\frac{1}{r}\frac{\partial}{\partial r}\left(r\overline{u'v'}\right) + \mu \nabla^2 u + F_x \tag{2.4}$$

and,

$$u\frac{\partial v}{\partial x} + v\frac{\partial v}{\partial r} = -\frac{1}{\rho}\frac{\partial p}{\partial r} - \frac{1}{r}\frac{\partial}{\partial r}\left(r\overline{v'^2}\right)$$

$$-\frac{\partial}{\partial x}\left(\overline{u'v'}\right) + \frac{\overline{w'^2}}{r} + \mu \nabla^2 v + F_r \tag{2.5}$$

and the continuity equation is:

$$\frac{\partial u}{\partial x} + \frac{1}{r}\frac{\partial (rv)}{\partial r} = 0 \tag{2.6}$$

If the only body force (F_i) is gravitational, then we may combine it with the pressure gradient to form the hydrodynamic pressure gradient as follows:

Let $P = p + \rho g r \sin \phi$ (2.7)

where P is the hydrodynamic pressure and ϕ is measured from the horizontal. Using this, and assuming turbulent shear predominates over viscous shear:

$$u\frac{\partial u}{\partial x} + v\frac{\partial u}{\partial r} = -\frac{1}{\rho}\frac{\partial P}{\partial x} - \frac{\partial}{\partial x}\overline{u'^2} - \frac{1}{r}\frac{\partial}{\partial r}\left(r\overline{u'v'}\right) \tag{2.8}$$

$$u\frac{\partial v}{\partial x} + v\frac{\partial v}{\partial r} = -\frac{1}{\rho}\frac{\partial P}{\partial r} - \frac{1}{r}\frac{\partial\left(r\overline{v'^2}\right)}{\partial r} - \frac{\partial\left(\overline{u'v'}\right)}{\partial x} + \frac{\overline{w'^2}}{r} \tag{2.9}$$

The terms on the right which involve the velocity fluctuations are frequently referred to as the "Reynolds stresses." Terms of the type $\overline{u'^2}$ are the normal Reynolds stresses.

B. Phenomenological Theories of Turbulent Momentum Transport

Boussinesq[25] suggested before 1900 than the Reynolds stresses might be related to the mean velocity gradient in a manner similar to that for laminar flows. He thus postulated a turbulent transport coefficient, ϵ, commonly referred to as "eddy viscosity" such that:

$$-\overline{u'v'} = \epsilon\frac{\partial u}{\partial y} \tag{2.10}$$

Prandtl,[42] on the basis of a simple mechanical model of turbulent momentum transport suggested the use of a "mixing length," ℓ, such that:

$$-\overline{u'v'} = \ell^2 \frac{\partial u}{\partial y}\left|\frac{\partial u}{\partial y}\right| \tag{2.11}$$

or

$$\epsilon = \ell^2 \frac{\partial u}{\partial y}$$

Later, Prandtl noted[41] that, whereas his mixing length theory was based on the notion that the turbulent momentum transport depended exclusively on the local characteristics of the flow, a more realistic model might be established by considering the overall nature of the average flow. Specifically, he suggested the relationship:

$$\epsilon = \kappa b \left(u_{max} - u_{min}\right) \tag{2.12}$$

where b = width of the mixing region, and

k is a proportionality constant.

This is referred to as the Prandtl "exchange coefficient hypothesis."

Reichardt's "inductive theory of turbulence," which is actually only a generalization of some experimental results, will be discussed later.

More recently, Hooper[27] has made use of some more fundamental concepts, including Kolmogaroff's idea of a critical eddy size, to derive a harmonic expression for the variation of the mixing length. His theory fits Nikuradse's data for fully-developed pipe flow quite well.

C. Free Jet Theories

The free turbulent jet was first discussed by Tollmien in 1926.[54] He empolyed Prandtl's mixing length theory, and showed that, for an axially symmetrical jet, the axial velocity is inversely proportional to the distance downstream. His development applies to the jet from a point source, or some distance downstream from a finite jet.

Tollmien assumed that the pressure is constant throughout the field of flow. Thus, the x-direction momentum is conserved:

$$2\pi\rho\int_0^\infty u^2 r\,dr = \rho M \qquad (M = \text{constant}) \qquad (2.13)$$

Then he assumes

$$u = \phi(x) f(\eta) \qquad \left(\eta = r/x\right)$$

Thus:

$$\phi^2(x)\int_0^\infty f^2(\eta)\, r\,dr = \rho M \qquad (= \text{constant})$$

or:

$$\phi^2(x)\, x^2 \int_0^\infty f^2(\eta)\,\eta\,d\eta$$

Thus, $\phi(x)$ is proportional to $1/x$, and:

$$u = \frac{A}{x} f(\eta) \qquad A = \text{constant} \qquad (2.14)$$

Now $F(\eta)$ is defined by:

$$F(\eta) = \int_0^{\eta} F(\eta)\, \eta\, d\eta$$

Noting that $u = \frac{AF'(\eta)}{x\eta}$, and employing the continuity equation, an expression is obtained for the radial velocity component:

$$v = \frac{AF'}{x} - \frac{AF}{x\eta} \tag{2.15}$$

The Reynolds equation involving the axial velocity (Equation (2.8)) is simplified by neglecting pressure variations and turbulent normal stresses. Prandtl's mixing length expression (2.11) is used to relate the Reynolds stress $(-\overline{u'v'})$ to the mean flow and the mixing length is assumed proportional to x:

$$\ell = cx \tag{2.16}$$

The result is:

$$v\frac{\partial u}{\partial r} + u\frac{\partial u}{\partial x} = -\frac{1}{r}\frac{\partial}{\partial r}\left[r c^2 x^2 \left(\frac{\partial u}{\partial r}\right)^2\right] \tag{2.17}$$

Making use of expressions (2.14) and (2.15), an ordinary differential equation in $F(\eta)$ is obtained:

$$F'F = c^2\left(F'' - \frac{F'}{\eta}\right)^2 \tag{2.18}$$

The constant c can be eliminated by the transformation:

$$\eta^+ = c^{-2/3}\eta$$

Since a series solution was to be sought, Tollmien found it convenient to transform the dependent variable also:

$$Z = \frac{d \ln F}{d \eta^+}$$

The final equation is:

$$Z' = \frac{2}{\eta^+} - Z^2 - \sqrt{Z} \qquad (2.19)$$

One boundary condition is:

$$\text{at } \eta = o, \; v = o \text{ or } F(o) = o$$

It is also known that u must be finite at $\eta = o$, and that $U(o)x = Af(o) = \text{constant}$.

Let A be so defined that $f(o) = 1$.

A series solution is established for $Z(\eta^+)$, but its convergence is poor in the neighborhood of η^+_r for which $Z(\eta^+_r) = 0$. An alternate series is developed for the solution in the region $\eta^+ > \eta^+_r$. Using both series, η^+_r is found to be 3.4 which is assumed to represent the edge of the jet. From experimental data, Tollmien determined that:

$$c = 0.0158$$

Then the rate of spread of the jet is:

$$b = 0.214x$$

The important result of this analysis is that all dimensionless profiles of $(\frac{ux}{A})$ in an ideal free turbulent jet are similar with respect to the variable (r/x). Near $x = o$, however, the solution represents no real

flow. By integrating volumetric flux around a closed surface including the jet source, it can be shown that no fluid enters at the source. Thus, all the material in the jet comes from the surrounding fluid. A certain amount of momentum, as indicated by Equation (2.13) is added to the system at the jet source. This, of course, is neither a realistic physical boundary condition, nor a practical mathematical one. It may be shown that the constant A is proportional to the square root of the kinematic momentum flux. M. Abramovich[1] has discussed this point.

In an actual jet, of course, a finite source is employed, and it has generally been observed that Tollmien's solution holds only at distances from the jet greater than about 8 source diameters. Thus, if the jet radius, as determined by experiments in the region of the developed jet is extrapolated to zero, the virtual source of the equivalent ideal jet may be found. Then at some point a distance x from this virtual source, if the velocity on the axis is found to be u_o, then A can be computed as $u_o x$.

Howarth[40] applied Taylor's vorticity transport theory to this problem, and obtained an alternate differential equation. He was unable to solve the equation using the mixing length relationship (Equation (2.16)) employed by Tollmien. He used some alternate expressions for the mixing length, but failed to achieve satisfactory agreement with experimental data.

Reichardt[43] studied the developed turbulent jet experimentally, and noted that the velocity profiles were nearly Gaussian. He then sought a Reynolds stress relation which would produce such a solution

when employed in the equations of motion. He hypothesized:

$$\overline{u'v'} = -\Lambda(x)\frac{\partial u^2}{\partial y} \tag{2.20}$$

When used in the Reynolds equation for a plane flow:

$$\frac{\partial u^2}{\partial x} = \Lambda(x)\frac{\partial^2 u^2}{\partial y^2} \tag{2.21}$$

The result is the same form as the heat conduction equation and is called Reichardt's momentum transfer law. Hinze[25] presents a critical discussion of Reichardt's work and concludes it is not of fundamental importance.

Görtler[23] applied Prandtl's momentum exchange hypothesis to the plane jet. We note from Equation (2.12) that for this relationship ϵ is dependent not on r, but only on x. Then the Reynolds equation governing the development of the turbulent jet can be transformed into an equation which is identical to that for a laminar mixing region. Schlichting[47] has discussed the application to round jets. The use of the exchange coefficient gives better agreement with the experimental results of Hinze and van der Hegge Zijnen,[26] although they point out that at the edge of the jet, experimental values were lower than those predicted. They suggest that this is due to the fact that the exchange coefficient should actually approach zero near the edge of the jet, rather than remain constant.

The discussion thus far has concerned only the "developed" jet. This means that entrance effects due to the finite source are not considered. It is observed, however, that if the jet is a uniform non-turbulent stream there is a region near the source wherein the flow is quite different than that from a point source. There is, initially, a core of fluid in the center of the jet in which the velocity is radially and axially invariant. In the region of this "potential core" the pressure is constant, as can be shown from Bernoulli's equation. This core is dissipated in about 4 jet diameters, and there follows a transition region in which the flow develops a self-preserving structure. Thus, it is observed that the flow some distance from the source is independent of the nature of the source. This is strictly true, of course, only for high jet Reynolds numbers for which the principle of Reynolds number structural similarity applies. This principle has been discussed in detail by Townsend.(55) The general features of the jet with finite source are shown in Figure 1.

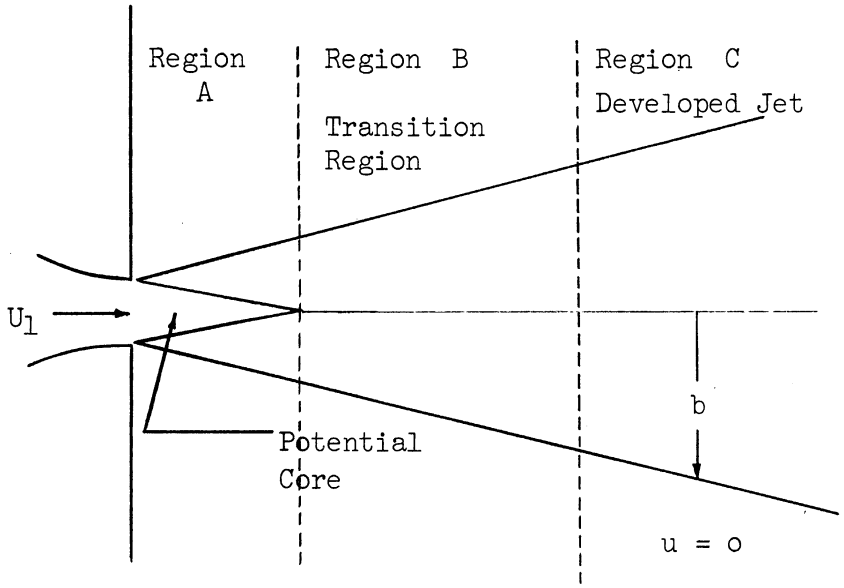

Figure 1. Features of Jet Flow with Finite Source.

Whereas the only parameter of the point source jet was the momentum constant, M, the circular jet with finite source has two parameters, a radius, R_1, and a velocity, U_1. Taking the axial velocity component as an example of the dependent variables, the general functional relationship may be written as:

$$\frac{u}{U_1} = f\left(\frac{r}{R_1}, \frac{x}{R_1}\right) \tag{2.22}$$

Kuethe[32] attempted to compute the flow in region A. He employed the Prandtl mixing length theory with $\ell = cb$ where b is the thickness of the mixing region. He then used a method of successive approximations to compute the velocity profile. His first approximation was:

$$u/U_1 = (1 - \theta^{2/3})^2 \tag{2.23}$$

where:

$$\theta = \left(\frac{r-a}{b}\right)$$

A good deal of calculation, involving numerical evaluation of integrals is involved in the method, but the results are in fair agreement with experimental measurements, from which it was determined that $c = 0.07$. His theory predicted a potential core length which is in good agreement with experimental observations:

$$\frac{x_c}{D_{jet}} = 4.44$$

D. Free Jets with Ambient Velocity

A problem which received considerable attention during World War II was that of a jet issuing into a fluid medium which was itself in uniform motion relative to the jet source. Both the core region (A) and the developed jet (C) were considered by Szablewski in Germany, and Squire and Trouncer in England. An additional parameter, the velocity of the ambient fluid, U_2, appears now, so that:

$$\frac{u}{U_1} = f\left(\frac{r}{R_1}, \frac{x}{R_1}, \frac{U_2}{U_1}\right) \tag{2.24}$$

Szablewski[51,52] made use of the Prandtl exchange coefficient hypothesis, and assumed power law velocity profiles in regions A and B. His solution involves a good deal of numerical evaluations, and is not of great fundamental importance. He obtained fair agreement with experimental results and determined values of k in (2.12) to be:

region A: $k = 0.0157$

region B: $k = 0.01$

Squire and Trouncer[49] noted that trigonometric functions did a fair job of fitting their experimental velocity profiles, and used Prandtl's mixing length theory to relate the Reynolds stress to the mean flow variables. In region A, they employed the following form of the velocity profile:

$$\frac{u}{U_1} = \frac{1}{2}\left(\frac{U_2}{U_1} - 1\right)\left[1 - \cos \pi\left(\frac{b-r}{b-a}\right)\right] \tag{2.25}$$

The mixing length was assumed proportional to the width of the mixing region:

$$\ell = c(b-a) \tag{2.26}$$

By comparison with experimental results, they found $C = 0.071$, in agreement with Kuethe's result for the free jet in a medium at rest. In region C, they made use of the profile:

$$u = U_2 + \left(\frac{u_o - U_2}{2}\right)\left(1 + \cos \pi \frac{r}{b}\right) \tag{2.27}$$

The mixing length is $\ell = Cb$.

From experimental data, they found $C = 0.082$. They had some limited success in applying the same analysis to region B, but found that c varied with x from 0.071 at the end of region A, to 0.082 in the developed jet.

Squire and Trouncer were also interested in the details of the irrotational flow outside the jet, and computed the hypothetical sink strength which would account for the inductive action of the jet. Due to the discontinuous model for the flow at the end of the potential core there is some peculiar behavior in the computed sink strengths. In general, however, this would seem a valuable approach to the potential flow field problem associated with the flow outside a free jet.

E. Confined Jets

If we confine the mixing field in a cylindrical tube, we introduce a new parameter, R_2 , so that equation (2.24) becomes:

$$\frac{u}{U_1} = f\left(\frac{r}{R_2}, \frac{x}{R_2}, \frac{U_2}{U_1}, \frac{R_2}{R_1}\right) \tag{2.28}$$

In addition, however, we have introduced a solid boundary in the problem so that the flow is no longer strictly a free turbulence shear flow. Indeed, there will be a boundary layer at the mixing tube wall which will eventually interact with the jet. If the boundary layer were to be considered in an analysis of the problem, a Reynolds number would be involved:

$$\frac{u}{U_1} = f\left(\frac{r}{R_2}, \frac{x}{R_1}, \frac{U_2}{U_1}, \frac{R_1}{R_2}, \frac{U_2 x \rho}{\mu}\right) \qquad (2.29)$$

All theoretical analyses to date have neglected the boundary layer.

A basic mechanical difference between the confined and free jets is that whereas momentum was conserved in the free jet, mass flux is conserved in the confined jet:

$$\rho \pi \int_0^{R_2} u r \, dr = \rho Q_t \quad \text{(constant)} \qquad (2.30)$$

Also, even if the ambient flow is uniform and non-turbulent, as is usually assumed, the jet will reach the wall at some point, and the flow will no longer be a jet flow, but a complex shear flow.

We note that the ambient velocity, U, can change from its initial value of U_2 as we move downstream. If, as fluid becomes entrained in the jet, this ambient velocity is reduced to zero before the jet reaches the wall, a back-flow develops to supply additional fluid to the jet. Thus is formed an eddy of recirculation.

In a confined jet, the integrated momentum changes downstream. In the core region, the pressure is constant, but thereafter, the pressure

rises as the jet spreads. Thus, the confined jet is a simple type of jet pump. An actual jet pump, of course, consists of a nozzle inside of a larger duct which converges to a cylindrical "mixing tube," and a diffuser completes the device. It is this practical application which has stimulated most of the research on confined jets.

Flügel[17] was the first to apply fluid mechanics theory to the jet pump. He used Prandtl's exchange coefficient hypothesis (2.12), in an integrated momentum equation, and assumed that the two streams have uniform velocities and are separated by a vortex sheet in which all the shear is concentrated. His work was enlightening with respect to the mechanism by which jet pumps operate, but it is of little quantitative value.

Ferguson[16] studied a two-dimensional confined jet, and attempted to predict the flow by assuming that the pressure is constant up to the point where the mixing layer reaches the wall. He used the results of a two-dimensional analysis of Kuethe to predice the length of this region, and employed some of the concepts of Flügel to compute the subsequent flow. He found that the results of this simplified analysis agreed fairly well with experimental results, but a variable value for a parameter in his shear expression was required.

Mikhail[39] has made a more recent study of a circular confined jet. He used the cosine velocity profile suggested by Squire and Trouncer, and the Prandtl mixing length equation in integrated momentum and continuity equations. He was unable to solve the resulting system

of differential equations without the use of some extensive simplifying assumptions, as he did not have a computer at his disposal.

Curtet, in France, has been studying confined jets for some time. Along with Craya at Grenoble, he has developed a theory for the developed jet region of a confined plane jet.[11] He makes use of an empirical velocity profile in an integrated form of Equation (2.8) which then contains only derivatives with respect to the axial variable. Then he notes from experimental data that all the coefficients of the derivatives can be expressed as multiples of a universal function of (y/x). He computes an average value for this function over the flow section, and thus obtains an ordinary differential equation. Finally, some results from experimental studies of the spread of free jets are used to evaluate the shear stress term. A Gaussian velocity profile (Equation (2.31) below) gave good agreement with experimental results, although a cosine distribution was later tried with satisfactory results. The extension of the theory to a cylindrical jet has not been completed.

$$\frac{u - U}{u_o - U} = e^{-\frac{\pi \eta^2}{4}} \qquad \left(\eta = \frac{r}{b}\right) \tag{2.31}$$

Recirculation was also considered by Curtet, who assumed that the reduction of the ambient velocity to zero in his computed results indicated that an eddy of recirculation occurred at that point. In spite of the fact that the flow must differ from that of the model on which the theory is based, this procedure permits a fairly accurate prediction of the occurence of an eddy.

Goslein and O'Brien,[24] Cunningham,[10] and Folsom,[18,19] have analyzed overall jet pump performance by means of overall energy and momentum balances. Various "efficiencies" are defined in an attempt to correlate overall ejector performance. Such an approach, however, supplies no information as to the mechanism of the momentum exchange or the rational design of a jet pump.

Because confined jets, and especially recirculation phenomena, are of interest in connection with turbulent jet flames, flame researchers have sought some fundamental parameter which governs the general behavior of confined jets. They are particularly interested in being able to predict the onset of circulation and the rate of recirculation. It is apparent from relation (2.28) that any such parameter must be a function of (U_2/U_1) and (R_2/R_1).

Thring and Newby[53] assumed that an enclosed jet grows at the same constant rate as in a free jet until it reaches the wall. They were interested in the mixing of two different fluids, air and fuel, and they concluded that the proper similarity parameter which governs the behavior of such a "cold flame model" is:

$$\left(\frac{\rho_1 Q_1}{\rho_1 Q_1 + \rho_2 Q_2}\right)\left(\frac{R_2}{R_1}\right)$$

For a single fluid system, this becomes, in terms of the groups of expression (2.28):

$$\frac{\left(R_2/R_1\right)}{1 + \left(\frac{U_2}{U_1}\right)\left[\left(\frac{R_2}{R_1}\right)^2 - 1\right]}$$

Curtet, in the course of his theoretical studies of plane confined jets, found that after integrating the equations of motion across the tube, the parameters appearing in the equation were (R_2/R_1) and a "momentum parameter," m . As generalized for a cylindrical jet, this parameter is:

$$m \equiv \frac{\pi R_2^2}{Q_t} \int_0^{R_2} \left(u^2 - \frac{U_1^2}{2} \right) 2\pi r\, dr \quad - \frac{1}{2} \tag{2.32}$$

Curtet's measurements indicated that this is a constant of the flow, or does not vary from one section to another. As will be demonstrated below this is precisely true only when wall friction is neglected, the flow external to the jet is non-turbulent and uniform, and there is no radial pressure gradient. The initial value of the Curtet similitude parameter is:

$$m_o = \frac{R_1^2 \left(U_1^2 - U_2^2 \right) + \frac{U_2^2 R_2^2}{2}}{\left(Q_t^2 / \pi^2 R_2^2 \right)} - \frac{1}{2} \tag{2.33}$$

Becker[5] has made a more general analysis of jet type flows, and demonstrated the fundamental significance of the parameter m for the particular kind of jet model considered by Curtet. Based on his unified analysis of jet flows, Becker suggests a more useful modification of the parameter m_o . He calls the new parameter the Craya-Curtet number, and gives it the symbol C_t :

$$C_t = \frac{1}{\sqrt{m_o}} \tag{2.34}$$

Becker's general treatment reveals that the Thring and Newby parameter is the proper similarity parameter only for an ideal or point source jet.

F. Experimental Studies

In addition to the experimental studies already mentioned above, which were carried out in conjunction with theoretical analyses, a number of other laboratory studies of heat, mass and momentum transport, as well as turbulence characteristics, in turbulent jets have been reported.

Alexander, Baron and Comings studied turbulent transport in jets at Illinois, and the final report of their work[2] contains a rather extensive discussion of phenomenological mixing theories as well as corrections necessary in the use of an impact tube to measure velocities in turbulent flows. Baron and Alexander[3] have noted that since the differential equation (Equation (2.21)) arising from the use of Reichardt's hypothesis is linear in u^2, the principle of superposition may be employed to compute velocities in flows involving parallel, interacting jets.

Forstall studied air jets with Shapiro,[21] and water jets with Gaylord.[20] Turbulent Schmidt and Prandtl numbers were determined from heat and mass transfer studies, and were found to differ little between the two fluids. Corrsin[8] and Uberoi[9] studied a round turbulent jet of heated air and used a hot wire system to determine velocity and temperature profiles as well as certain parameters of the turbulence. They found that the transport of heat occurred more rapidly than that of momentum. Hinze and van der Hegge Zijnen[26] suggested on the basis of

their studies that the mechanism of turbulent heat transfer is different from that for momentum transport.

Laurence, at NACA,[36] has completed an extensive hot wire study of the intensity, scale, and spectrum of turbulence in a free gas jet. Rosler and Bankoff[44] studied free air and water jets by means of hot wire anemometers. A special technique was developed for making hot wire measurements in a liquid. Their jet source was a long round tube, not a converging nozzle, so that the initial profile was that for fully-developed turbulent pipe flow. This was verified experimentally, but the remainder of their measurements were made at distances from the jet efflux of 10 or more jet tube diameters so that only the developed jet was studied.

Donald and Singer[14] employed a dye and chemical indicator technique to study, visually, the flow in the ambient fluid as well as in the mixing region of a submerged water jet. They were able to make photographic records of the core and mixing region geometries as well as streamlines outside the mixing region.

Viktorin[60] was the first to study the confined jet experimentally, by measuring velocities in a jet issuing into a large pipe. He was unsuccessful in an attempt to predict his results by means of Flügel's theory.

Martin and Rice[38] studied the effect of nozzle cross-section geometry on jet pump performance. Locher[37] applied dimensional analysis to the scale-up of laboratory tests in the design of a very large jet pump.

Becker[4,5] studied recirculation in confined jets by means of oilfog-marked air. He found that recirculation eddies occur when the

Craya-Curtet number is less than 0.75. Curtet discovered,[12] in his studies of plane confined jets that for values of the parameter m_o, defined in Equation (2.32), somewhat less than the value for which a steady recirculation eddy occurred, the flow became periodic with an eddy being alternately generated and swept away at the two confining walls. The period of the oscillation was found to follow the relationship:

$$\frac{R_2^2}{\varphi_t T} = C_1 \left(\frac{\varphi_1}{\varphi_t} \right) + C_2$$

where T = period of oscillation

C_1, C_2 are constants

Curtet and Ricou[13] investigated the effects of turbulence in the secondary flow on the mixing process and found that the mixing process was greatly accelerated by fairly low turbulence intensities in the stream.

G. General References

The book by Pai[40] is hardly more than a sketchy abstraction of the literature, and is currently out of print. Extensive bibliographies on jets have been compiled by Forstall and Shapiro,[21] and by Krzywoblocki.[31] The very recent treatise by Abramovich[1] contains many interesting discussions of jet flows, although the works of Curtet, Squire and Trouncer and Szablewski are not mentioned.

CHAPTER III

RECIRCULATION IN CONFINED JETS

It is known that under certain circumstances a recirculation eddy will exist in the mixing tube as a stable part of the flow. The pattern of the flow in the neighborhood of such an eddy is shown in Figure 2.

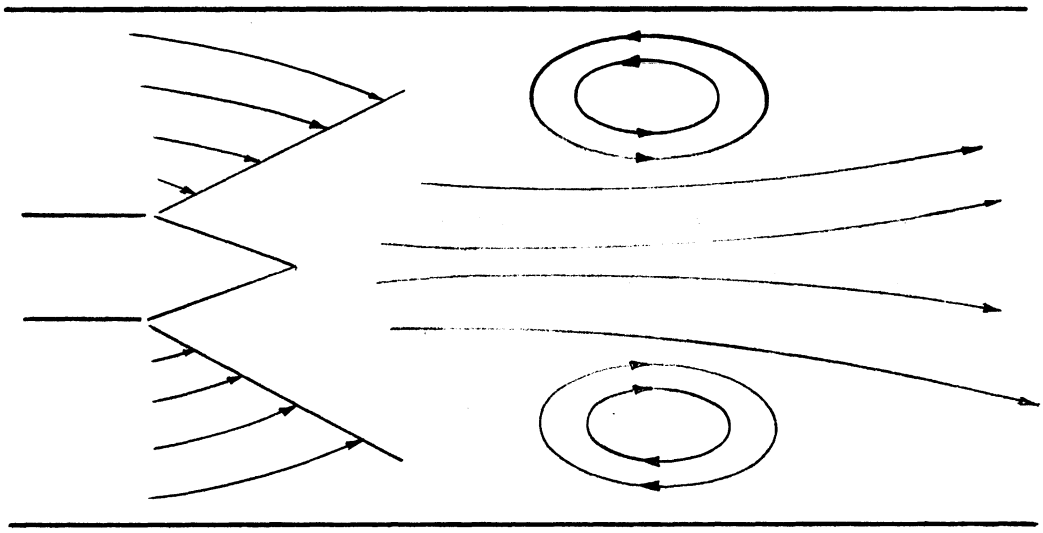

Figure 2. Eddy of Recirculation.

This phenomenon can be explained in several ways. Curtet describes recirculation quite simply as the mechanism which supplies fluid to be inducted into the thirsty mixing region after all the secondary flow has been swallowed up. He was interested in predicting when recirculation will occur, and assumed that the reduction of the ambient velocity to zero in his computed results indicated that an eddy of

recirculation occurred at that point. For a plane, confined jet, he computed[11] that the criterion for the existence of an eddy of recirculation in the mixing tube was:

$$m_o > 0.91$$

Becker found, experimentally,[4] for a circular jet that the condition was:

$$C_t < 0.75$$

Abramovich has a slightly more formal description of recirculation. He says[1] that mixing in a confined field results in a pressure rise, and that if this pressure rise is sufficiently high, it will retard the ambient flow to zero, resulting in recirculation. In other words, the positive pressure gradient saps the momentum from the ambient fluid, and may reduce this momentum to zero if the pressure rises sufficiently before the mixing region reaches the wall. This picture serves as a guide for the formalization of the recirculation problem, and it will now be demonstrated that the criterion for the occurrence of an eddy of recirculation may be derived from fundamental observations of confined jet flows without recourse to a detailed analysis of the equations of motion.

The model commonly employed in dealing with the developed jet region of a confined jet is shown in Figure 3. The velocity in the mixing region or jet is self preserving and its profile can be represented with reasonable fidelity by empirical distributions such as the harmonic distribution (Equation (2.27)) of Squire and Trouncer, and the Gaussian distribution (Equation (2.31)). These distributions are plotted for comparison in Figure 4. The velocity outside the mixing region is irrotational and there is no radial pressure gradient. This simple model was found by Curtet to represent the actual flow with surprising accuracy.

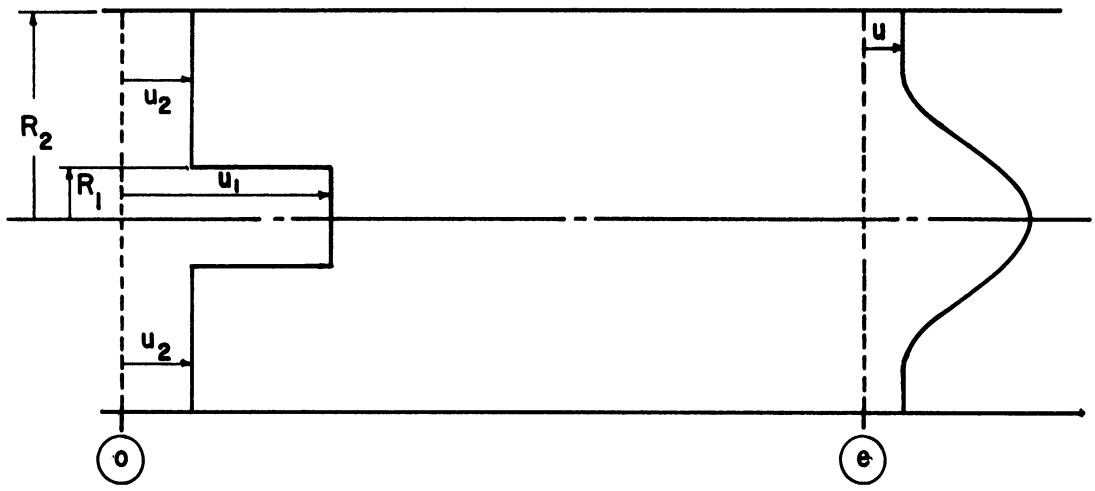

Figure 3. Confined Jet Model.

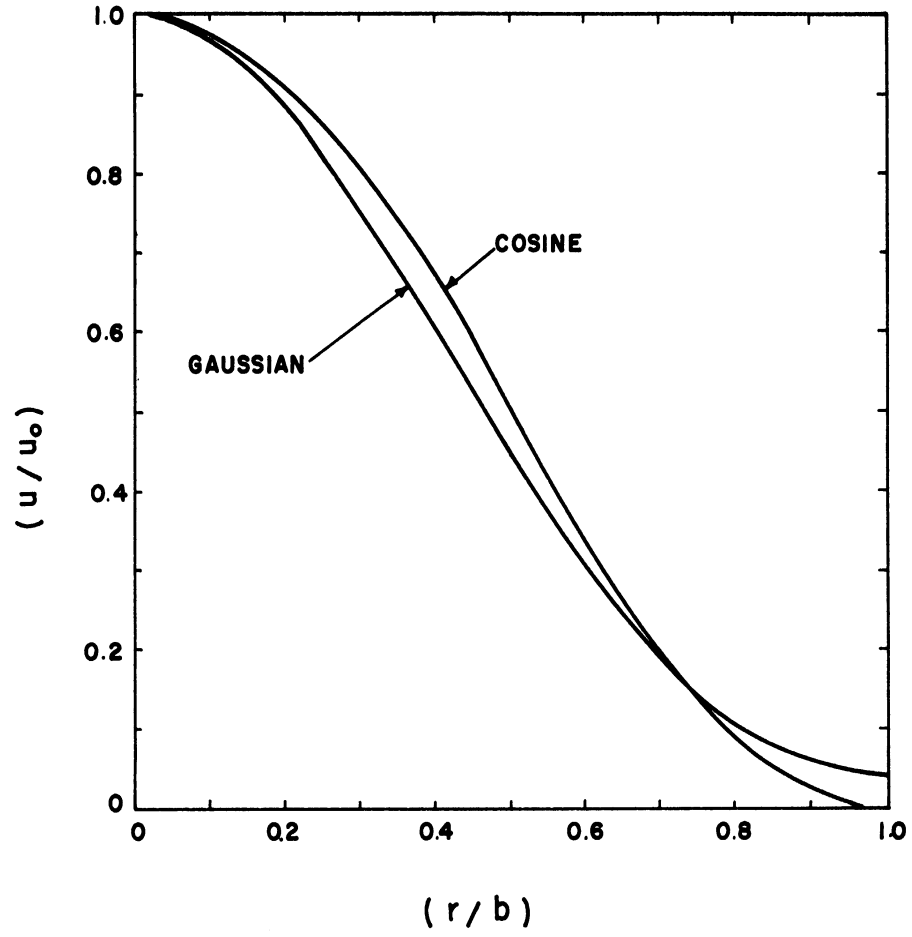

Figure 4. Velocity Distribution Functions.

The uniform velocity outside the jet is related to the pressure through the Bernoulli equation:

$$U \frac{dU}{dx} = - \frac{1}{\rho} \frac{dP}{dx} \tag{3.1}$$

Now as the jet spreads, the pressure rises, and, according to Bernoulli, the velocity falls accordingly. If the pressure rises sufficiently so as to reduce the velocity outside the jet, U, to zero before the jet expands to the wall $(b = R_2)$ then recirculation will occur. The condition for the virtual occurrence of an eddy is that $U = 0$ at the same time that $b = R_2$. We wish to develop a quantitative criterion for this condition in terms of the flow parameters (U_2/U_1) and (R_2/R_1).

An overall momentum balance between the entrance to the mixing tube and some point down stream which is labelled point "e" is:

$$(P_o - P_e)\pi R_2^2 + \int_0^{x_e} \tau_w 2\pi R_2 dx = \left[\rho \int_0^{R_2} u^2 2\pi r dr\right]_e - \left[\rho \int_0^{R_2} u^2 2\pi r dr\right]_o \tag{3.2}$$

The momentum flux at the entrance is simply:

$$\rho \int_0^{R_2} u^2 2\pi r dr = \pi \rho \left[U_1^2 R_1^2 + U_2^2 \left(R_2^2 - R_1^2\right)\right] \tag{3.3}$$

Inserting this result in Equation (3.2), and dividing by $\pi \rho U_1^2 R_1^2$:

$$\frac{P_e - P_o}{\rho U_1^2} - \int_0^{x_e} \frac{2\tau_w \, dx}{\rho U_1^2 R_2} = \left(\frac{R_1}{R_2}\right)^2 + \left(\frac{U_2}{U_1}\right)^2 \left[1 - \left(\frac{R_1}{R_2}\right)^2\right]$$

$$- 2\int_0^1 \left(\frac{u}{U_1}\right)^2 \left(\frac{r}{R_2}\right) d\left(\frac{r}{R_2}\right) \qquad (3.4)$$

The particular case to be considered here is that at point e :

$$U = 0$$

$$b = R_2$$

If a momentum factor, β , is defined as follows:

$$\beta \equiv \frac{\frac{1}{A}\int u^2 dA}{\left[\frac{1}{A}\int u \, dA\right]^2} = \frac{\int_0^1 u^2 \left(\frac{r}{R_2}\right) d\left(\frac{r}{R_2}\right)}{2\left[\int_0^1 u \left(\frac{r}{R_2}\right) d\left(\frac{r}{R_2}\right)\right]^2} \qquad (3.5)$$

then Equation (3.4) may be written as:

$$\frac{P_e - P_o}{\rho U_1^2} - \int_0^{x_e/R_2} \frac{2\tau_w}{\rho U_1^2} d\left(\frac{x}{R_2}\right) = \left(\frac{R_1}{R_2}\right)^2 + \left(\frac{U_2}{U_1}\right)^2 \left[1 - \left(\frac{R_1}{R_2}\right)^2\right] - \beta_e \left(\frac{\bar{u}_e}{U_1}\right)^2 \qquad (3.6)$$

The velocity ratio in the last term can be represented in terms of the initial conditions by means of the condition of constant volume flux at every cross section:

$$Q_t \equiv U_1 R_1^2 \pi + \pi U_2 (R_2^2 - R_1^2) = \pi R_2^2 \bar{u}_e \qquad (3.7)$$

Using this result in Equation (3.6):

$$\frac{P_e - P_o}{\rho U_1^2} - \int_0^{x_e/R_2} \frac{2\tau_w}{\rho U_1^2} d\left(\frac{x}{R_2}\right) = \left(\frac{R_1}{R_2}\right)^2 + \left(\frac{U_2}{U_1}\right)^2 \left[1 - \left(\frac{R_1}{R_2}\right)^2\right] - \beta_e \left(\frac{Q_t}{\pi R_2^2 V_1}\right)^2 \qquad (3.8)$$

Integrating Bernoulli's equation from the entrance to point e :

$$\frac{P_e - P_o}{\rho} = -\frac{1}{2}\left(U_e^2 - U_2^2\right)$$

But virtual recirculation corresponds to $U_e = 0$. So:

$$\frac{P_e - P_o}{\rho} = \frac{1}{2} U_2^2 \qquad (3.9)$$

The condition for eddy generation is that the pressure recovered by redistribution of the velocity up to the point where the jet reaches the wall, as given by Equation (3.8), be greater than the pressure difference given above. This condition is:

$$\int_0^{x_e/R_2} \frac{2\tau_w}{\rho U_1^2} d\left(\frac{x}{R_2}\right) + \left(\frac{R_1}{R_2}\right)^2 + \left(\frac{U_2}{U_1}\right)^2 \left[1 - \left(\frac{R_1}{R_2}\right)^2\right] - \beta_e \left(\frac{Q_t}{\pi R_2^2 V_1}\right)^2 > \frac{1}{2}\left(\frac{U_2}{U_1}\right)^2 \qquad (3.10)$$

If wall friction is neglected, this inequality can be rearranged to give:

$$\frac{\left(\frac{R_1}{R_2}\right)^2 + \left(\frac{U_2}{U_1}\right)^2 \left[1 - \left(\frac{R_1}{R_2}\right)^2\right] - \frac{1}{2}\left(\frac{U_2}{U_1}\right)^2}{\left(Q_t / \pi R_2^2 V_1\right)^2} > \beta_e \qquad (3.11)$$

The left hand member of the inequality is simply related to the Curtet similitude parameter, m , so that the condition for eddy formation is:

$$m_o + \frac{1}{2} > \beta_e \tag{3.12}$$

In terms of the Craya-Curtet number:

$$C_t < \frac{1}{\sqrt{\beta_e - 1/2}} \tag{3.13}$$

The results for the two distributions considered are:

1. Harmonic profile

   $u = \frac{u_o}{2} \left[1 + \cos \left(\frac{\pi r}{R_2}\right) \right]$

   $\beta_e = 1.95$

   $(C_t)_{crit.} = 0.83$

2. Gaussian profile

   $u = u_o \, C^{-\pi\left(\frac{r}{R_2}\right)^2}$

   $\beta_e = 1.72$

   $(C_t)_{crit.} = 0.91$

The presence of wall shear would tend to reduce the maximum pressure recovered, and would thus decrease the critical value of C_t . A velocity distribution with a greater momentum integral, i.e., higher value of β_e, would also yield a lower value of $(C_t)_{crit.}$ As has already been pointed out, Becker found the value of 0.75 experimentally for a circular gas jet.

Several important conclusions may be drawn from the above developments. One is that the parameters m_o or C_t are truly similitude parameters only when wall friction, irrotationality in the ambient

fluid, and radial pressure gradients are negligible. Another is that these parameters serve as criteria for recirculation only when the velocity profiles are of similar form in the developed jet region.

CHAPTER IV

DESCRIPTION OF CONFINED JET WITH TURBULENT SOURCE

A. Introduction

If we wish to study the effect of turbulence in the initial jet, it is desirable that we know something about the structure of the turbulence. One way of achieving a turbulent jet source with known characteristics is to use the efflux from a long, smooth circular tube. Now, for sufficient Reynolds number, we will obtain a turbulent stream whose characteristics have been studied in detail. Although the principle of Reynolds number similarity tells us that for high local Reynolds numbers, the structure of the turbulence is not dependent on the Reynolds number, the time average dynamic variables are affected by the Reynolds number due to the role played by the fluid properties near the wall. Thus, as compared to the confined jets already discussed, one new group is added to the general relationship:

$$\frac{u}{\bar{u}_1} = f\left(\frac{r}{R_2}, \frac{x}{R_1}, \frac{U_2}{\bar{u}_1}, \frac{R_1}{R_2}, \frac{R_1 \bar{u}_1 \rho}{\mu}\right) \tag{4.1}$$

since the jet tube velocity is not uniform, but has a profile dependent upon the jet tube Reynolds number. Thus, if:

$$\beta_1 = \frac{\int_0^{R_1} u^2 \, 2\pi r \, dr}{\bar{u}_1^2 \pi R_1^2} \tag{4.2}$$

then the Curtet similarity parameter as defined by (2.32) is:

$$m_o = \frac{R_1^2\left(\beta_1 \bar{u}_1^2 - U_2^2\right) + \frac{U_2^2 R_2^2}{2} - \frac{Q_t^2}{2\pi^2 R_2^2}}{\left(Q_t/\pi R_2\right)^2} \qquad (4.3)$$

Thus, it would appear that the Reynolds number dependence is easily incorporated into the Curtet parameter. Actually, an additional amount of energy enters the system in the form of turbulent energy in the jet tube efflux. To account for this, Rosler and Bankoff[44] define a modified vairation of the definition of β which includes turbulent contributions to the energy. They estimate, however, that for turbulent pipe flow, the correction amounts to less than .05%.

Some features of the flow in a confined jet with turbulent source are discussed below to establish a general picture of the mechanisms involved, and to provide a basis for the quantitative analysis of the system which is presented in the next chapter.

B. Wake Due to Jet Tube Wall

At the end of the jet tube there is a wake, due to the finite thickness of the tube wall, and the no-slip condition on both the inside and outside of the tube. This results in a minimum in the axial velocity profile. The only theoretical treatment of the role played by the wake in jet mixing is that of Chapman and Korst[7] which considers only the simplest case of the plane jet boundary with uniform pressure. None of

increases as we move closer to the wall. Townsend[56] suggests the relation:

$$\frac{u}{\bar{u}_1} = \frac{U_o}{\bar{u}_1} - C\sqrt{\frac{\tau_o}{\rho \bar{u}_1^2}}\, f\left(\frac{r}{R_1}\right) \qquad (4.5)$$

The terms $(U_o/\bar{u}_1)$ and the dimensionless wall shear stress, are functions of the Reynolds number. A satisfactory agreement with experiment is found for $r/r_o < 0.9$ if:

$$\frac{u}{\bar{u}_1} = \frac{U_o}{\bar{u}_1} - 7.5\sqrt{\frac{\tau_o}{\rho \bar{u}_1^2}}\left(\frac{r}{R_1}\right)^2 \qquad (4.6)$$

Detailed studies of the turbulence characteristics of pipe flow have been carried out of Laufer[35] and Sanborn[46] using hot-wire anemometers.

It is necessary in the present study to know something about what happens to the stream which leaves the jet tube with the well-known characteristics described above. In his studies of turbulent boundary layers, Townsend[57,58] has hypothesised the existence of the "equilibrium layer." This hypothesis is based on considerations of the concept of structural similarity and the relative importance of the terms in the "turbulent energy balance." This relationship, derivable from the Reynolds equations, can be interpreted as a statement that the kinetic energy associated with the velocity fluctuations is constantly being dissipated or transformed into heat by viscous shear, and replenished by several mechanisms.

One form of the turbulent energy balance is:

$$\overline{u'v'}\frac{\partial u}{\partial r} + \frac{1}{r}\frac{\partial}{\partial r}\left(\frac{1}{2}\overline{q^2 v' r}\right) = -\frac{1}{r}\frac{\partial\left(\overline{p'v'}r\right)}{\partial r} + \nu\Gamma \qquad (4.7)$$

$$q^2 = u'^2 + v'^2 + w'^2$$

Γ = dissipation + viscous transport

For a steady state, the amount of kinetic energy associated with the velocity fluctuation in a small volume of fluid is constant. Townsend suggests that when the rate of turbulent energy dissipation by conversion to heat is nearly balanced by the rate of turbulent energy generation by working against Reynolds stresses, the flow in that region is determined almost solely by the distribution of shear stress within the region and is independent of the conditions outside of it. In other words, when the other terms in the turbulent energy equation, including the convection terms, are very small compared to the generation and dissipation terms, the flow in that region is essentially independent of the remainder of the flow, and may be considered self-preserving. Laufer's experimental results suggest an application of some of Townsend's ideas to the problem at hand.

Laufer's measurements of the terms in the mechanical energy balance (Equation (4.7)) are summarized in Figure 6. We will be interested in the structure of the flow away from the wall, since when the wake has disappeared, that portion of the jet near $r = a$ will have already changed in its structure and velocity profile due to rapid momentum transport just after the jet entrance. We note that the outer portion of the jet flow is characterized by large production and dissipation

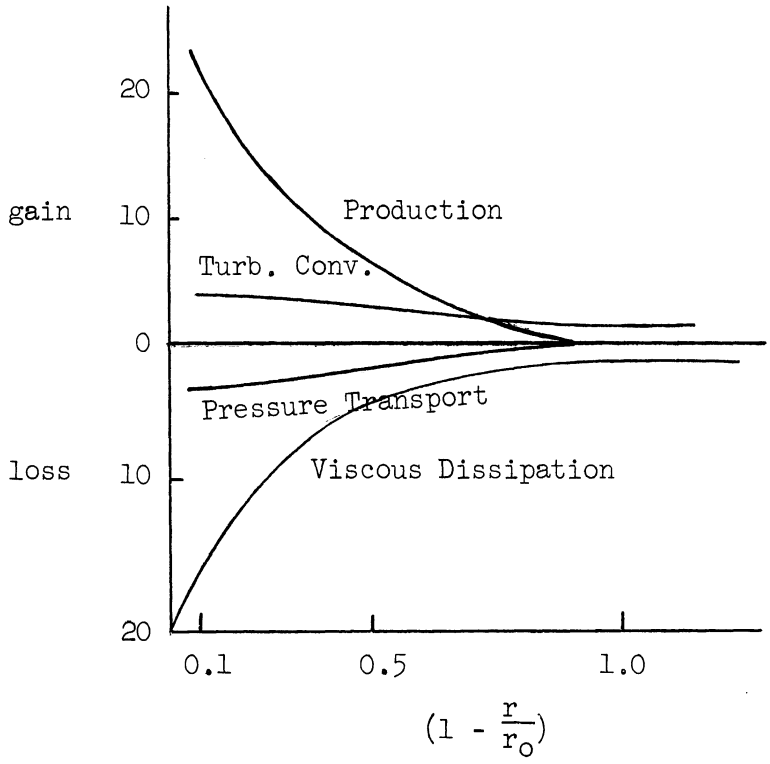

Figure 6. Turbulent Energy Balance for Pipe Flow at $R_e = 5 \times 10^4$ (Laufer, NACA R 1174).

terms. We might expect, then, that in this region and in the region internal to it, the structure of the trubulence does not change axially, except by the action of momentum exchange at edge of the region. Now, if the structure is not changing axially, then the Reynolds stress is the same as it was in the pipe flow, and we can see from the Reynolds equation that the velocity profile remains the same. Thus, corresponding to the "potential core" of ordinary jets, we have an equilibrium turbulent core which extends from the entrance to the point downstream were, by means of shear, the core has been dissipated to the point where turbulent

convection becomes a significant contribution to the turbulent energy.

D. Flow Outside the Equilibrium Core

Since the streamlines are initially parallel, the pressure at the entrance is radially uniform. Furthermore, the pressure gradient in the axial direction for the flow in the annular region surrounding the mixing region is initially zero. The pressure on the axis falls, however, as has been noted in the discussion of the equilibrium core. Thus, a radial pressure gradient is developed which tends to push fluid toward the axis. Fluid is induced into the mixing region, then, not only by turbulent momentum transport, but by the radial pressure gradient. The streamlines will be deflected toward the axis, and the pressure will begin to fall at the wall.

Features of the hydrodynamic pressure behavior in a confined jet with turbulent source are shown in Figure 7.

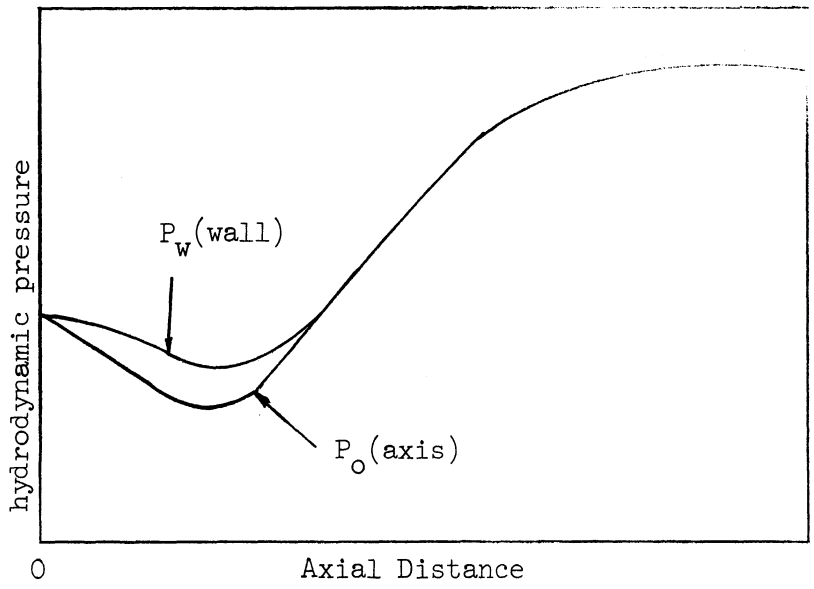

Figure 7. Pressure Gradients in Confined Jet with Fully Developed Turbulent Source.

E. Flow Downstream of the Equilibrium Core

When the equilibrium core has been dissipated to a certain extent by shear at its outer edge, turbulent convection becomes a significant term in the turbulent energy balance, so that the flow near the axis is no longer an independent equilibrium flow. Because the streamlines in this region are parallel, however, they will tend to remain so in the absence of a radially varying force field. It is true, of course, that pressure and turbulent normal stresses will vary across this region, but the radial gradients are probably not large enough to cause a rapid divergence of the flow. Thus, there will still be a core of fluid in which the velocity profile is nearly that of the flow at the entrance, but whose turbulent structure is changing. This will be called the "kinematic core."

In order to determine the general nature of the pressure behavior associated with this kinematic core, Equation (2.8) will be employed. If the turbulent normal stress is neglected, and expression (2.10) is used, the radius may be set equal to zero to obtain the gradients on the axis. The result is:

$$u_o \frac{du_o}{dx} = -\frac{1}{\rho}\frac{\partial P}{\partial x} + \left[\frac{1}{r}\frac{\partial}{\partial r}\left(\epsilon r \frac{\partial u}{\partial r}\right)\right]_{r=0} \qquad (4.8)$$

but, if $du_o/dx = 0$;

$$\frac{dP_o}{dx} = \rho\left[\frac{1}{r}\frac{\partial}{\partial r}\left(\epsilon r \frac{\partial u}{\partial r}\right)\right]_{r=0} \qquad (4.9)$$

or:

$$\frac{dP_o}{dx} = \rho\left[\frac{\epsilon}{r}\frac{\partial}{\partial r}\left(r\frac{\partial u}{\partial r}\right) + \frac{\partial u}{\partial r}\frac{\partial \epsilon}{\partial r}\right]_{r=0} \qquad (4.10)$$

but

$$\left(\frac{\partial u}{\partial r}\right)_{r=0} = 0$$

and, if ϵ is nearly constant in the neighborhood of the axis

$$\left[\frac{\epsilon}{r}\frac{\partial}{\partial r}\left(r\frac{\partial u}{\partial r}\right)\right]_{r=0} = 2\epsilon\left(\frac{\partial^2 u}{\partial r^2}\right)_{r=0}$$

then:

$$\frac{dP_o}{dx} = 2\rho\left[\epsilon\frac{\partial^2 u}{\partial r^2}\right]_{r=0} \qquad (4.11)$$

Thus, the axial pressure must continue to fall in the kinematic core region. Only when the velocity on the axis begins to fall, can the pressure rise.

When the velocity at the axis begins to fall, and the pressure begins to rise, the flow is a very complex one, as it no longer contains a core of known and constant turbulent structure or velocity, and is not self-preserving in the sense of Townsend's definition[55] of that term. Experiments with finite jet sources, however, have indicated that

the flow rapidly develops a self-preserving structure. In the confined jet with potential core studied by Becker[5] as well as the free jet with turbulent core studied by Rosler and Bankoff,[44] this development was found to be reasonably complete at 8 to 10 jet diameters downstream of the entrance. Becker[5] observed little effect of the jet source Reynolds number on the developed flow for jet Reynolds numbers greater than 30,000.

For the axial component of velocity, the similarity of the flow may be represented as follows:

$$\frac{u(r,x) - U(x)}{u_o(x) - U(x)} = f\left[\frac{r}{b(x)}\right] \tag{4.12}$$

Various researchers have reported that both the Gaussian distribution (Equation (2.31)) and a harmonic distribution (Equation (2.25)) fit observed velocity profiles reasonably well in the developed jet region.

When the jet spreads to the wall, or when the mixing region meets the wall boundary layer, the flow is no longer a jet flow, but a shear flow with boundary for which few simplifying assumptions can be made. A long distance downstream, fully developed pipe flow will obtain.

F. The Boundary Layer

The only data available for the growth of a boundary layer on the inside wall of a tube are those for flow in the hydrodynamic entry region. Langhaar's theoretical treatment[33] gives results for the laminar case, which are in good agreement with Nikuradse's experimental

data. Shapiro, Siegel and Kline[48] applied boundary layer theory to predict the wall shear stress for such flows. For that situation, however, there is a favorable pressure gradient, and separation does not occur. For the problem under study here, there may be a severe adverse pressure gradient. This has an important effect on both separation and transition-to-turbulence in the boundary layer. All avaliable data concerning these phenomena involve flows over flat plates. If the boundary layer thickness is small compared to the radius of curvature of the surface, however, the results are the same. Since, in the present situation, the behavior of the flow near the entrance, where the boundary layer is quite thin, is of specific interest, a discussion of separation and transition in boundary layers on flat plates is in order.

A falling pressure, like that in the core region, tends to inhibit both separation of the boundary layer and transition to turbulence. When the pressure begins to rise, however, this adverse pressure gradient promotes both the transition and the separation. The criterion for separation of a laminar boundary layer, as discussed by Schichting[47] is, for a flat plate:

$$\frac{U U''}{U'^2} < 11 \qquad (4.13)$$

Thus, for the boundary layer in a confined jet, separation will always accompany the disappearance of the core, unless transition to turbulence occurs first. This is because turbulent boundary layers are considerably more stable than laminar ones. The transition to turbulence occurs when:

$$\frac{U\rho\delta^*}{\mu} > \left(Re_\delta\right)_{critical} \qquad (4.14)$$

The critical Reynolds number for flat plates depends on the level of turbulence in the flow outside the boundary layer, the magnitude of the pressure gradient and the boundary layer thickness. For no pressure gradient:

$$(Re_\delta)_{crit} = 420$$

With an adverse pressure gradient, it can be considerably less. If the boundary layer becomes turbulent withour separating, then it will proceed into the region of pressure rise. Uram[59] has reviewed research on axisymmetric turbulent boundary layers in an adverse pressure gradient.

Becker[5] postulates that since the boundary layer development is strongly influenced by the axial pressure gradient, it is characterized by the Craya-Curtet number. It must be recalled, however, that Becker considered jets with poential core, in which the initial pressure gradient is always nearly zero. In the case of the jet with fully developed turbulent source, however, there is initially a negative pressure gradient whose magnitude depends primarily on the jet tube Reynolds number. Based on the above observations, then, it seems probable that the jet tube Reynolds number would have a strong effect on the boundary layer development in such a flow.

CHAPTER V

MATHEMATICAL MODEL OF FLOW

A. Philosophy and Objectives

It was desired to establish a model for the flow which, if it produced results in agreement with experimental data, could be used to study certain features of the flow for many conditions other than those for which experiments were carried out. It was intended that the analysis serve as a means of studying the characteristics of the flow, rather than just solve a particular boundary value problem. An integral analysis based on the qualitative features of the flow presented in the previous section seemed in order. Thus, the mathematical model would provide a means of testing the validity of the hypotheses set forth.

Certain of the assumptions employed in previous confined jet work, to simplify the problem for mathematical analysis, are not strictly valid when there is an axial pressure gradient in the core region. These assumptions have been modified, and an approximate analysis has been formulated which, it was hoped, would predict the major characteristics of the flow, at least over a prescribed range of conditions. The following analysis is based on a uniform flow external to the mixing region. This is a reasonable approximation only when the uniform flow region is relatively small, (R_1/R_2 large), and the axial pressure gradient small, ($(R_e)_1$ small).

If the turbulent normal stresses are small compared to the hydrodynamic pressure, Equation (2.8) becomes:

$$u\frac{\partial u}{\partial x} + v\frac{\partial u}{\partial r} = -\frac{1}{\rho}\frac{\partial P}{\partial x} - \frac{1}{r}\frac{\partial}{\partial r}\left(r\overline{u'v'}\right) \qquad (5.1)$$

Equation (5.1) will be applied to each region of the flow to predict the development of the pressure and velocity profiles in the axial direction. It is assumed in each case that the boundary layer is very thin so that its displacement thickness can be neglected in the continuity integral, and its momentum thickness may be neglected in the momentum integral.

Figure 8 shows the system under consideration, and clarifies the terminology. The equilibrium and kinematic core regions are considered separately, but following Squire and Trouncer, the analysis of the developed jet will be extended to cover the transition region.

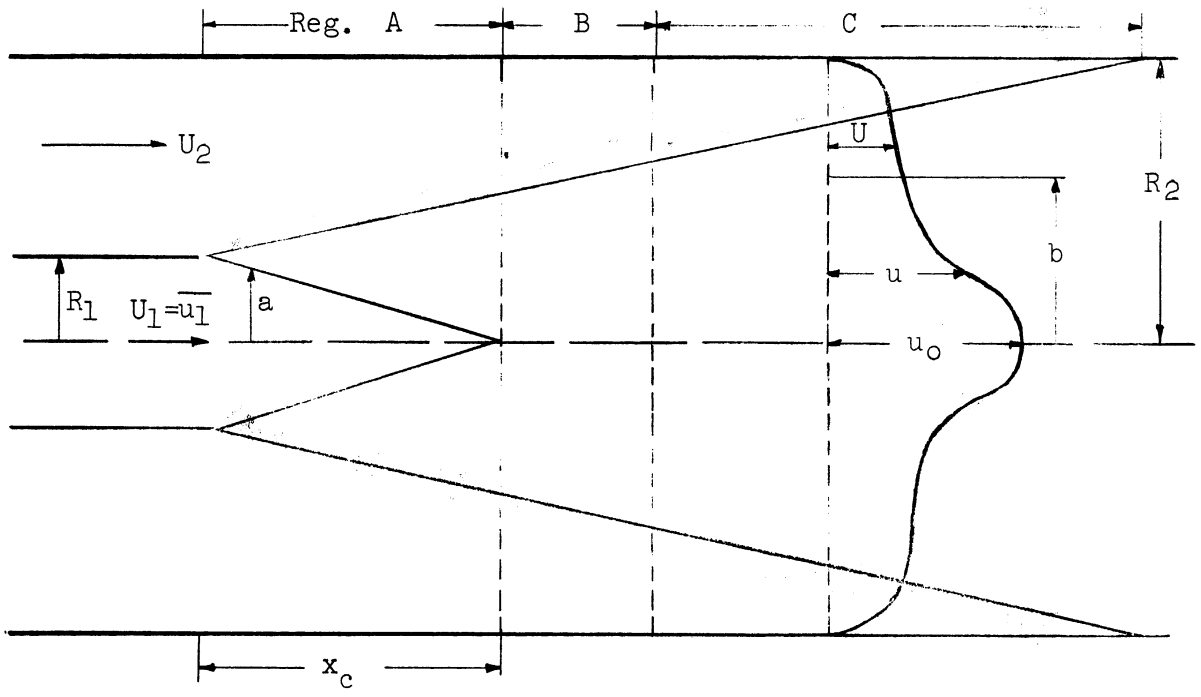

Figure 8. Sketch of System Considered in Establishment of Mathematical Model.

B. Equilibrium Core Region

If the existence of an equilibrium core is hypothesised on the basis of the arguments in the preceding section, then the velocity, pressure and shear stress in the core are those for turbulent flow in a smooth tube. For such a flow, the wall shear stress is simply related to the pressure gradient:

$$\tau_w = \frac{R_1}{2} \frac{dP_0}{dx} \tag{5.2}$$

Also, the shear stress is proportional to the radius:

$$\frac{\tau}{\tau_w} = \frac{r}{R_1} \tag{5.3}$$

The dimensionless pressure gradient is a unique function of the Reynolds number:

$$-\frac{dP_0}{dx} \frac{R_1}{\rho \bar{u}_1^2} = \gamma(Re_1) \tag{5.4}$$

If the shear is predominantly turbulent, then the shear stress referred to above is the Reynolds stress:

$$\tau = -\rho \overline{u'v'} \tag{5.5}$$

Of course, near the wall viscous shear becomes predominant, but we are interested here only in those vestiges of the turbulent tube flow which

may be present in the equilibrium core. Thus, by the time the wall wake has dissipated, the core will already have diminished in size so that the portion remaining is the turbulent core of the tube flow for which Equation (5.5) is valid. Sanborn's measurements support this argument. Then the Reynolds stress distribution in the core is given by:

$$\overline{u'v'} = \frac{r\,\tau_w}{R_1} = \frac{r\,\overline{u}_1^2\,\gamma}{2R_1} \tag{5.6}$$

For the present, let us consider the jet flow starting at some value of $x = x_0$ where the wake has been dissipated, and a , the radius of the equilibrium core is less than 0.9. Under these circumstances, Townsend's parabolic profile given be Equation (4.6) is a good representation of the velocity. In terms of the dimensionless pressure gradient, this profile is:

$$\frac{u}{\overline{u}_1} = \frac{U_0}{\overline{u}_1} - 5.3\sqrt{\gamma}\left(\frac{r}{R_1}\right)^2 \tag{5.7}$$

Outside the mixing region, a uniform flow with axial velocity = U will be considered. For the mixing region, let us assume a polynomial in (b-r)/(b-a) may be used to represent the velocity profile:

$$\frac{u}{U} = \delta_0 + \delta_1\frac{(b-r)}{(b-a)} + \delta_2\left[\frac{b-r}{b-a}\right]^2 + \delta_3\left[\frac{b-r}{b-a}\right]^3 \tag{5.8}$$

But at r = b , we have

$$u = U \quad ; \qquad \frac{\partial u}{\partial r} = 0$$

Then

$$\delta_o = 1, \text{ and}$$

$$\delta_1 = 0,$$

and Equation (5.8) becomes:

$$\frac{u}{U} = 1 + \delta_2 \left[\frac{b-r}{b-a}\right]^2 + \delta_3 \left[\frac{b-r}{b-a}\right]^3 \qquad (5.9)$$

The coefficients δ_2 and δ_3 which are functions of x, can be determined from the conditions at $r = a$, where u and $(\partial u / \partial r)$ are specified by Equation (5.7). They are:

$$\delta_2(x) = 3\left(\frac{U_o}{\overline{u_1}} - \frac{U}{\overline{u_1}}\right) - \frac{5.3\sqrt{\gamma}\, a}{(R_1)^2}(2b + a) \qquad (5.10)$$

and

$$\delta_3(x) = 2\left[\left(\frac{U}{\overline{u_1}} - \frac{U_o}{\overline{u_1}}\right) + \frac{5.3\sqrt{\gamma}}{(R_1)^2} a b\right] \qquad (5.11)$$

The ratio $U_o/\overline{u_1}$ is as shown in Figure 5.

In the core, the pressure is radially uniform. It will be assumed that, for the purposes of this model, the radial pressure gradient is limited to the mixing region. Thus, the pressure outside the mixing region will be equal to the wall pressure. Summarizing, we have:

$$P = P_o \qquad o \le r \le a$$

$$P = P_w \qquad b \le r \le R_1$$

$$P_o \le P \le P_w \qquad a \le r \le b$$

Furthermore, it is apparent from the qualitative arguments summarized in Figure 7, that, if P represents the excess pressure over that at the entrance:

$$P_o < P_w < 0$$

and

$$\frac{dP_w}{dx} = 0 \quad \text{at} \quad x = 0$$

This can be formalized as shown below.

$$\frac{dP_w}{dx} = \lambda(x) \frac{dP_o}{dx} \tag{5.12}$$

where $\lambda(x)$ is a monotonically increasing function of x with $\lambda(o) = 0$. Lacking a basis for any more elaborate form, (x) will be assumed linear in x :

$$\lambda(x) = Bx \tag{5.13}$$

For the uniform flow region, the flow is essentially irrotational so that:

$$U \frac{dU}{dx} = -\frac{1}{\rho} \frac{dP_w}{dx} \tag{5.14}$$

For a given value of B and $(Re)_1$, it may be seen that $P_o(x)$, $P_w(x)$ and $U(x)$ can be easily computed. The mean velocity distribution is then specified by a and b . A system of ordinary differential equations will now be developed, the solution to which will be the desired functions: $a(x)$ and $b(x)$. The two required differential equations will be obtained by integrating the continuity Equation (2.6), and the simplified Reynolds Equation (5.1).

The total axial mass flux must be constant. Thus:

$$\int_0^{R_2} u\, 2\pi r\, dr = Q_t \qquad \text{(constant)} \tag{5.15}$$

The velocity is not a continuous function, however, so that the integral must be divided into three parts before it can be evaluated

$$\frac{Q_t}{2\pi} = \int_0^a u r\, dr + \int_a^b u r\, dr + \int_b^{R_2} u r\, dr$$

The velocities in each integral are:

$0 \leq r \leq a$ $\quad u = u(r)$; Equation (5.7)

$a \leq r \leq b$ $\quad u = u(r)$; Equation (5.9)

$b \leq r \leq R_2$ $\quad u = U$

In its derivative form Equation (5.15) is:

$$\frac{1}{2\pi}\frac{dQ_t}{dx} = \frac{d}{dx}\int_0^a u r\, dr + \frac{d}{dx}\int_a^b u r\, dr + \frac{R_2^2}{2}\frac{dU}{dx} = 0 \tag{5.16}$$

Carrying out the indicated integrations we obtain an equation of the form:

$$\Phi_1(x)\frac{dq}{dx} + \Phi_2(x)\frac{db}{dx} + \Phi_3(x)\frac{dU}{dx} = 0 \tag{5.17}$$

Integrating Equation (5.1) between the limits a and b :

$$\int_a^b u\frac{\partial u}{\partial x} r\, dr + \int_a^b v\frac{\partial u}{\partial r} r\, dr + \int_a^b \frac{1}{\rho}\frac{\partial P}{\partial x} r\, dr = -\int_a^b \frac{\partial}{\partial r}\left(r\overline{u'v'}\right) dr \tag{5.18}$$

the stress term on the right integrates directly to give:

$$-\int_a^b \frac{\partial}{\partial r}\left(r\overline{u'v'}\right)dr = \left(-r\overline{u'v'}\right)_{r=b} - \left(-r\overline{u'v'}\right)_{r=b} \qquad (5.19)$$

But at $r = b$, the stress disappears, and at $r = a$ it is given by Equation (5.6). Thus:

$$-\int_a^b \frac{\partial}{\partial r}\left(r\overline{u'v'}\right)dr = \frac{a^2\,\overline{u_1}^2\,\gamma}{2R_1} \qquad (5.20)$$

It is positive because the core is tending to accelerate the neighboring fluid.

The third term on the left is the integral of the pressure gradient. It may be represented in terms of a properly averaged gradient:

$$\frac{1}{\rho}\int_a^b \frac{\partial P}{\partial x}\,r\,dr = \frac{1}{\rho}\left(\frac{dP}{dx}\right)_{avg.}\left(\frac{b^2-a^2}{2}\right)$$

Now the precise distribution of the pressure in the mixing region is not known, but it is the purpose of the integral approach to avoid solving the second Reynolds Equation (2.9) by making use of approximate models for radial variations. To implement the integral method here, the simplest average will be taken. Thus:

$$\frac{1}{\rho}\int_a^b \frac{\partial P}{\partial r}\,r\,dr = \frac{1}{\rho}\left(\frac{dP_o}{dx} + \frac{dP_w}{dx}\right)\left(\frac{b^2-a^2}{4}\right)$$

or, employing Equation (5.12):

$$\frac{1}{\rho}\int_a^b \frac{\partial p}{\partial x} r\,dr = \frac{1}{\rho}\frac{dP_o}{dx}(1+\lambda)\left(\frac{b^2-a^2}{4}\right) \tag{5.21}$$

Substituting Equations (5.20) and (5.21) in (5.18):

$$\int_a^b u\frac{\partial u}{\partial x} r\,dr + \int_a^b v\frac{\partial u}{\partial r} r\,dr + (1+\lambda)\frac{(b^2-a^2)}{4\rho}\frac{dP_o}{dx} = \frac{a^2\bar{u}_1^{\,2}\gamma}{2R_1} \tag{5.22}$$

As is demonstrated in Appendix A, the two remaining integrals on the left may be put into a simpler form. The resulting equation is:

$$\frac{d}{dx}\int_a^b u^2 r\,dr + (u_a - U)\frac{d}{dx}\int_0^a u r\,dr - U\frac{d}{dx}\int_a^b u r\,dr + (1+\lambda)\frac{(b^2-a^2)}{4\rho}\frac{dP_o}{dx} = \frac{a^2\bar{u}_1^{\,2}\gamma}{2R_1} \tag{5.23}$$

The pressure gradient can be eliminated by means of Equation (5.4), and the final equation, in general form, is:

$$\Theta_1(x)\frac{da}{dx} + \Theta_2(x)\frac{db}{dx} = \frac{\bar{u}_1^{\,2}\gamma}{2R_1}\left[a^2 + \frac{(1+\lambda)(b^2-a^2)}{a}\right] \tag{5.24}$$

Equations (5.17), and (5.24) form the required system for the determination of a(x) and b(x) . The boundary conditions are:

at $x = x_o$; $a = a_o$

$b = b_o$

We recall that x_o is some point downstream of the wall wake. Since Townsend's profile (Equation (5.7)) holds only for $r/R_1 \leq 0.9$, a_o was taken as 0.9 with b_o computed from the integrated continuity equation.

C. The Kinematic Core

In this region, the velocity profile in the core is still represented by Equation (5.7), but the stress distribution is no longer represented by Equation (5.6). In fact, the turbulent structure of the core is changing rapidly in this region, and it will be necessary to make maximum use of intuition and previous experimental observations to establish a mathematical model. It is important to note that the disappearance of the equilibrium structure in the core will cause it to dissipate more rapidly due to convective communication with the high shear mixing region. Thus, it is a very short region.

The general form of the velocity distribution will be assumed the same as in the previous discussion. Thus, Equations (5.7) and (5.9) are still valid. The core pressure is no longer given by Equation (5.4), however, and P_w and U are no longer known independently. If Equations (5.12) and (5.14) are still valid, there are now three dependent variables a, b, U which prescribe the mean flow.

The integration of the continuity equation then gives:

$$\phi_1(x)\frac{da}{dx} + \phi_2(x)\frac{db}{dx} + \phi_3(x)\frac{dU}{dx} = 0 \qquad (5.25)$$

In the momentum integral Equation (5.18), a relationship for the shear stress term will be required. Employing Squire and Trouncer's mixing length, Equation (2.26), we have:

$$-\overline{u'v'} = \ell^2 \frac{\partial u}{\partial r}\left|\frac{\partial u}{\partial r}\right| = -\ell^2\left(\frac{\partial u}{\partial r}\right)^2$$

with

$$\ell = c(b-a)$$

or:

$$-\overline{u'v'} = -c^2(b-a)^2\left(\frac{\partial u}{\partial r}\right)^2 \tag{5.26}$$

Equation (5.19) is still valid, and the right hand term of Equation (5.18) is:

$$-\int_a^b \frac{\partial}{\partial r}\left(r\overline{u'v'}\right)dr = a c^2(b-a)^2\left(\frac{\partial u}{\partial r}\right)^2_{r=a} \tag{5.27}$$

The derivative $\left(\frac{\partial u}{\partial r}\right)_{r=a}$ is given by Equation (5.7). It is:

$$\frac{\partial u}{\partial r} = \frac{-2(5.3)\sqrt{\gamma}\, r\, \pi_1}{R_1^2} \qquad 0 \le r \le a \tag{5.28}$$

and:

$$\left(\frac{\partial u}{\partial r}\right)^2_{r=a} = \frac{4(5.3)^2 \gamma a^2 \pi_1^2}{R_1^4}$$

The pressure integral is evaluated as before, and dP_o/dx can be eliminated by means of Equations (5.12) and (5.14). The momentum integral equation becomes:

$$\theta_1(x)\frac{da}{dx} + \theta_2(x)\frac{db}{dx} + \theta_3(x)\frac{dU}{dx} = \frac{4(5.3)^2\gamma_2^3\bar{u}_1^2c^2(b-a)^2}{R_1^4} \qquad (5.29)$$

There is no straightforward method of obtaining the required third equation. If the change in the nature of the core turbulence does not immediately influence the behavior of the flow at the outer edge of the mixing region, however, then we might assume that the jet continues to spread at the rate computed at the end of the equilibrium core region:

$$\frac{db}{dx} = \left(\frac{db}{dx}\right)_{\text{end of core region}} = b'_o \qquad (5.30)$$

Now the system is complete and consists of Equations (5.25), (5.29) and (5.30).

D. The Developed Jet

In this region, the core has disappeared and the velocity on the axis falls. The jet region is characterized by the approach to structural similarity, and it might be expected, following the arguments of Prandtl and Hinze, that a reasonable form for the Reynolds stress relation is the constant exchange coefficient law:

$$-\overline{u'v'} = \kappa b(u_o - U)\frac{\partial u}{\partial r} \qquad (5.31)$$

For sinplicity, the mean axial velocity will be assumed to follow the Squire and Trouncer harmonic relationship (Equation (2.27)).

If the radial pressure g4adient is small, the Reynolds equation (Equation (5.1)) is

$$u\frac{\partial u}{\partial x} + v\frac{\partial u}{\partial r} = U\frac{dU}{dx} + \frac{\kappa b(u_o - U)}{2b}\frac{\partial}{\partial r}\left(r\frac{\partial u}{\partial r}\right) \tag{5.32}$$

From Equation (2.27)

$$\frac{\partial u}{\partial r} = -\frac{\pi(u_o - U)}{2b}\sin\left(\frac{\pi r}{b}\right) \tag{5.33}$$

and

$$\frac{\partial}{\partial r}\left(r\frac{\partial u}{\partial r}\right) = \frac{-\pi(u_o - U)}{2b}\left[\sin\frac{\pi r}{b} + \frac{\pi r}{b}\cos\frac{\pi r}{b}\right] \tag{5.34}$$

Then Equation (5.32) becomes

$$u\frac{\partial u}{\partial x} + v\frac{\partial u}{\partial r} - U\frac{dU}{dx} = \frac{-\kappa\pi(u_o - U)^2}{2r}\left[\sin\frac{\pi r}{b} + \frac{\pi r}{b}\cos\frac{\pi r}{b}\right] \tag{5.35}$$

A system of three ordinary differential equations will now be developed, the solution to which will be (b, U, u_o)(x). One will be obtained by integration of the continuity equati on resulting in:

$$\phi_1(x)\frac{db}{dx} + \phi_2(x)\frac{dU}{dx} + \phi_3(x)\frac{du_o}{dx} = 0 \tag{5.36}$$

The second will be obtained by setting $r = o$ in Equation (5.35) to give:

$$u_o \frac{du_o}{dx} - U\frac{dU}{dx} = \left\{ \frac{-\kappa\pi(u_o - U)^2}{2r} \left[\sin\frac{\pi r}{b} + \frac{\pi r}{b}\cos\frac{\pi r}{b} \right] \right\}_{r=0}$$

Applying L'Hopitals' rule to the right hand term:

$$u_o \frac{du_o}{dx} - U\frac{dU}{dx} = -\frac{\kappa\pi^2(u_o - U)^2}{b} \tag{5.37}$$

The third equation will be obtained by integrating Equation (5.35) over the interval from $r = 0$ to b. Nothing that the shear stress disappears at both limits, the integral equation is:

$$\int_0^a u\frac{\partial u}{\partial x} r\,dr + \int_0^b r\frac{\partial u}{\partial r} r\,dr - U\frac{dU}{dx}\frac{b^2}{2} = 0$$

Employing again the development given in Appendix A, this equation may be simplified to the following form:

$$\frac{d}{dx}\int_0^b u(u-U) r\,dr - U\frac{b^2}{2}\frac{dU}{dx} = 0 \tag{5.38}$$

Then, the final equation is of the form:

$$\Theta_1(x)\frac{db}{dx} + \Theta_2(x)\frac{dU}{dx} + \Theta_3(x)\frac{du_o}{dx} = 0 \tag{5.39}$$

Equations (5.36), (5.37), and (5.39) make up the required system.

E. Numerical Analysis

In each of the regions considered, the problem has been reduced to that of solving a system of two or three simultaneous, non-linear, ordinary differential equations. Most numerical methods for the solution of ordinary differential equations are based on truncated Taylor series expansions. With boundary conditions of the type encountered here, the Runge-Kutta methods are quite convenient, especially if a computer is available. The most frequently encountered Runge-Kutta method is the fourth order method, which employs the first five terms of the Taylor series expansion, and involves an error of the order of $(\Delta x)^5$. There is some freedom in the choice of an averaging technique, and the most popular for use with computers is that due to Gill.

The Runge-Kutta-Gill subroutines generally available for use with digital computers solve systems of the type:

$$\frac{dy_1}{dx} = f_1(y_1, y_2, \cdots, x)$$
$$\frac{dy_2}{dx} = f_2(y_1, y_2, \cdots, x) \qquad (5.40)$$

The systems arising from the developments here are of the type:

$$\sum f_i(y_1, y_2, \cdots, x)\frac{dy_i}{dx} = F(x)$$

These must then be solved simultaneously for the individual derivatives. A computer program to solve the resulting system was developed. The algorithm was written in the "MAD" language for use in the IBM 7090 computer at the University of Michigan Computing Center, and is given in Appendix B.

The dimensionless pressure gradient, γ, in the equilibrium core was computed by means of the formula established by Blasius.[6]

$$\gamma = 0.079\ (\mathrm{Re})^{-\frac{1}{4}}$$
$$3000 \leq \mathrm{Re} \leq 100{,}000 \tag{5.41}$$

CHAPTER VI

EXPERIMENTAL APPARATUS AND PROCEDURES

A. The System Studied

In order to gain new insight into the phenomenon of confined jet mixing, velocity profiles and wall static pressures were measured at various distances from the jet source, in a system which differed somewhat from that employed in previous confined jet studies. Thus, the entering jet was a fully-developed, turbulent pipe flow rather than a uniform potential flow, and the ratio of mixing tube to jet diameters was lower than in previous studies.

The specific purposes of the laboratory study were: to determine the detailed behavior of this new kind of jet, especially near its entrance, to test the validity of the similarity criteria of Craya and Curtet for a nonuniform jet source, and to verify the hypotheses set forth above concerning the nature of the flow.

B. Description of Equipment

Figures 9 and 10 are a schematic diagram and a photograph, respectively, of the experimental equipment which was located on the third floor of the Fluids Engineering Building. The fluids were pumped into the jet tube and secondary entrance section from a constant head tank by means of two centrifugal pumps. The use of pumps, rather than independent, elevated constant head systems permitted operation over a wider range of conditions, and provided a critical test of the applicability of previous knowledge about jet mixing where industrial fluid handling equipment was used.

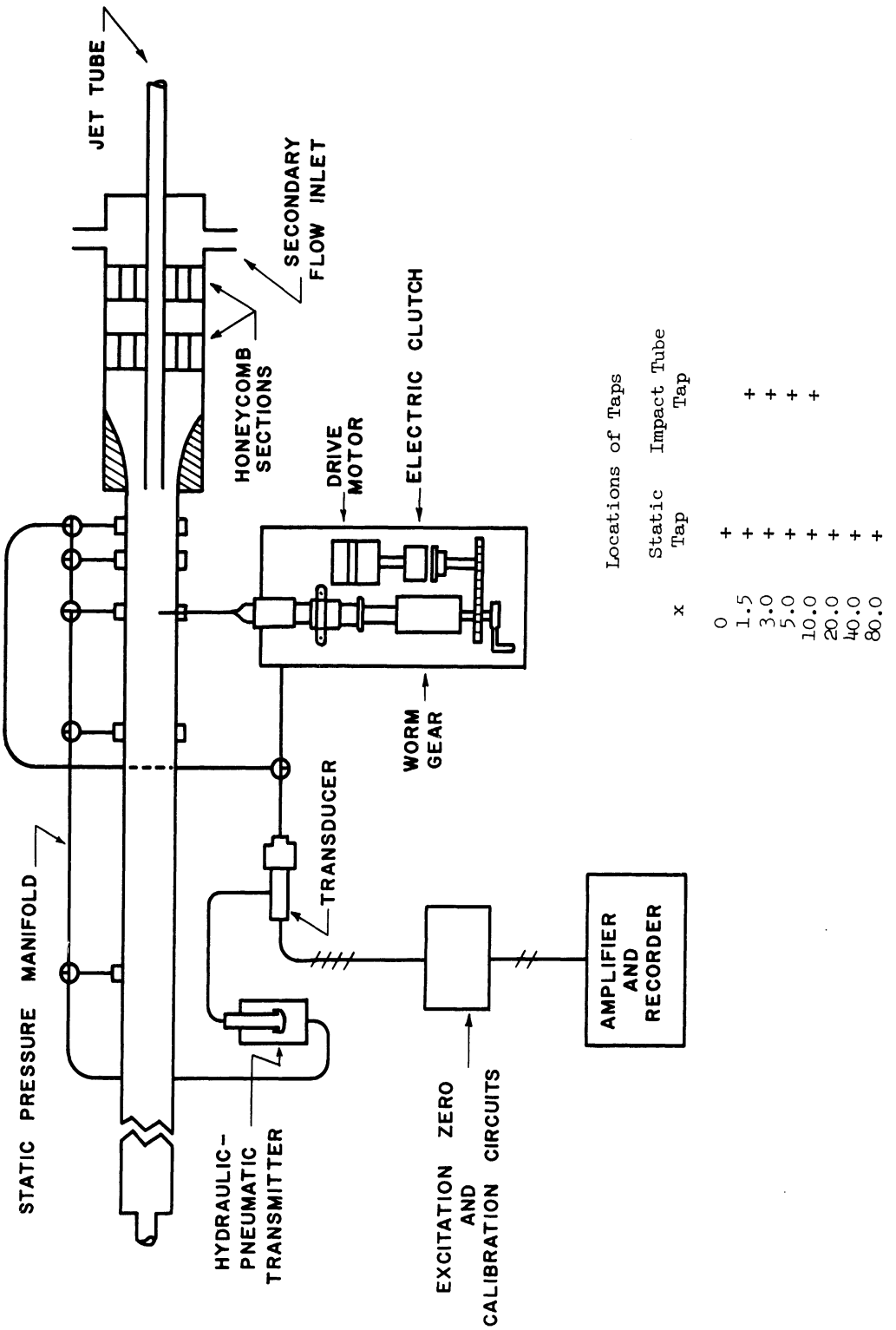

Figure 9. Elements of Experimental System.

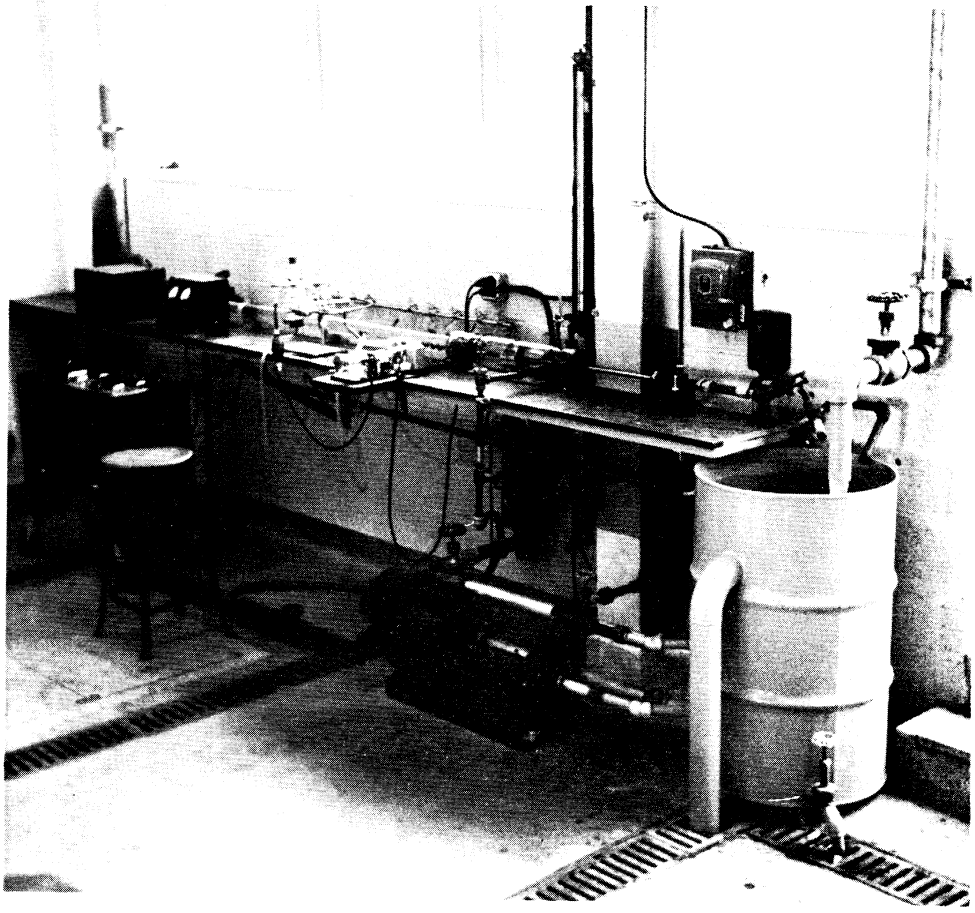

Figure 10. Photograph of Equipment.

Thin-walled brass tubes were employed as jet sources. Although several authors have formulated analyses of turbulent flow development at the entrance to round tubes, their analyses are based on an initially flat velocity profile. For such an initial condition, Latzko[34] predicts that fully-developed flow will obtain at a distance from the entrance of $1.25\ r_o(Re)^{\frac{1}{4}}$. For the maximum Reynolds number and tube diamerer employed in this study, this value is less than 20. When, as in the case here, the initial condition is more complex, or unknown, the only course is to make the tube much longer than that suggested by Latzko's result. Accordingly, the jet tubes used were more than 50 radii in length.

The outer tube of the mixing chanber was 2 inches in diameter and 80 inches in length so that the downstream exit would have little effect on the mixing process. Two jet tubes were used; one with a 1" diameter, and one with a $\frac{1}{2}$" diameter. The mixing tube and secondary flow entrance chamber were clear plastic with $\frac{1}{4}$" walls. The secondary flow entrance section was 4" I.D., 2' long, and contained two, 3-inch honeycomb sections. A piece of aluminum stock was machined to form a convergent channel which became cylindrical where the 2-inch I.D. test section began.

The primary (jet) and secondary flows were pumped through rotameters from a 55-gallon drum equipped with a large inlet and runoff duct so that a constant level could be maintained. The fluid leaving the end of the test section could be drained or recycled to the reservoir.

The mixing tube was tapped on each side as shown in Figure 9 at various distances downstream from the jet entrance. On one side the taps were fitted with brass fittings and rubber seals so that an impact tube could be inserted for velocity measurements. On the opposite side the taps were connected to a manifold system which permitted their use both in supplying a reference pressure for the impact tube total head measurements and also in measuring the difference in wall pressure between any two taps.

All pressure differences were measured by means of one of two Statham pressure transducers employing resistance-bridge strain-gauges. The characteristics of these transducers are given in Table I. Direct current excitation was employed and a Sanborn pre-amplifier, amplifier, and recorder were used to amplify the millivolt output and supply a visual record of it. A specially-built device provided for external calibration and zeroing circuits and also a choice of two excitation voltages from dry batteries. Figure 12 is a schematic diagram of the calibration and zeroing circuits.

So that a continuous record might be obtained for the velocity profiles, the impact tube was moved slowly across the mixing tube by means of a motor-driven worm gear device. This was a specially-modified JKM syringe drive unit equipped with a high-torque motor and an impact tube carriage made from a hypodermic syringe. Figure 11 is a photo of the impact tube carriage and drive unit.

The impact tube itself is identical to that used by Knudsen in his study of velocity profiles in anuli.[29] The point of a number 19

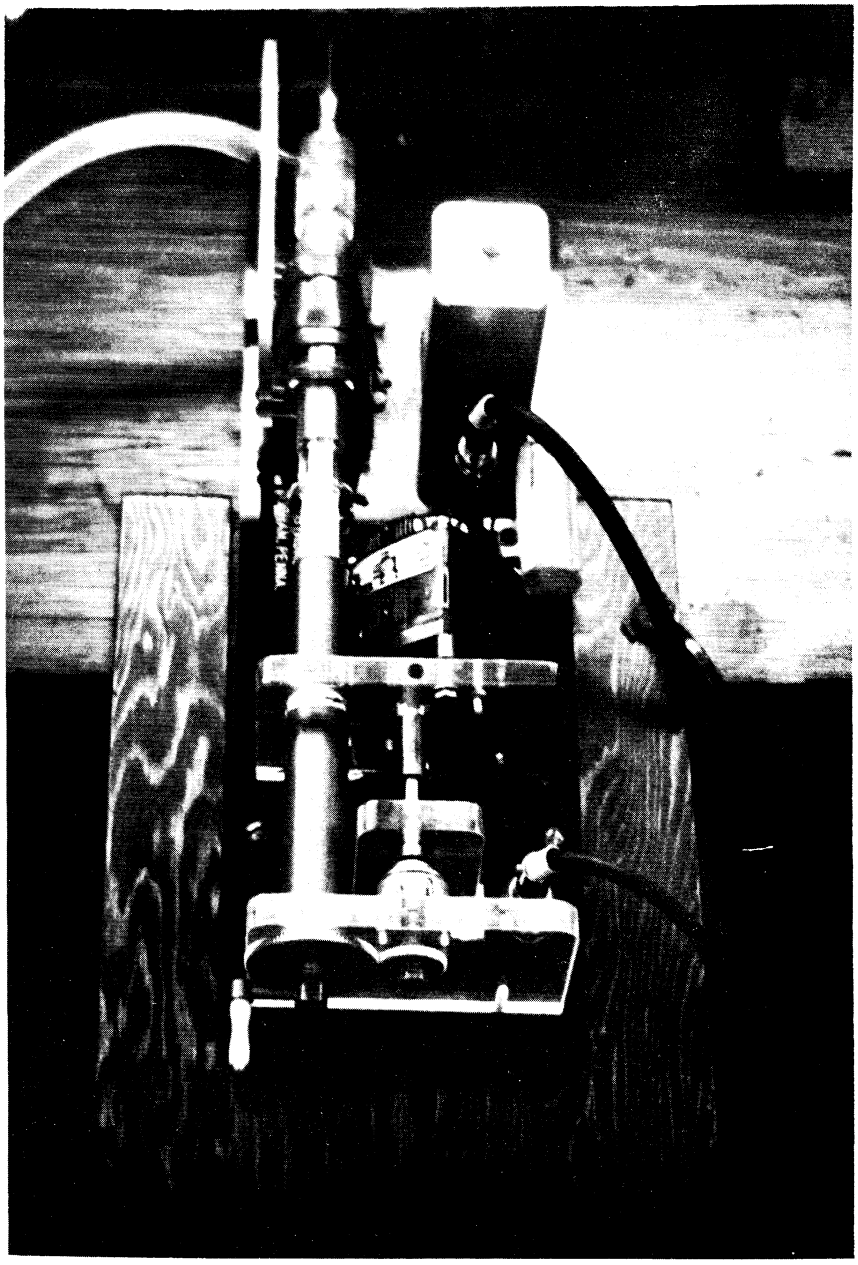

Figure 11. Photograph of Impact Tube Drive Unit.

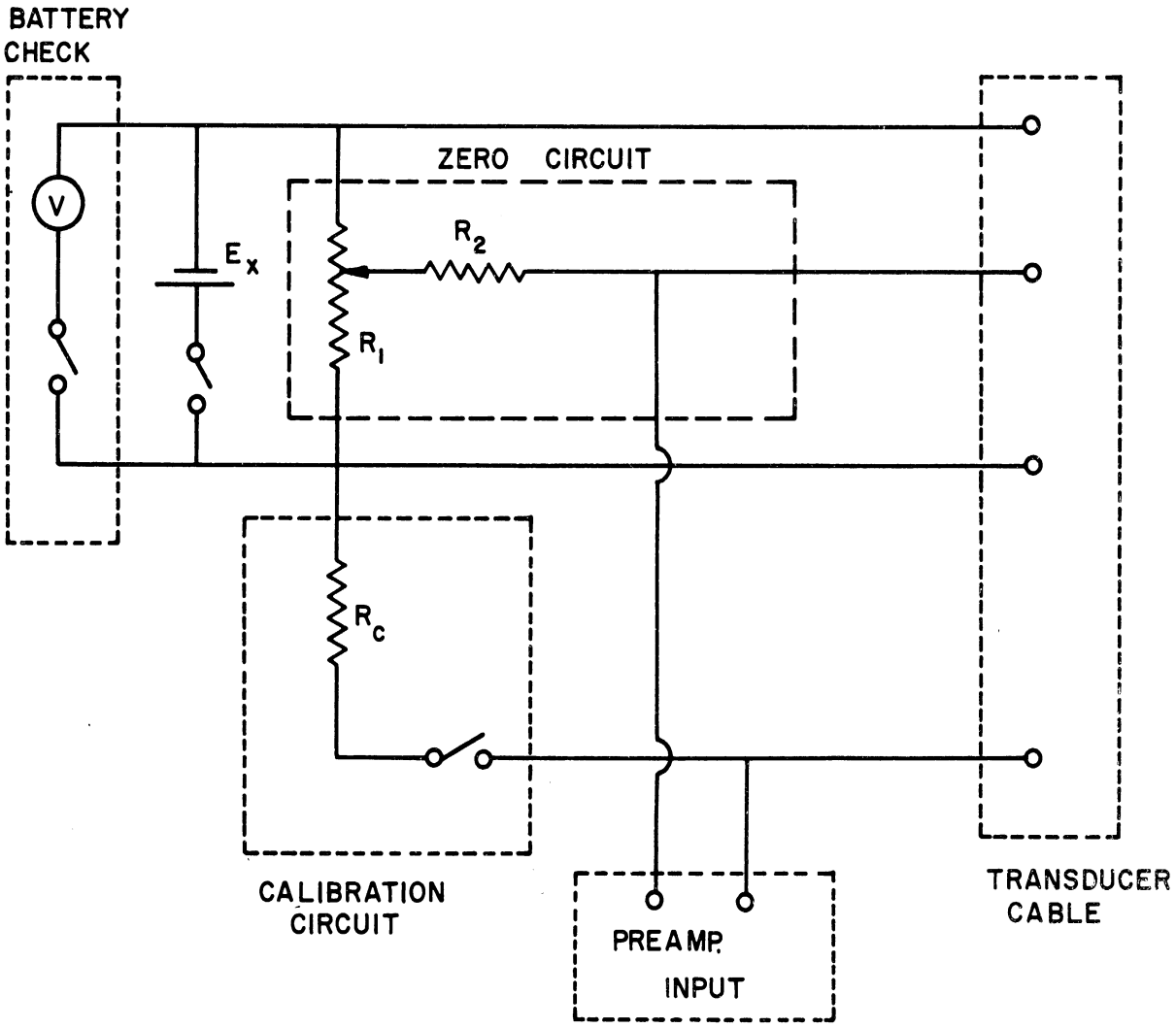

R_1 = 10K wire-wound potentiometer

Transducer Range	± 0.3 psi	± 0.7 psi
E_x	12 v	15 v
R_2	33 K Ω	35 K Ω
R_c	60 K Ω	25 K Ω

Figure 12. Transducer Excitation, Calibration and Zero Circuits.

hypodermic needle was sawed off, and a small slot sawed in one side at the end. Then the end was sealed with epoxy resin, leaving a rectangular hole in the side of the tube.

TABLE I

TRANSDUCER CHARACTERISTICS

Serial Numbers	11141	11157
Model Number	PM5TC ± 0.3-350	PM5TC ± 0.7-350
Pressure Range	± 0.3 psi	± 0.7 psi
Excitation	12 v	14 v
Calibration factor microvolts/volt/psi	7229	4800

C. Velocity Profiles

The impact tube, mounted on its special carriage, was positioned at the wall of the mixing tube, and an electric clutch turned on, engaging the constant speed drive unit. The impact tube traversed the mixing tube at the rate of 0.156 inches per minute. The symmetry of the pressure records indicated that the hydraulic and electronic circuits of the pressure measuring system were not introducing any significant lag between the pressure sensing probe and the recording. The impact tube was connected to the positive side of a strain gauge pressure transducer. The reference side was attached through the protective pressure transmitter and a manifold system to a tap in the mixing tube wall opposite that

employed for the impact tube. The transducer output was fed to the recorder, thus providing a continuous record of the pressure difference. One such record is shown in Figure 13.

D. Wall Static Pressures

By means of the manifold-valve system, the pressure difference between any two wall taps could be measured. A sample record of such a measurement is shown in Figure 14.

E. Data Analysis

In laminar flow measurements, a small correction factor is commonly employed in the interpretation of pitot tube pressures. For low velocities such as those involved in these studies, which were less than 10 ft/sec, this correction has been shown[3] to be less than 0.1%.

In turbulent flows, however, additional uncertainties are encountered because impact tubes measure mean square values. Goldstein[22] and Fage[15] have discussed this problem, and conclude that if the radial velocity component is small, reasonable accuracy can be obtained by using the wall static pressure as the reference pressure. This was the procedure followed in the measurements reported in this thesis. Baron et. al.[3] point out that there is no rational basis for correcting turbulent impact tube measurements, as quantitative detailed knowledge of the turbulent structure is generally unknown. Knudsen[29] reported that his tests showed good accuracy could be obtained with an impact tube of the type used here, by use of the simple formula:

$$u = \sqrt{2\Delta P/\rho} \qquad (6.1)$$

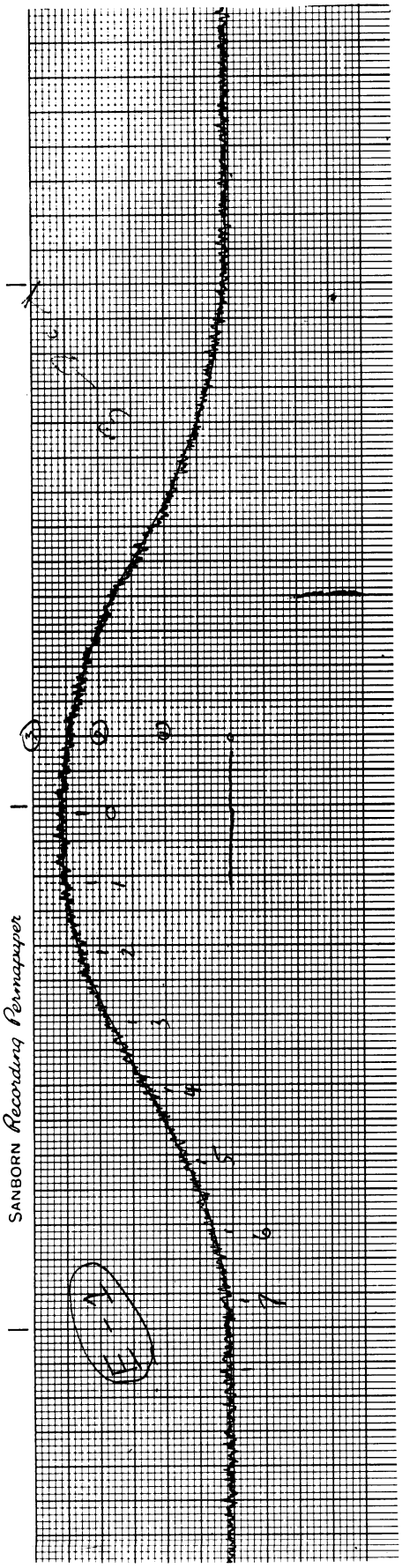

Figure 13. Sample Impact Tube Record.

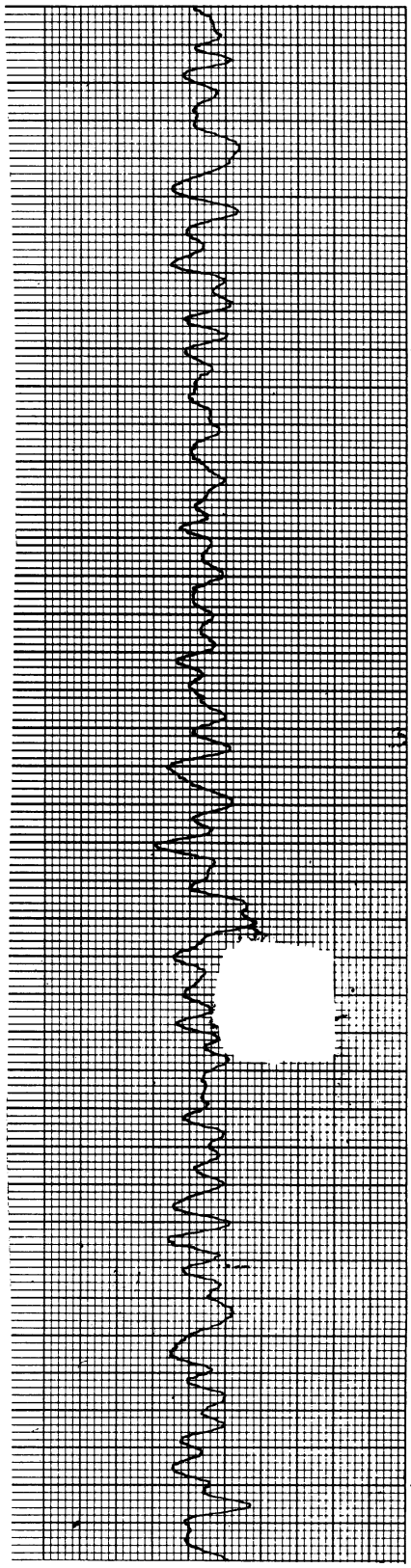

Figure 14. Sample Wall Static Pressure Record.

The pressure difference corresponding to a given voltage output is:

$$\Delta P = C E \tag{6.2}$$

where C = transducer constant, psf/millivolt

E = transducer output, millivolts

There was no way of measuring the radial hydrodynamic pressure gradient, so that in cases for which such gradients were significant, as was particularly true of the studies involving the small jet tube, an indeterminant error in the calculated velocities was inevitable. The maximum errors due to radial pressure gradients would occur in the higher Reynolds number flows from the $\frac{1}{2}$" jet tube. For those runs it has been estimated that the error is in the range of 2-4%.

Because of the limited sensitivity of the available amplifier and recorder, and the superimposed fluctuations resulting from worn pump impellers, accurate determinations of velocities in the region external to the mixing region were not possible. Thus, boundary layer development could not be followed, but average velocities in the ambient flow region were estimated by computing the uniform velocity necessary to satisfy the continuity equation. Data for the region wherein velocities were measured were plotted on paper whose vertical grid spacing was proportional to the square of the abscissa. Then, since

$$\int u r\,dr = \frac{1}{2}\int u\,d(r^2) \tag{6.3}$$

the volumetric flow rate corresponding to this portion of the flow could be computed from the area under this curve as obtained by means of a

planimeter. Knowing the total flow rate, as determined from rotameters, the average velocity in the remainder of the tube could be determined. If the computed average was negative, then an eddy of recirculation was known to have been present. The existence of such eddies was verified visually by injecting dye into the jet tube stream.

Records of differences between wall static pressures were more simply determined. Due to worn shafts and impellers in the centrifugal feed pumps, however, the pressures fluctuated rapidly about their norminal values. This produced fluctuations in the recordings of pressure differences as shown in Figure 14. To obtain the average value of the reading, a planimeter was used to measure the area under a certain length of trace. Equation (6.2) was employed to compute the pressure difference from the average recorder reading.

The transducer constant, C, is computed from the relationship:

$$C = \frac{1}{FE_x}, \qquad (6.4)$$

where F is a calibration factor supplied by the manufacturer, and E_x is the excitation voltage supplied to the transducer. A vacuum tube voltmeter was used to determine the exact voltage output of the dry cells employed, and a high resistance voltmeter was used to check on cell stability. When cell voltages began to drop, new ones were installed.

CHAPTER VII

EXPERIMENTAL RESULTS

Conditions studied with the $\frac{1}{2}$-inch diameter jet tube are listed in Table II, and the results are shown in Figures 15 through 23. Corresponding information concerning studies made with the 1" jet tube is given in Table III and Figures 24 through 30. Each figure contains the complete data on velocity profiles and wall pressures for each experimental condition. The dashed line on the velocity plot represents the initial profile computed as follows:

$0 \leq r \leq R$, universal velocity profile

$R_1 \leq r \leq R_2$ average secondary velocity

The velocity profiles are numbered as follows:

Number	Distance from Jet Tube Exit, Inches
1	1.5
2	3.0
3	5.0
4	10.0

In drawing the wall static pressure curves, maximum use was made of intuition and indirect information, as the small number of experimental measurements did not always provide a complete picture of the distribution. When recirculation occurred, for example, an inflection was expected. Also, for large values of x, it was known that the slope should be approaching its value for developed pipe flow.

TABLE II

MEASUREMENTS WITH $\frac{1}{2}$" DIAMETER JET TUBE

Figure	$(Re)_1$	C_t	U_2/U_1	Recirculation Observed
15	12,000	1.21	0.22	
16		1.54	0.34	
17	18,000	0.251	-0-	X
18		0.56	0.075	X
19		0.80	0.15	
20	26,000	0.251	-0-	X
21		0.67	0.10	X
22		0.88	0.16	
23	29,000	0.66	0.09	X

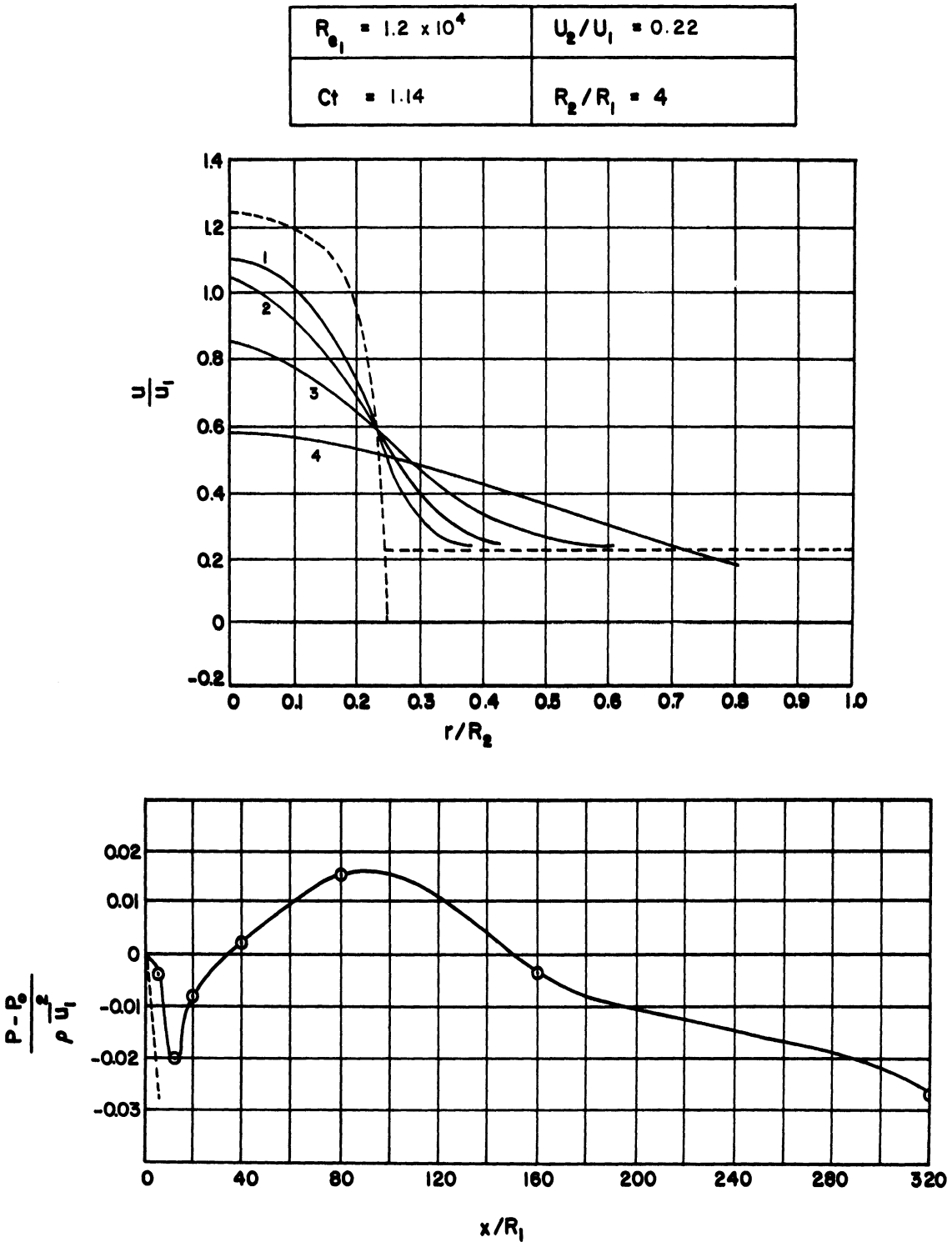

Figure 15. Experimentally Measured Velocity Profiles and Wall Static Pressures for the 1/2" Diameter Jet Tube.

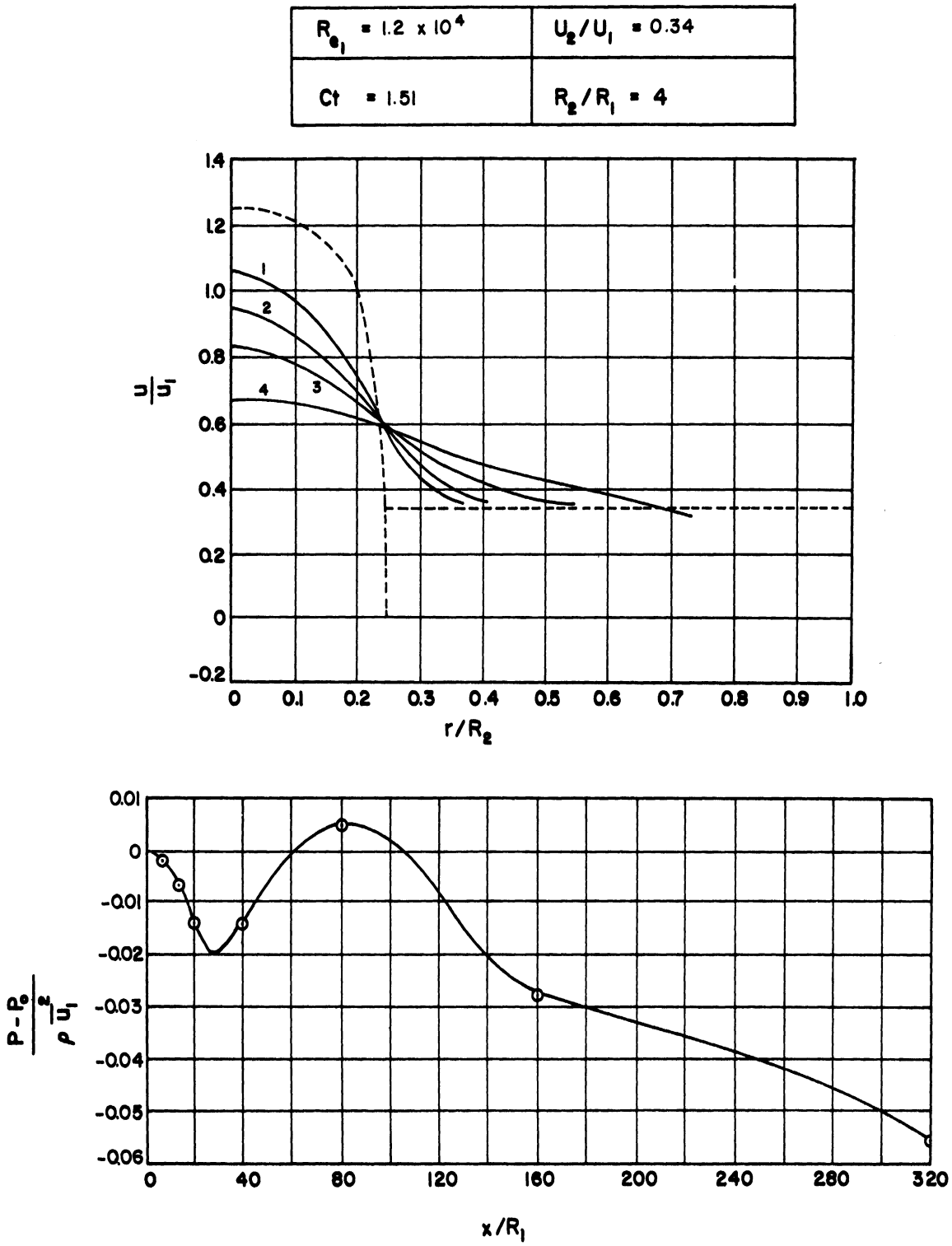

Figure 16. Experimentally Measured Velocity Profiles and Wall Static Pressures for the 1/2" Diameter Jet Tube.

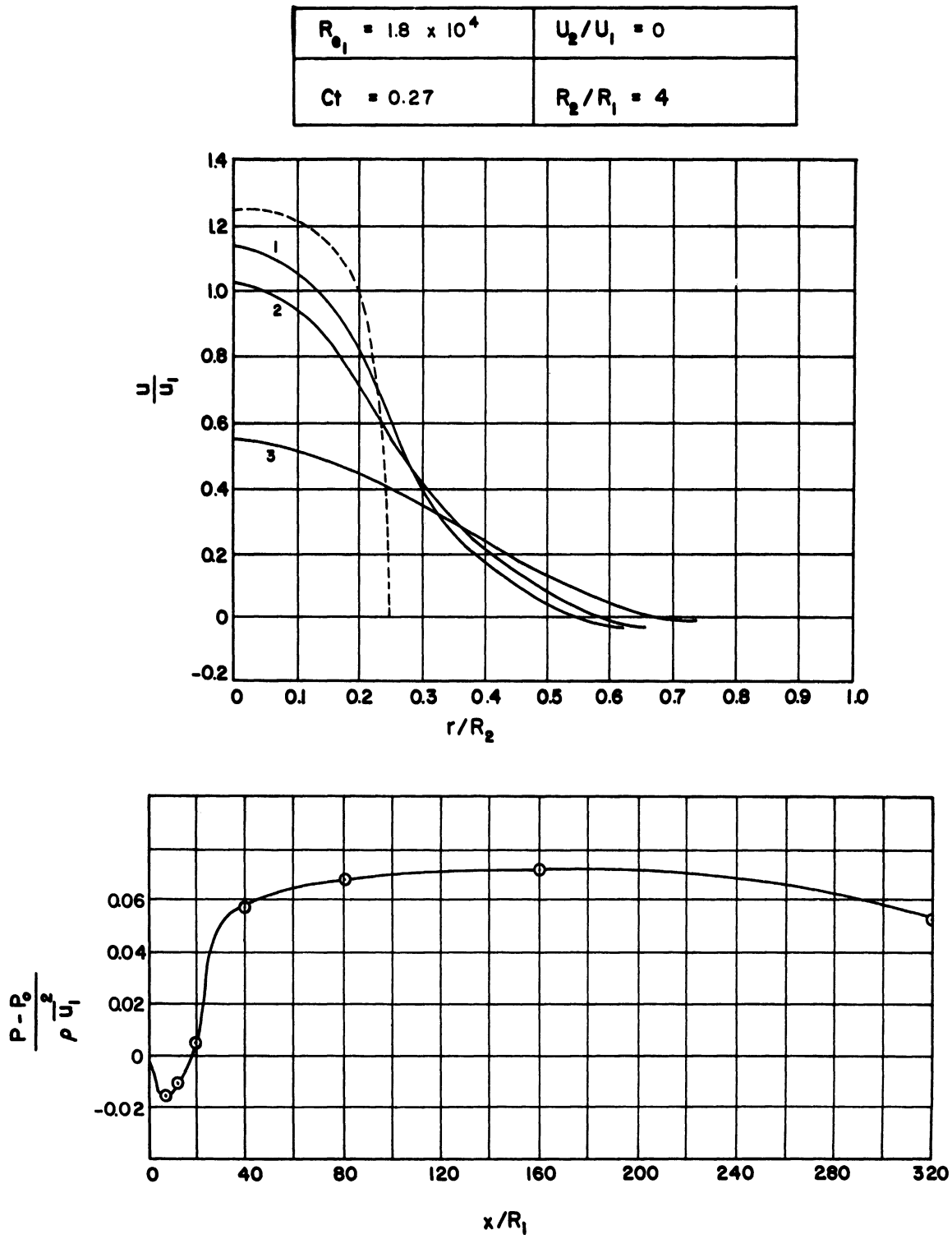

Figure 17. Experimentally Measured Velocity Profiles and Wall Static Pressures for the 1/2" Diameter Jet Tube.

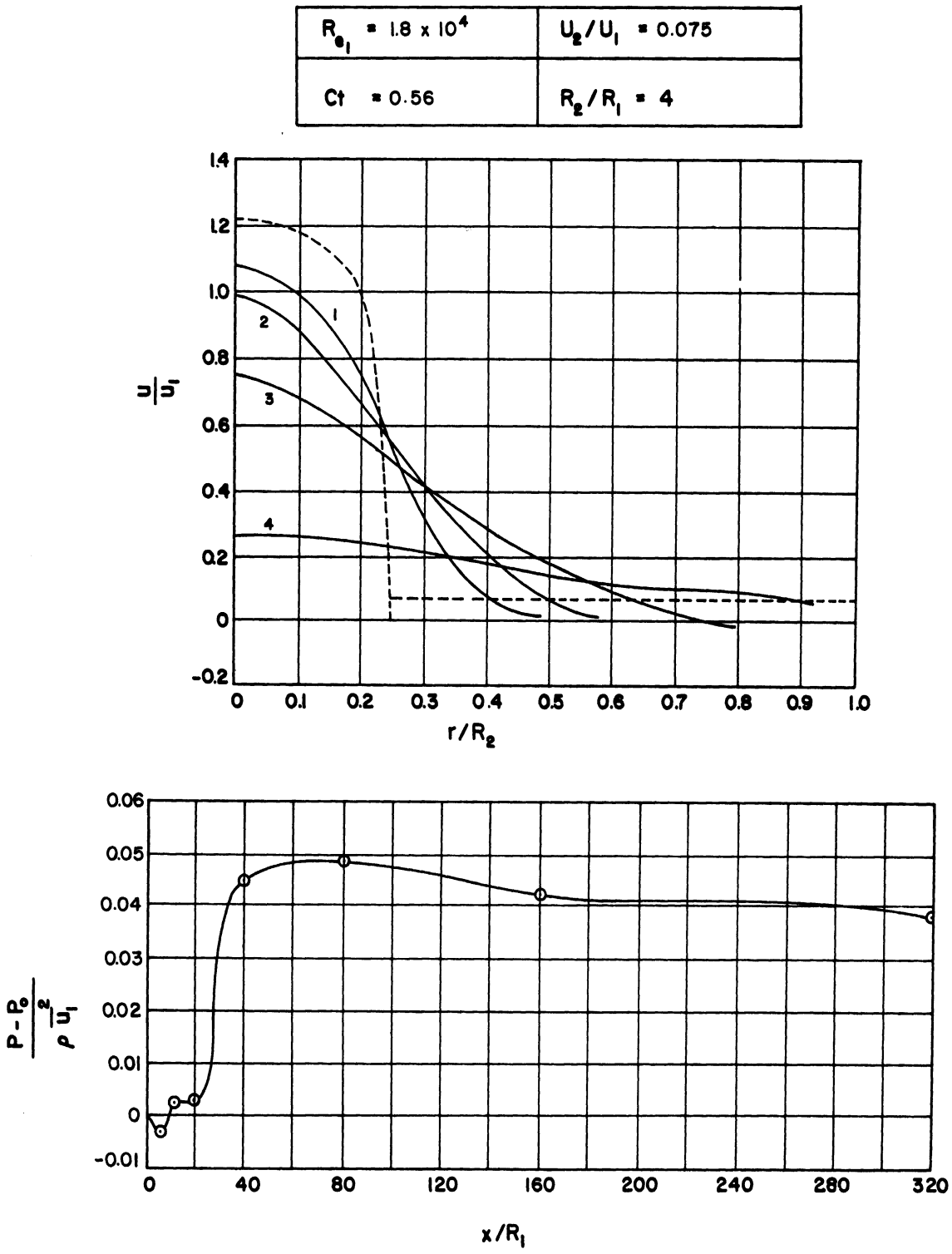

Figure 18. Experimentally Measured Velocity Profiles and Wall Static Pressures for the 1/2" Diameter Jet Tube.

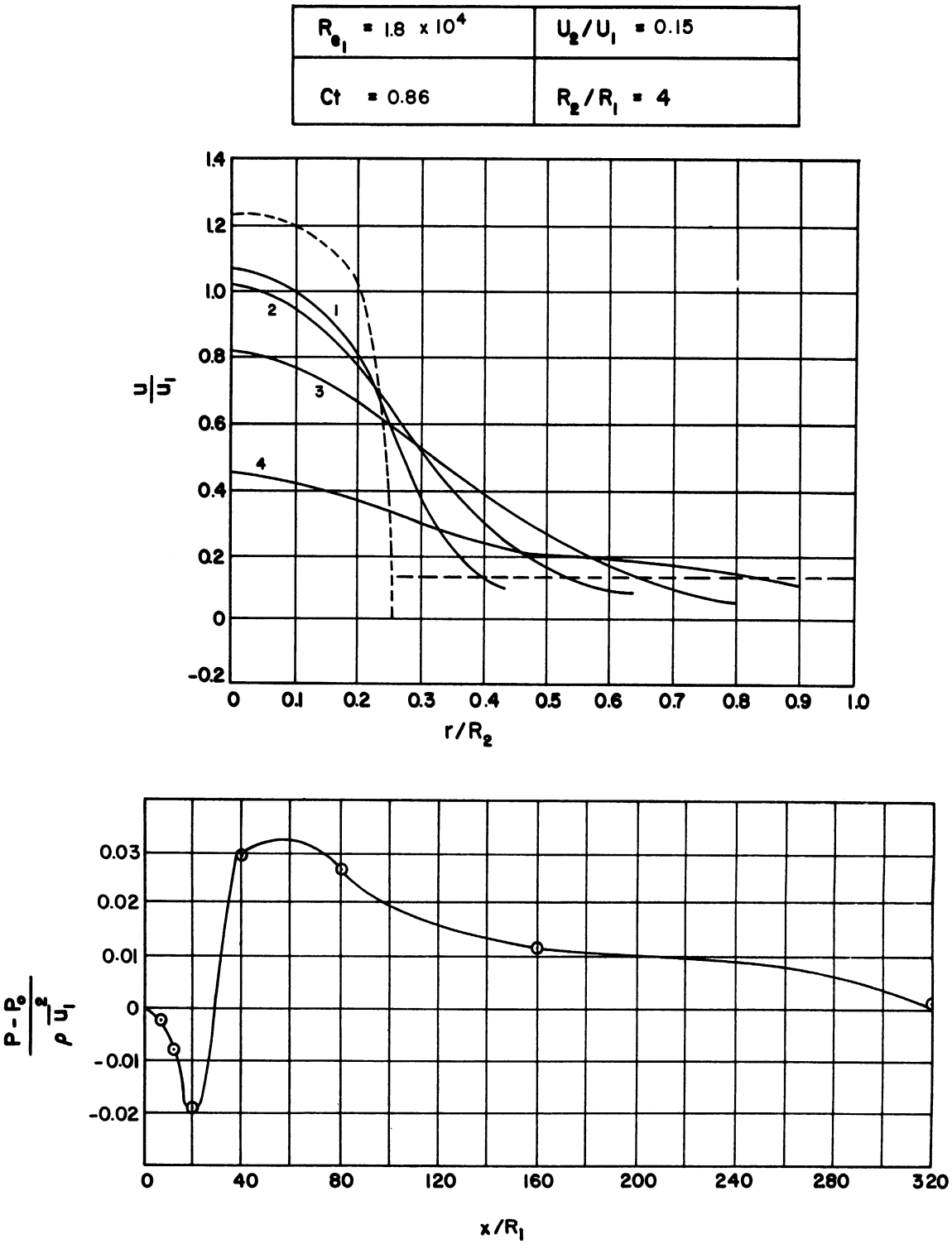

Figure 19. Experimentally Measured Velocity Profiles and Wall Static Pressures for the 1/2" Diameter Jet Tube.

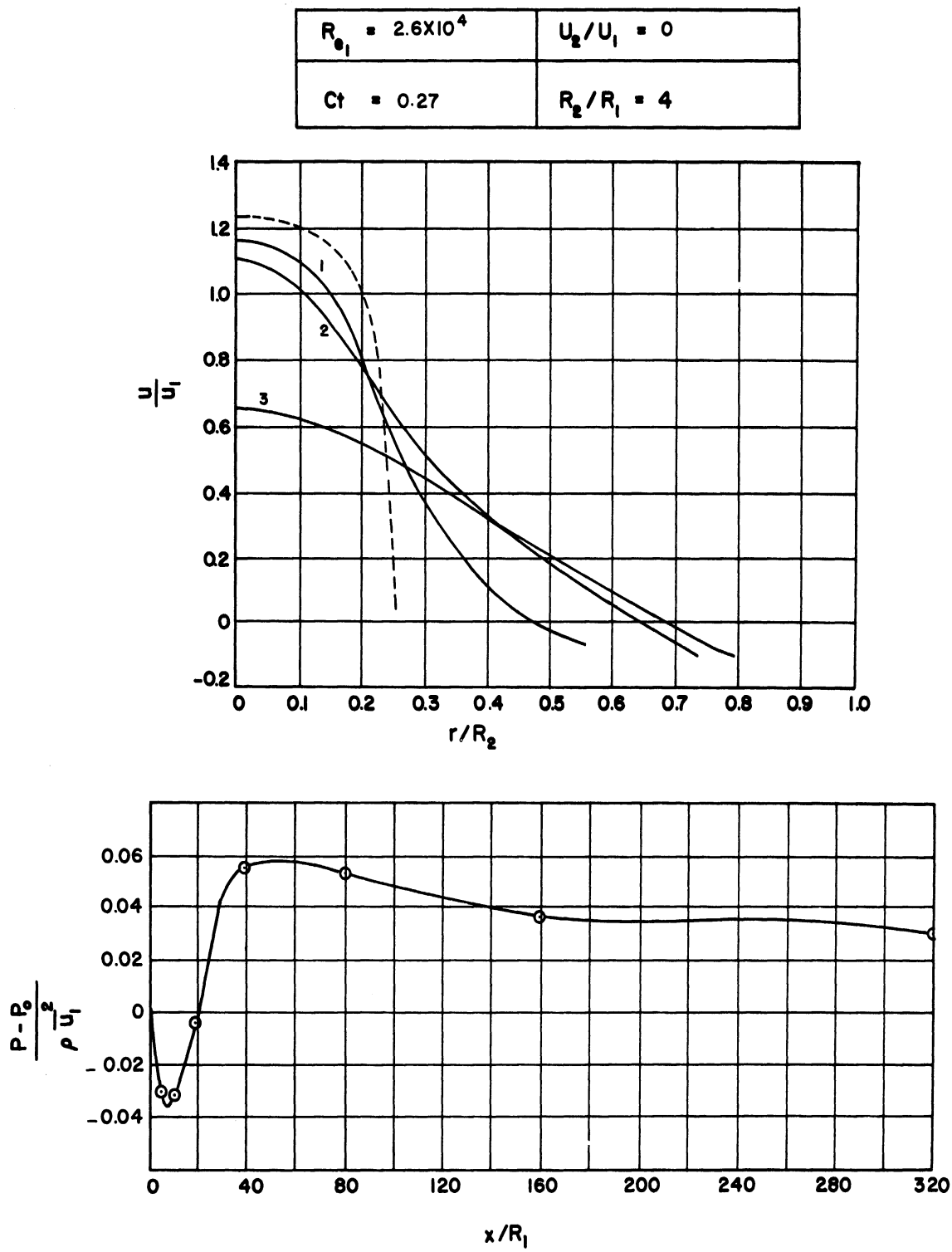

Figure 20. Experimentally Measured Velocity Profiles and Wall Static Pressures for the 1/2" Diameter Jet Tube.

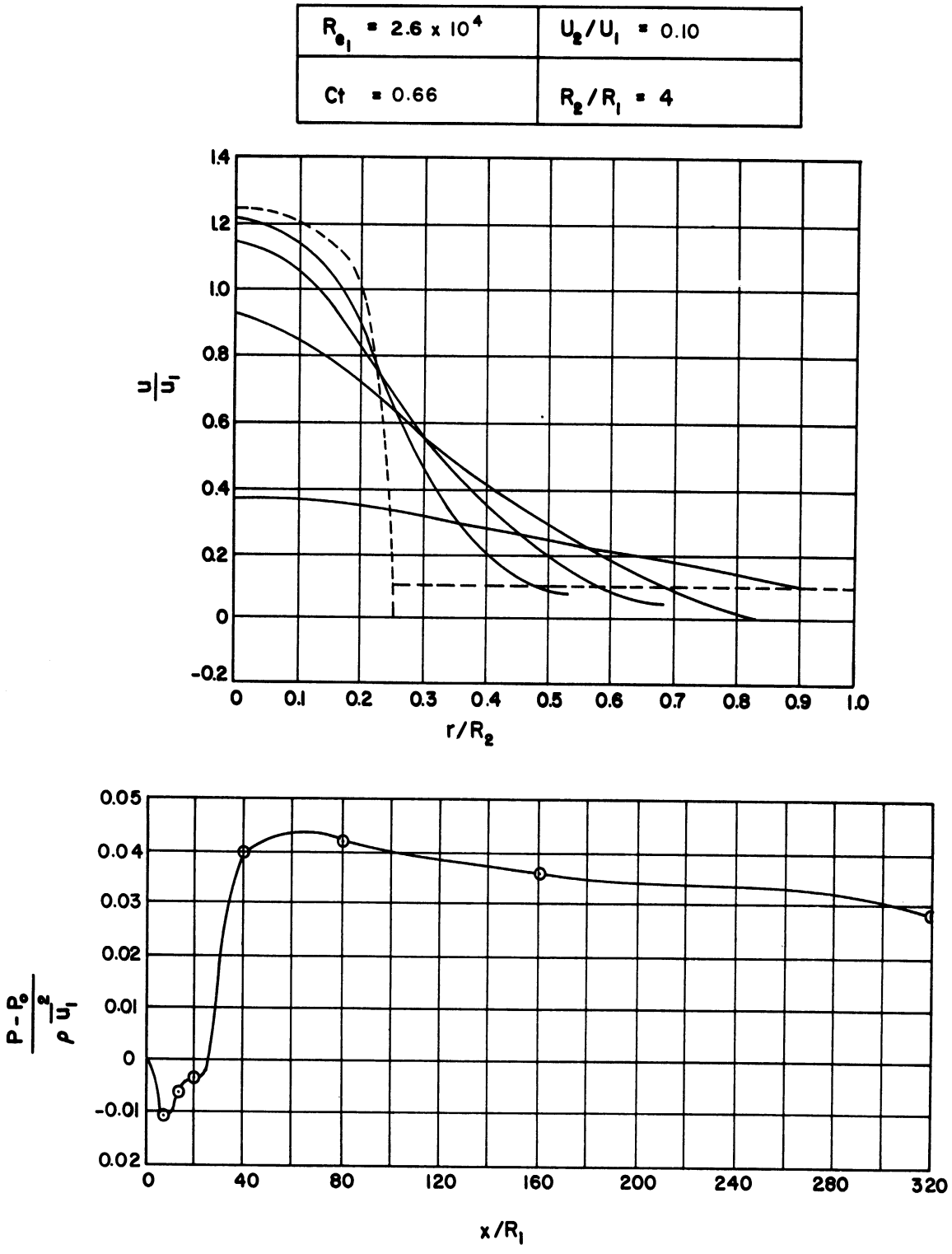

Figure 21. Experimentally Measured Velocity Profiles and Wall Static Pressures for the 1/2" Diameter Jet Tube.

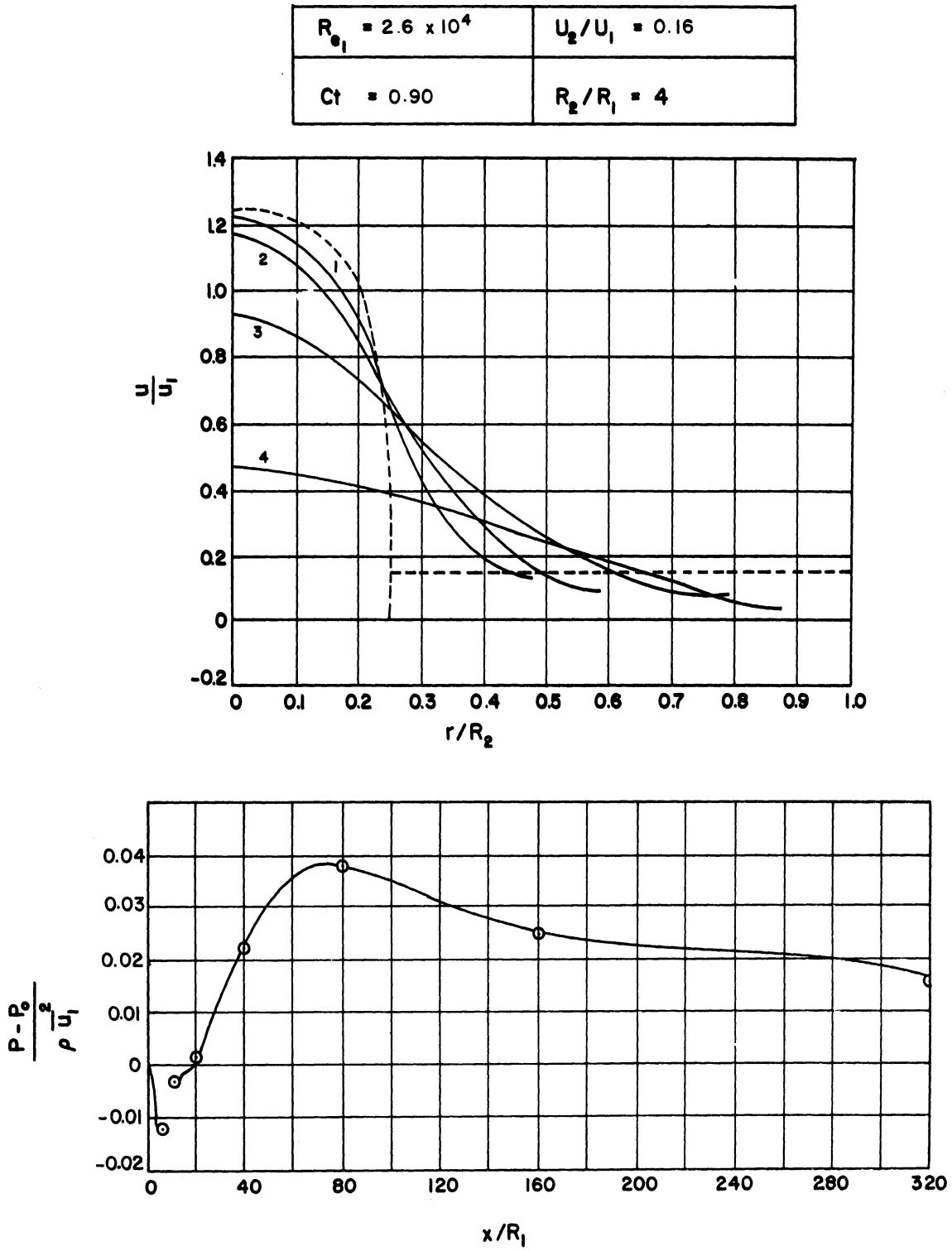

Figure 22. Experimentally Measured Velocity Profiles and Wall Static Pressures for the 1/2" Diameter Jet Tube.

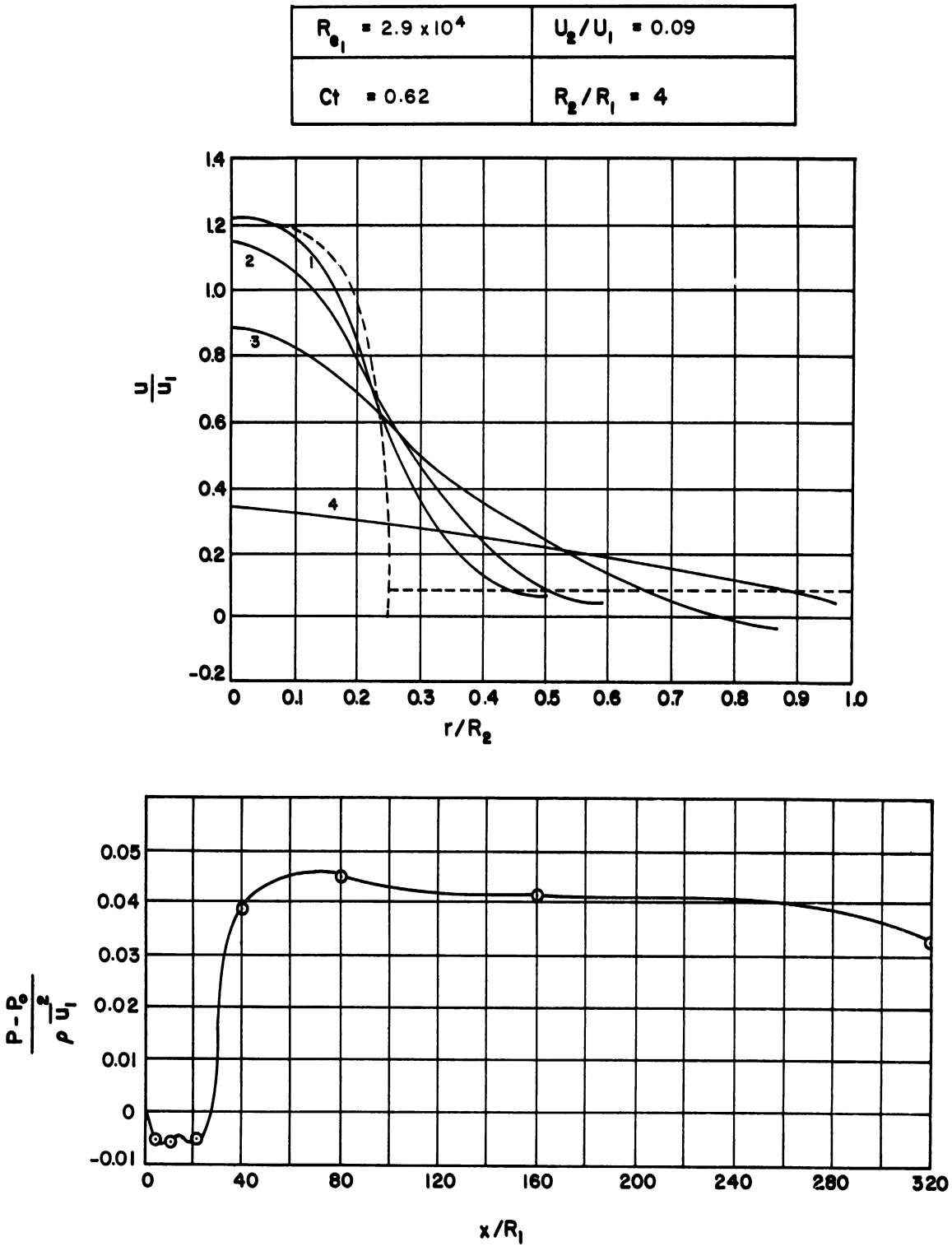

Figure 23. Experimentally Measured Velocity Profiles and Wall Static Pressures for the 1/2" Diameter Jet Tube.

TABLE III

MEASUREMENTS WITH 1" DIAMETER JET TUBE

Figure	$(Re)_1$	C_t	U_2/U_1	Recirculation Observed
24	14,000	1.21	0.47	
25		1.54	0.70	
26	28,000	0.50	-0-	X
27		0.71	0.12	X
28		0.88	0.24	
29	42,000	0.50	-0-	X
30		0.65	0.08	X

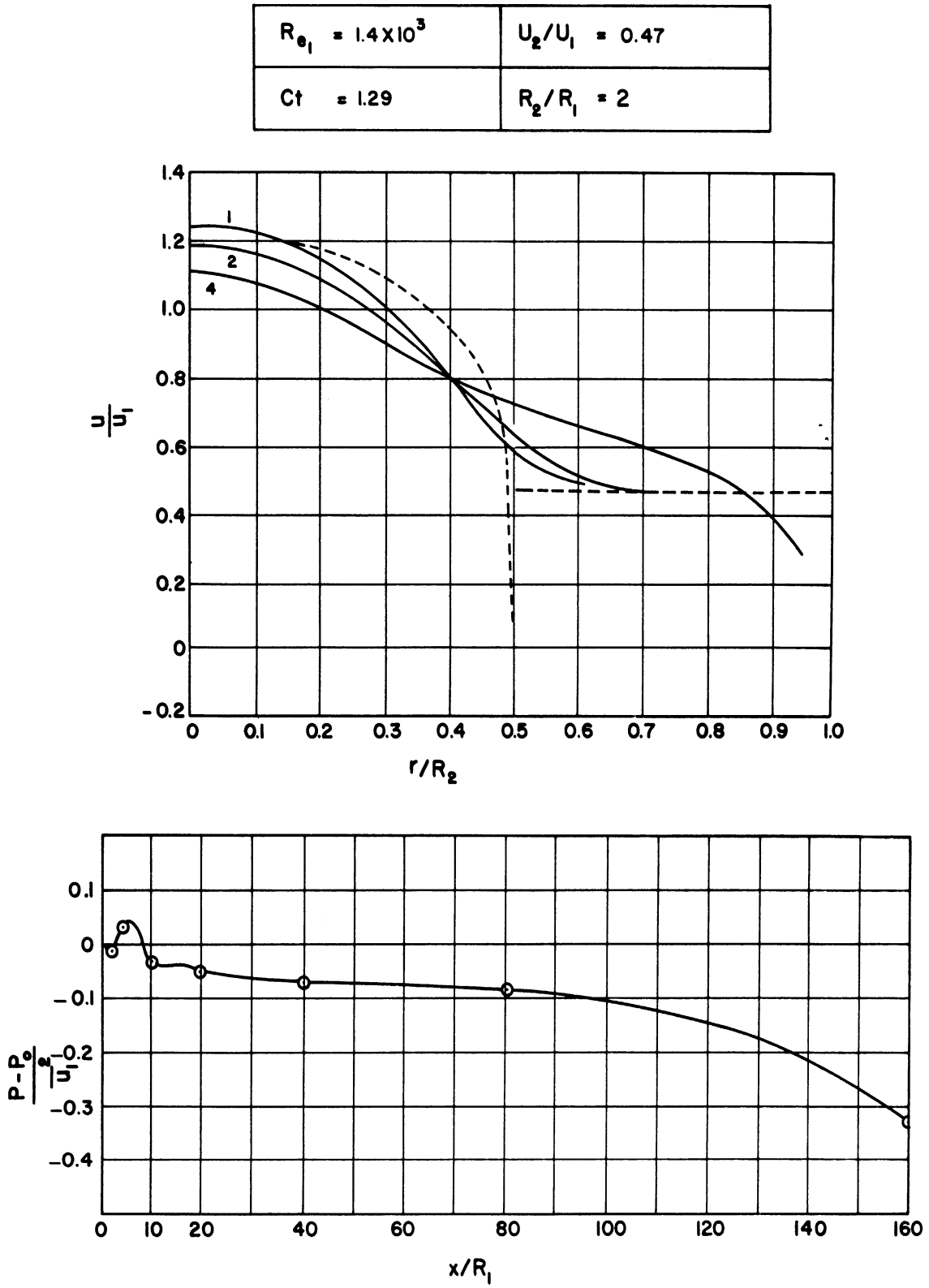

Figure 24. Experimentally Measured Velocity Profiles and Wall Static Pressures for 1" Diameter Jet Tube.

$R_{\theta_1} = 1.4 \times 10^3$	$U_2/U_1 = 0.72$
$Ct = 1.64$	$R_2/R_1 = 2$

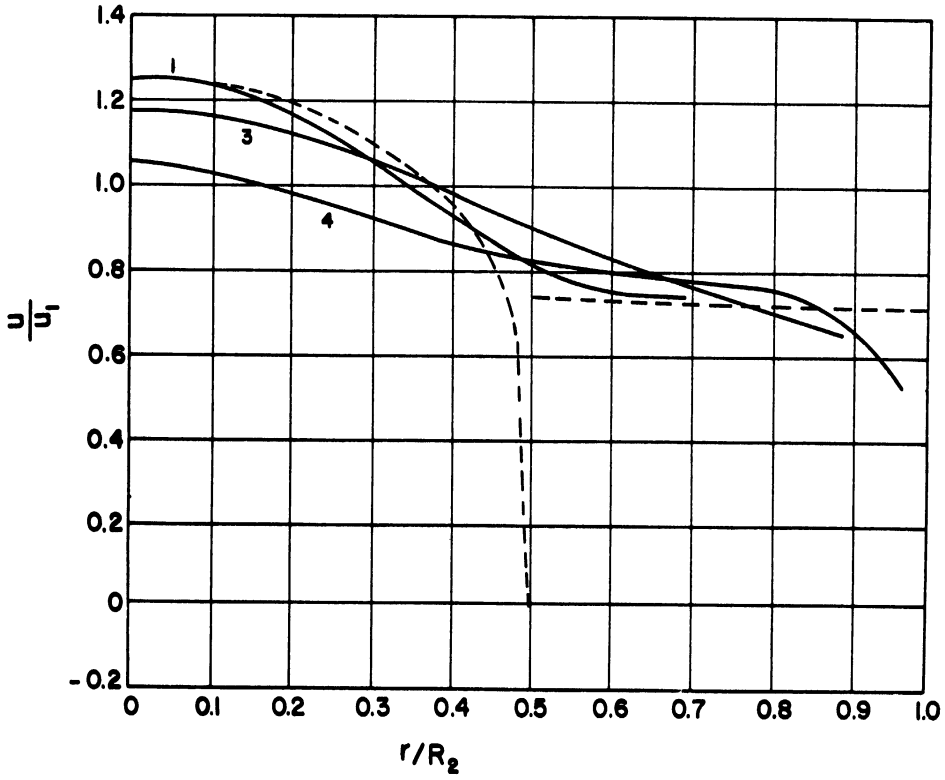

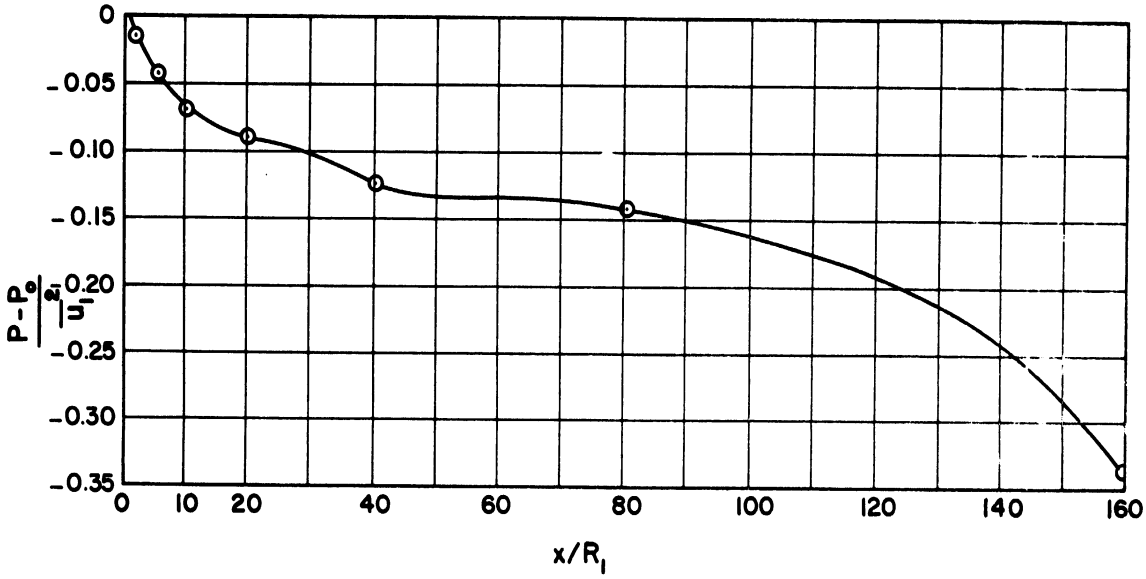

Figure 25. Experimentally Measured Velocity Profiles and Wall Static Pressures for 1" Diameter Jet Tube.

$R_{\theta_1} = 2.8 \times 10^3$	$U_2/U_1 = 0$
$Ct = 0.5$	$R_2/R_1 = 2$

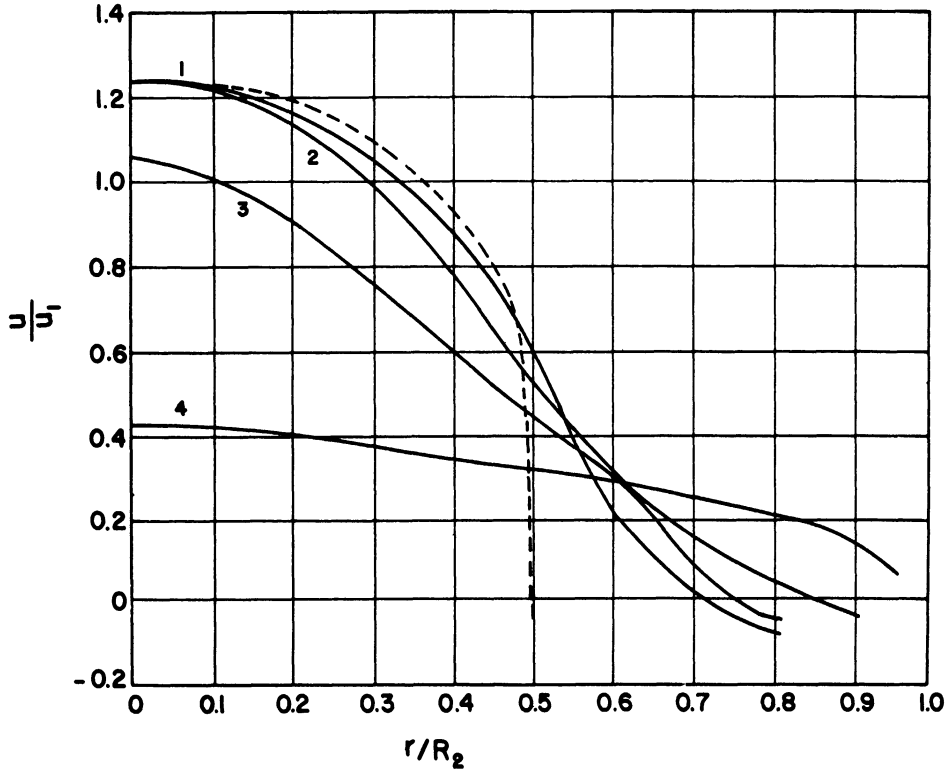

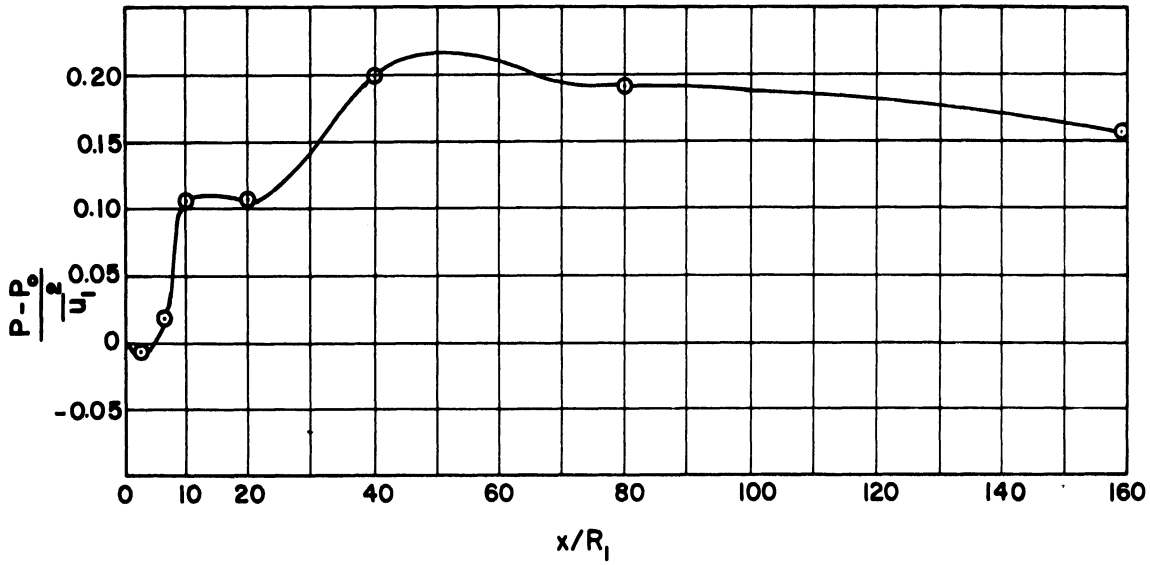

Figure 26. Experimentally Measured Velocity Profiles and Wall Static Pressures for 1" Diameter Jet Tube.

$R_{\theta_1} = 2.8 \times 10^3$	$U_2/U_1 = 0.12$
$Ct = 0.71$	$R_2/R_1 = 2$

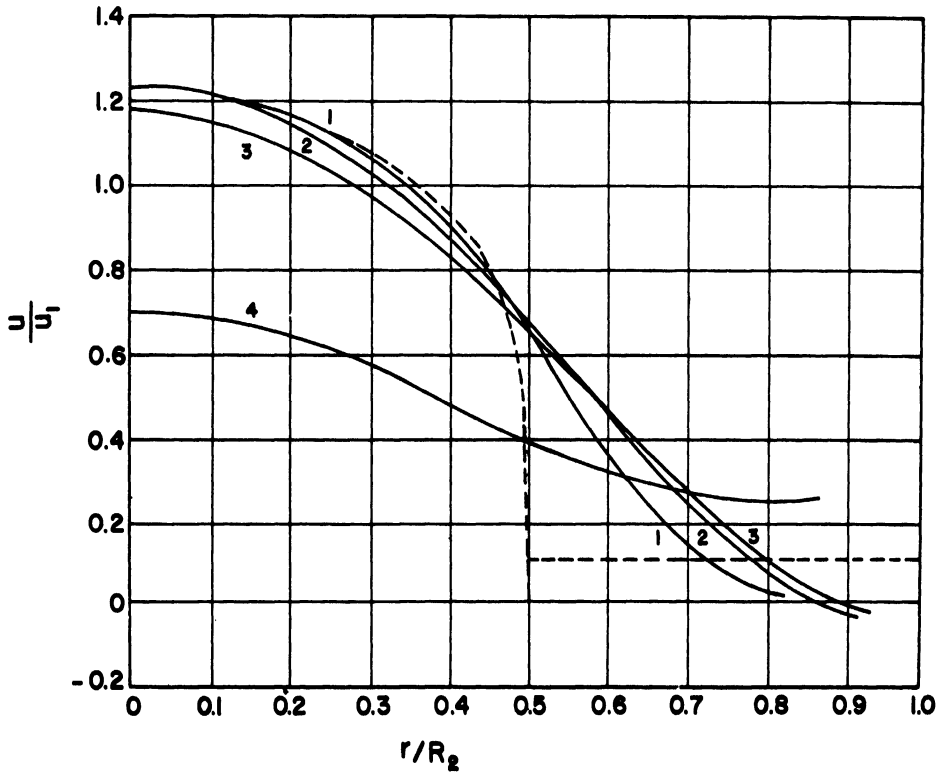

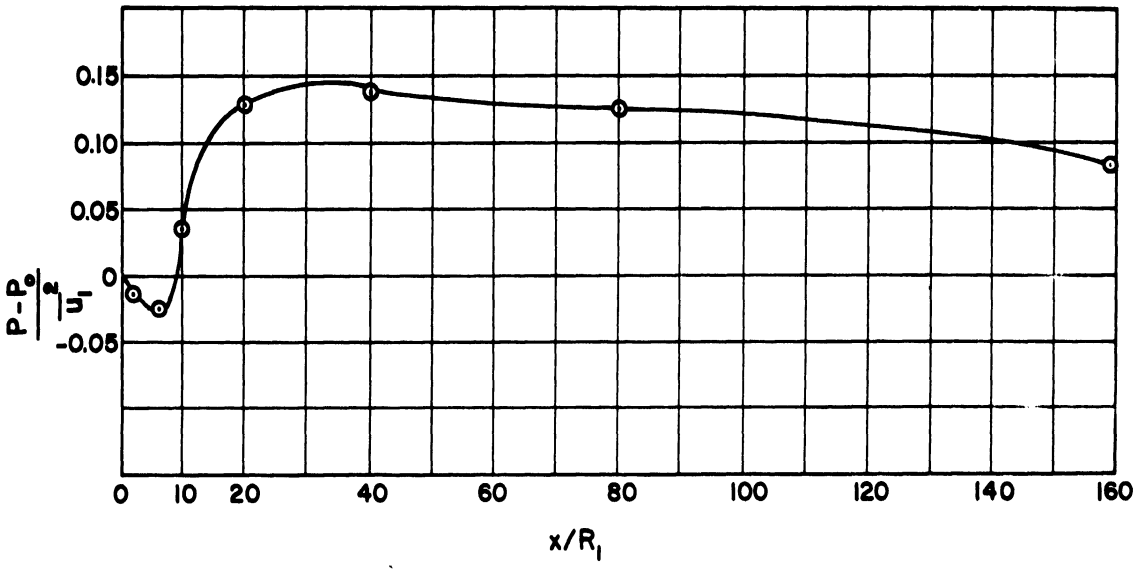

Figure 27. Experimentally Measured Velocity Profiles and Wall Static Pressures for 1" Diameter Jet Tube.

$R_{\theta_1} = 2.8 \times 10^4$	$U_2/U_1 = 0.24$
$Ct = 0.88$	$R_2/R_1 = 2$

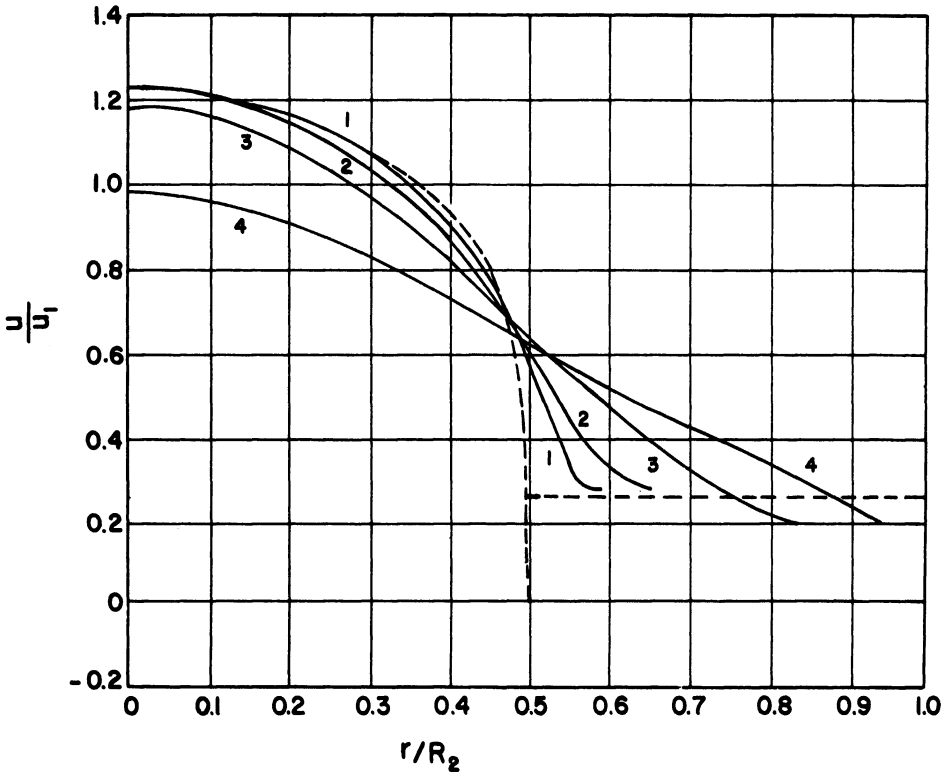

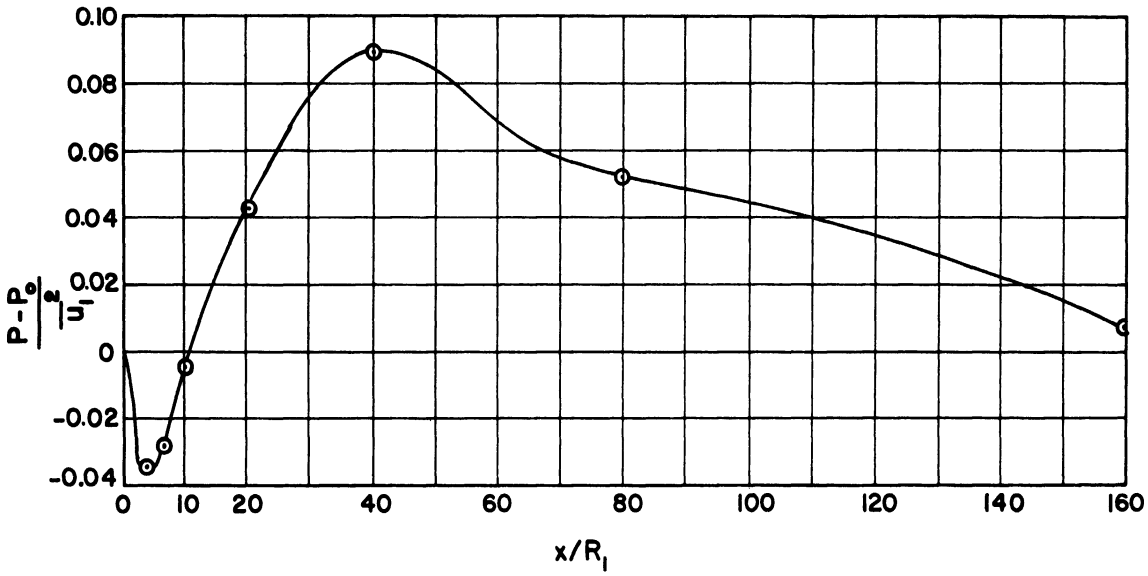

Figure 28. Experimentally Measured Velocity Profiles and Wall Static Pressures for 1" Diameter Jet Tube.

$R_{\theta_1} = 4.2 \times 10^3$	$U_2/U_1 = 0$
Ct = 0.5	$R_2/R_1 = 2$

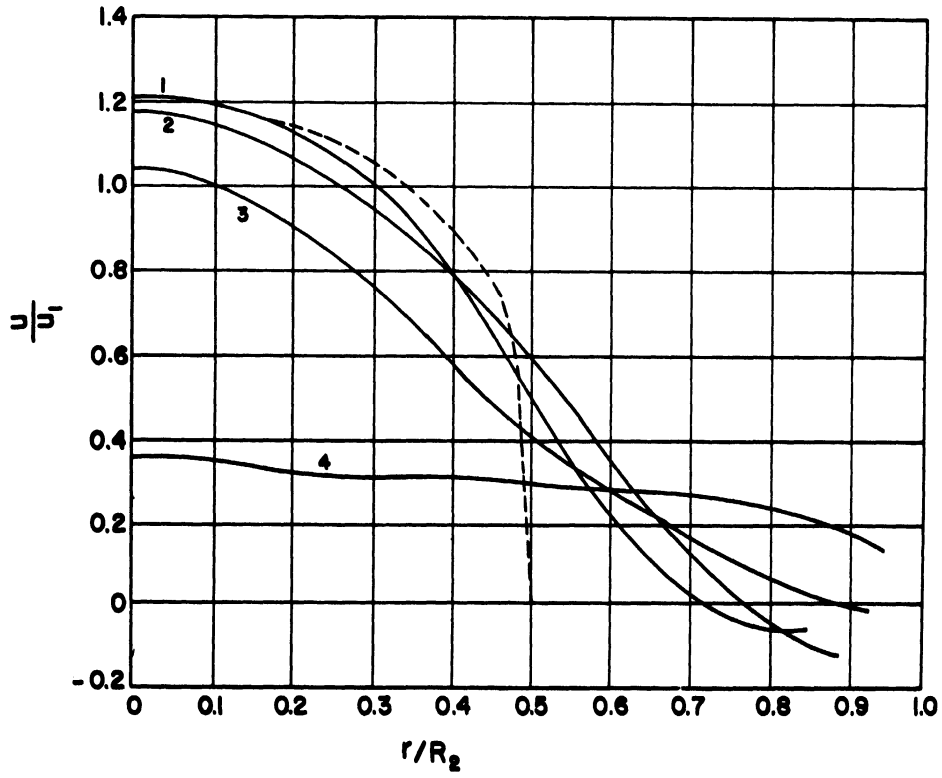

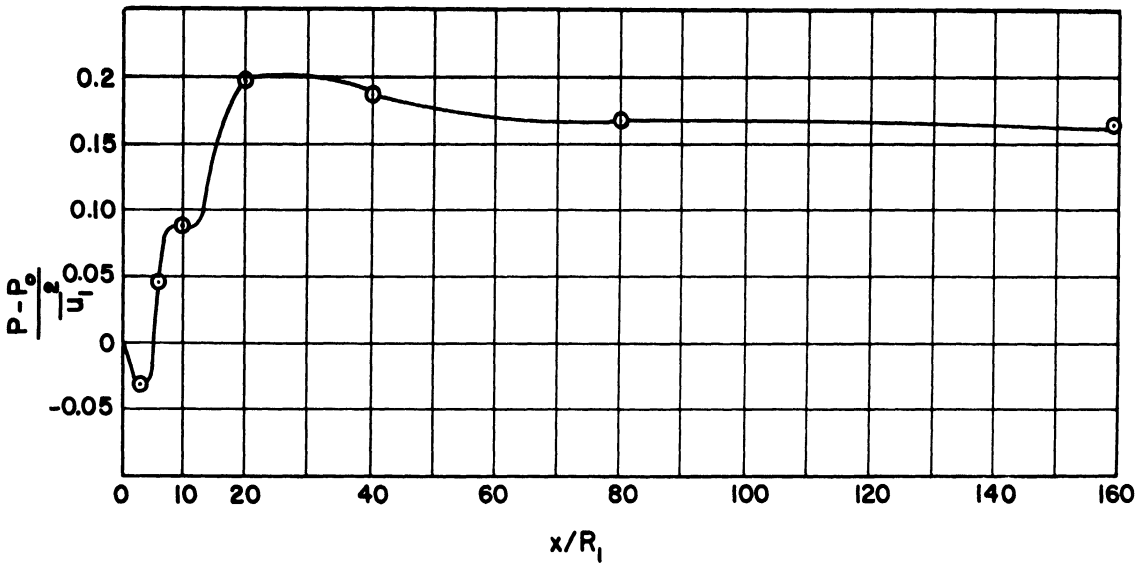

Figure 29. Experimentally Measured Velocity Profiles and Wall Static Pressures for 1" Diameter Jet Tube.

$R_{\theta_1} = 4.2 \times 10^3$	$U_2/U_1 = 0.08$
$Ct = 0.68$	$R_2/R_1 = 2$

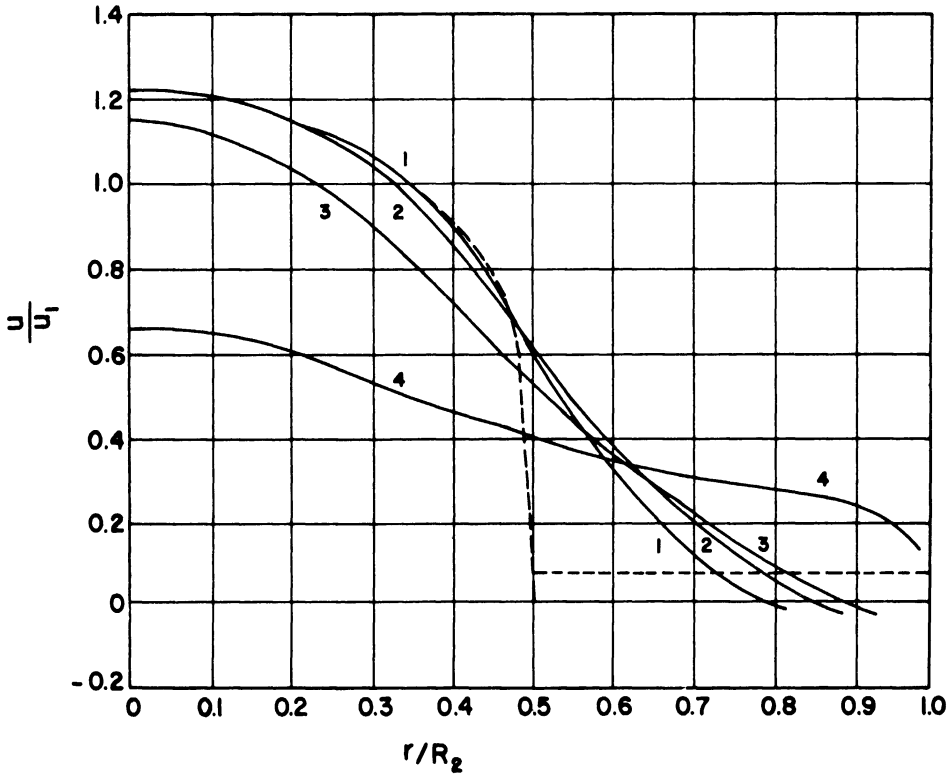

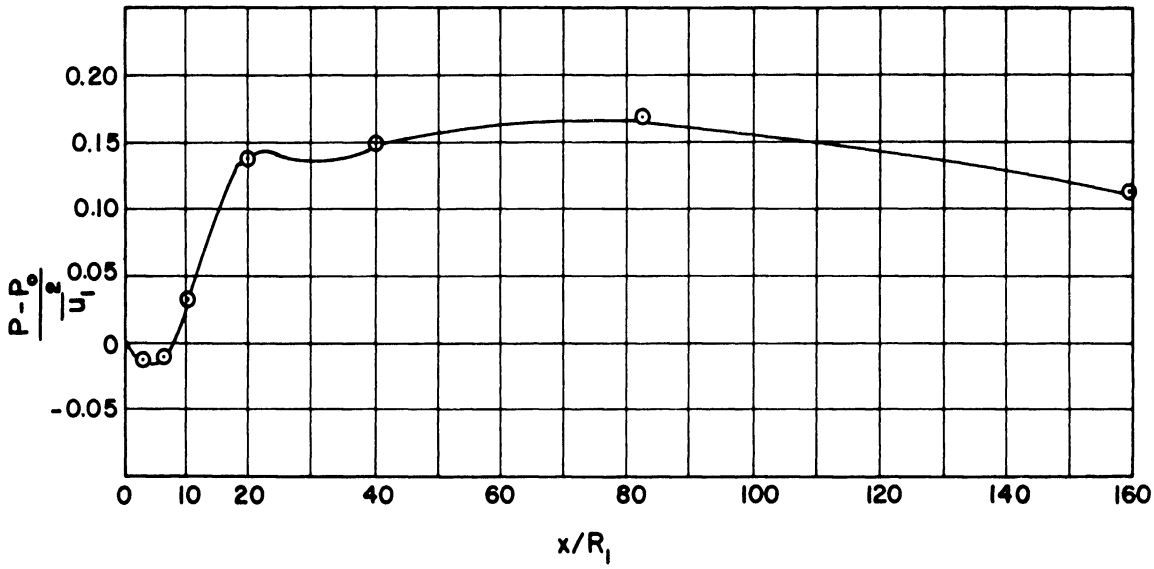

Figure 30. Experimentally Measured Velocity Profiles and Wall Static Pressures for 1" Diameter Jet Tube.

CHAPTER VIII

DISCUSSION OF EXPERIMENTAL RESULTS

A. Introduction

Several general conclusions may be drawn from examination of the experimental results. First, the length of the core divided by the jet tube radius varies considerably. Exact location of the point where the velocity on the axis begins to fall is not possible as traverses were made only at arbitrarily selected points, but it seems apparent that the jet Reynolds number has an important effect on the length defined above. This length will be referred to as the "core length". The dependency on jet Reynolds number is in contrast with the case of a jet with potential core for which, x_c/R_1 is always about 8 regardless of jet Reynolds number.

It may also be noted that in the experiments involving the smaller jet tube, some degree of similarity in the velocity profiles exists a short distance downstream of the point at which the core disappears. In Chapter III it was shown that such a similarity is a necessary condition for the validity of the Curtet similarity principle. For the larger jet tube, however, $(R_2/R_1 = 2)$ the jet spreads to the wall in such a short distance of the core disappearance that there is little opportunity for the flow to develop any similarity. Thus, these flows contain no region of developed jet flow of the type analyzed by Curtet.

After the jet reaches the wall, the positive pressure gradient decreases as the velocity redistributes itself, gradually approaching its fully developed tube flow configuration, until the loss in integrated

velocity head nearly offsets the wall shear stress so that the pressure levels out. Finally, the pressure gradient will approach its value for pipe flow. For all of the experimental studies, the Reynolds number, based on the mixing tube diameter and average velocity, was sufficient for turbulent flow.

B. Maximum Pressure Recovery

A characteristic of the flow in a confined jet which is of practical importance is the maximum pressure recovery obtained in the mixing tube. It is of interest to compare this maximum pressure rise with that predicted by an overall momentum balance. Consider the control volume shown in Figure 31:

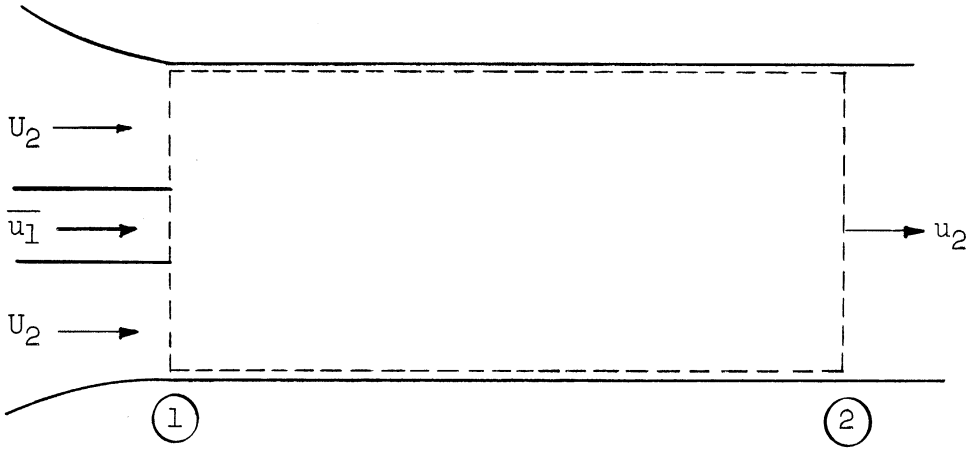

Figure 31. Control Volume for Momentum Balance.

In a manner analagous to that of the derivation of Equation (3.8), the overall momentum balance can be written as shown below if wall friction is neglected and the nonuniformity of the initial jet profile is

accounted for by the use of a momentum factor, β_1,

$$\frac{P_{max} - P_1}{\rho \bar{u}_1^2} = \beta_1 \left(\frac{R_1}{R_2}\right)^2 + \left(\frac{U_2}{\bar{u}_1}\right)^2 \left[1 - \left(\frac{R_1}{R_2}\right)^2\right] - \beta_2 \left\{\frac{U_2}{\bar{u}_1^2}\left[1 - \left(\frac{R_1}{R_2}\right)^2\right] + \left(\frac{R_1}{R_2}\right)^2\right\}^2 \qquad (8.1)$$

Streeter[50] has computed β_1 as a function of the tube friction factor, and his equation is:

$$\beta_1 = 1 + 4\gamma \qquad (8.2)$$

Employing the Blasius Equation (5.41) to compute $\gamma(Re)$, we find that for all of the conditions studied experimentally, β_1 does not differ greatly from 1.02. Using this value, the maximum pressure recovery was computed as a function of the velocity ratio for the two radius ratios employed. The results are shown in Figures 32 and 33 along with the values measured in the laboratory.

It may be noted that the maximum pressure rise corresponds to fairly small values of β_2. This indicates that when the jet reaches the wall, if β_2 has a value of the order of 1.8 as computed in Chapter II, then considerable additional pressure rise occurs after the mixing region fills the tube. Furthermore, nearly all of the available momentum is converted to pressure head before the wall shear begins to dominate the pressure development.

C. Recirculation

When $U_2 = 0$, as was the case in the experiments whose results are shown in Figures 17, 20, 26, and 29, the secondary flow is shut off

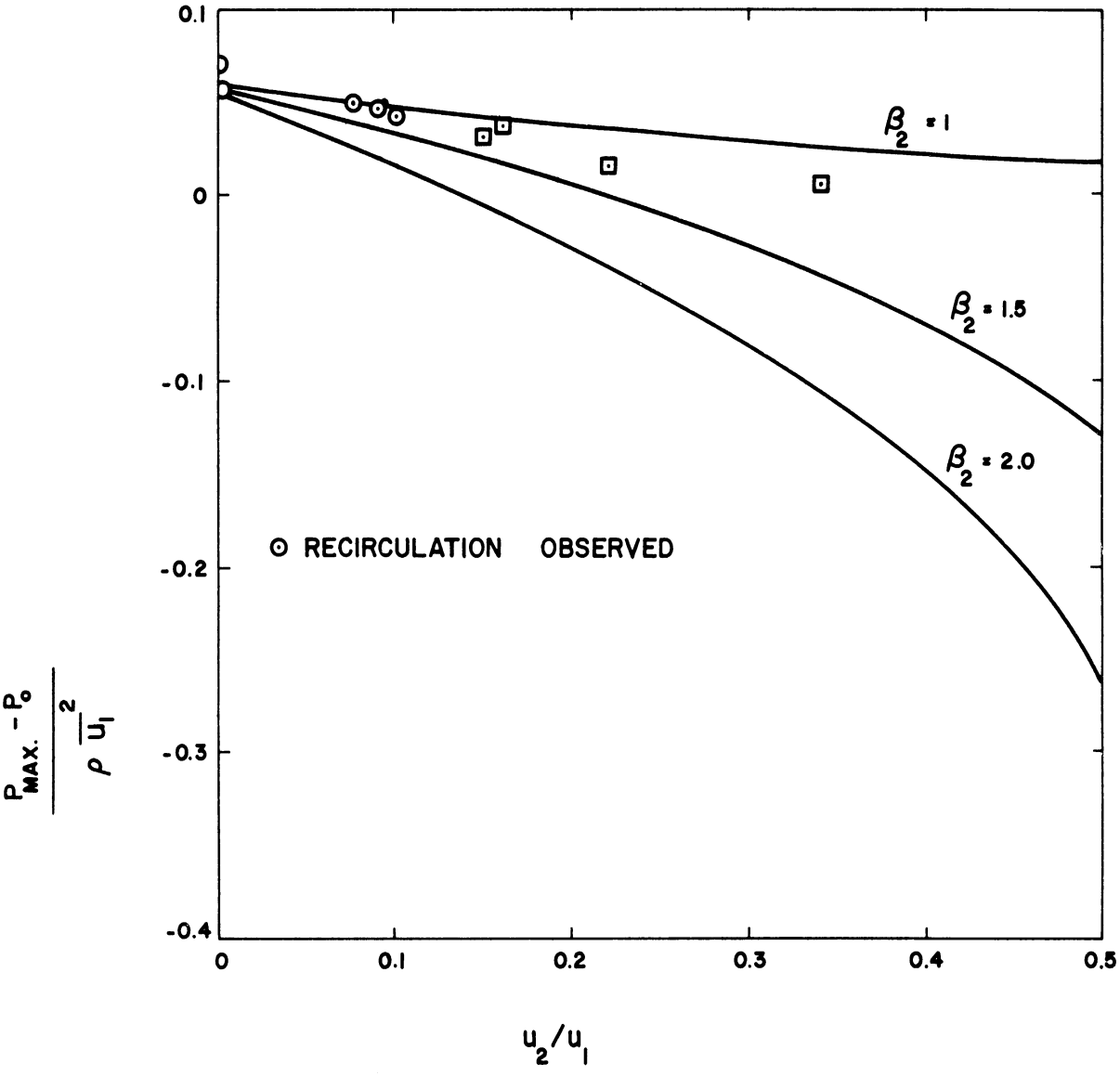

Figure 32. Maximum Pressure Rise 1/2" Jet Tube.

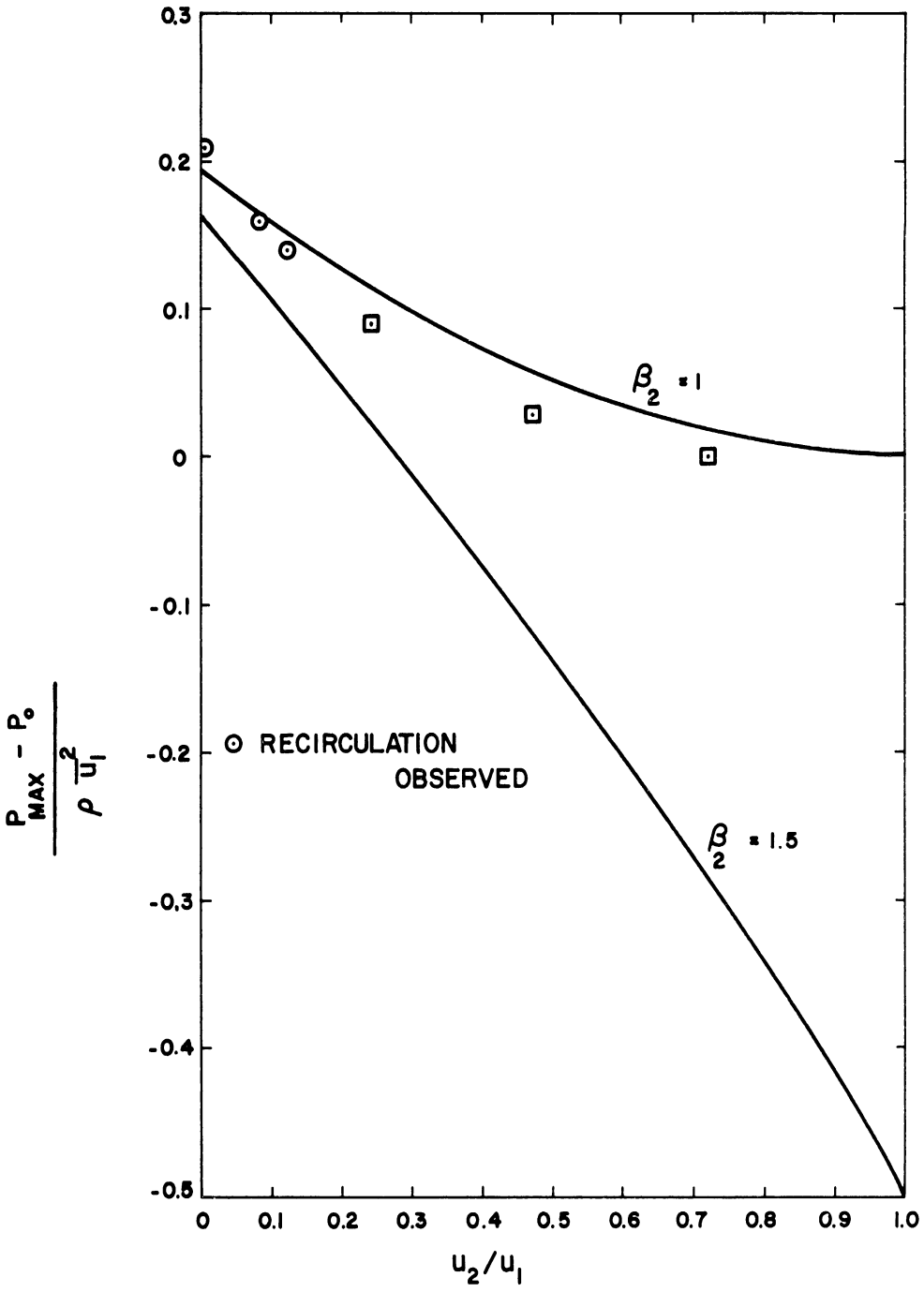

Figure 33. Maximum Pressure Rise 1" Jet Tube.

entirely so that all the fluid inducted into the mixing region must come from downstream. Thus, an eddy of recirculation stands at the entrance to the mixing tube. The maximum pressure rise for a given jet velocity occurs for this condition. If a small secondary flow is supplied, the eddy moves downstream into the mixing tube as seen in Figures 18, 20, 21, 23, 27, and 30. There is a dip in pressure corresponding to the rapid change in the velocity distribution associated with the eddy.

In Chapter III, criteria for the occurrence of an eddy of recirculation were discussed, and it was concluded that under certain circumstances, the similitude parameter of Curtet governs recirculation phenomena in confined jets. Due to the increased radial pressure gradient near the source, however, and the absence of a developed jet region for larger values of R_1/R_2, the system under study here deviates somewhat from the model upon which Curtet's developments were based. Nevertheless, the value of C_t, the Becker modification of the Curtet parameter, was computed for each of the flows studied experimentally. In order to illustrate the effect of Craya-Curtet number on recirculation over the range of Reynolds numbers involved, Figure 34 was prepared. It may be noted that a value of Ct of about 0.78 separates the recirculatory flows from those in which no eddy was observed. This compares with the value of 0.75 found by Becker[5] in his experiments with the more common confined jet system.

Thus, even for the larger jet tube, in which case strictly similar velocity profiles were not developed, the integrated momentum did not vary sufficiently from one test to another to destroy the

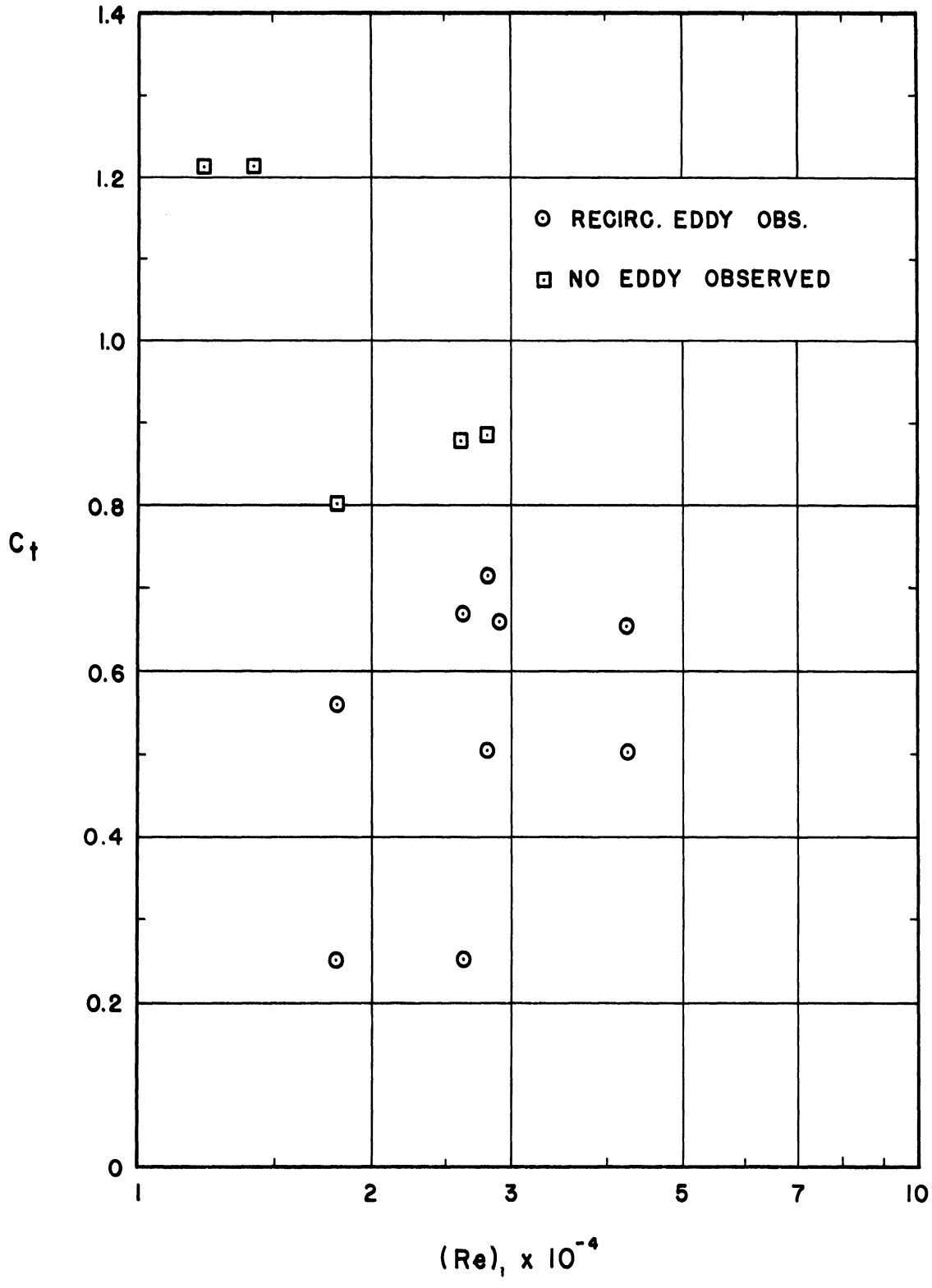

Figure 34. Dependency of Recirculation on Reynolds and Craya-Curtet Numbers.

general validity of the recirculation analysis given in Chapter III. A detailed experimental study aimed specifically at defining the conditions for the existence of an eddy of recirculation would no doubt indicate, however, that for larger ratios of jet tube to mixing tube diameter, the single parameter criteria would not be exactly valid.

CHAPTER IX

CALCULATIONS BASED ON MATHEMATICAL MODEL

A. Flow Near the Source

It was pointed out in Chapter IV that the analysis presented there of the flow in the initial regions of the jet was based on assumptions which are valid only for larger values of R_1/R_2. Since a computer program was prepared to solve the system of differential equations derived in that analysis, it was quite easy to obtain numerical results for a large number of conditions. For the smaller jet tube ($R_2/R_1 = 4.0$), the computed results were not in quantitative agreement with experimental results. For $R_2/R_1 = 2$, however, the computed results for the core region were in good agreement with experimental results.

The computed velocities at $x/R_1 = 3$ for conditions corresponding to the experimental results plotted in Figure 24 are shown in Figure 35. As pointed out above the agreement with experiment is good in this region prior to the decrease in the velocity on the axis. Since, in the case of the larger jet tube, a self-preserving structure or developed jet flow was never attained, the developments of Section 4, Chapter V could not be applied here.

In order to learn more about the behavior of the flow near the source, the length of the region for which the velocity on the axis is constant (the core length) was computed from the mathematical model for a variety of Reynolds numbers and velocity ratios. The results are shown in Figure 36. As might have been expected, the length of the core increases with jet tube Reynolds number and velocity ratio. It is also of

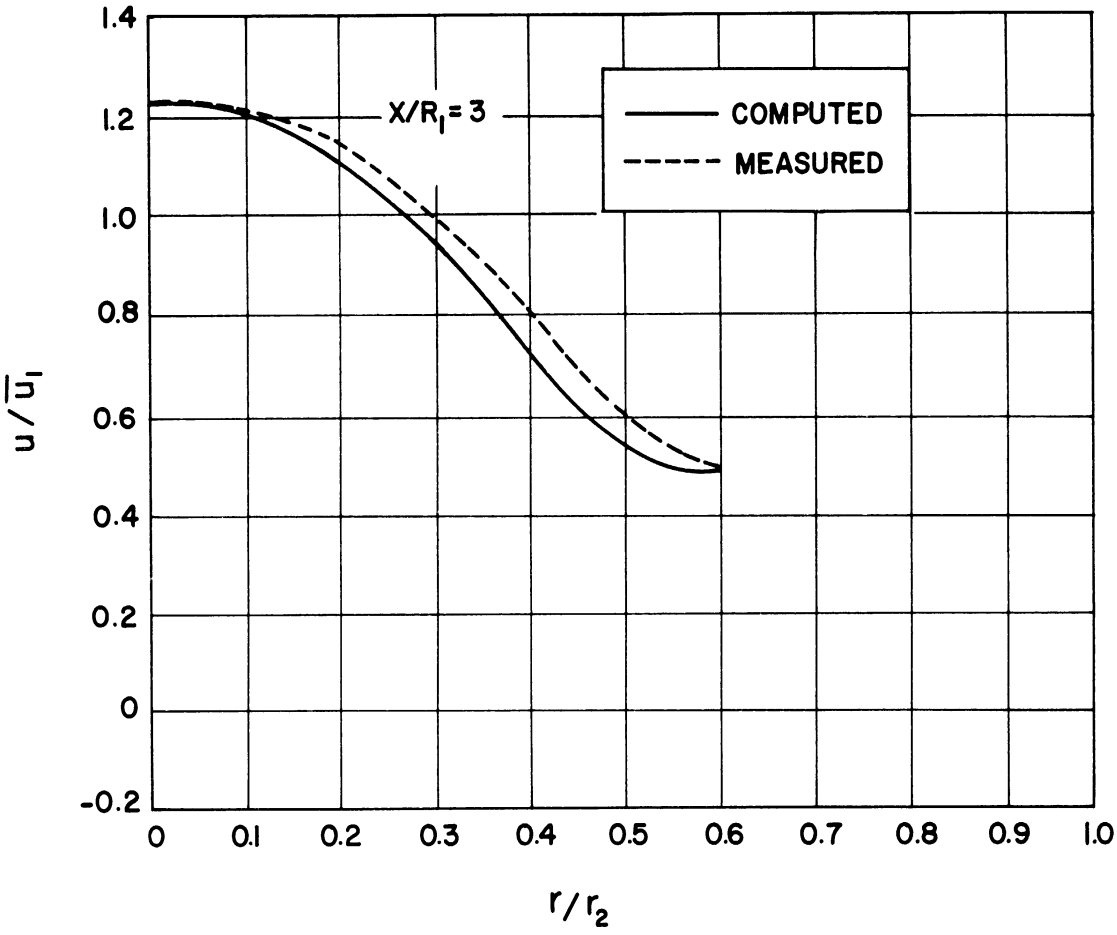

Figure 35. Computed Velocity Profile at $x/R_1 = 3$
Conditions of Figure 24.

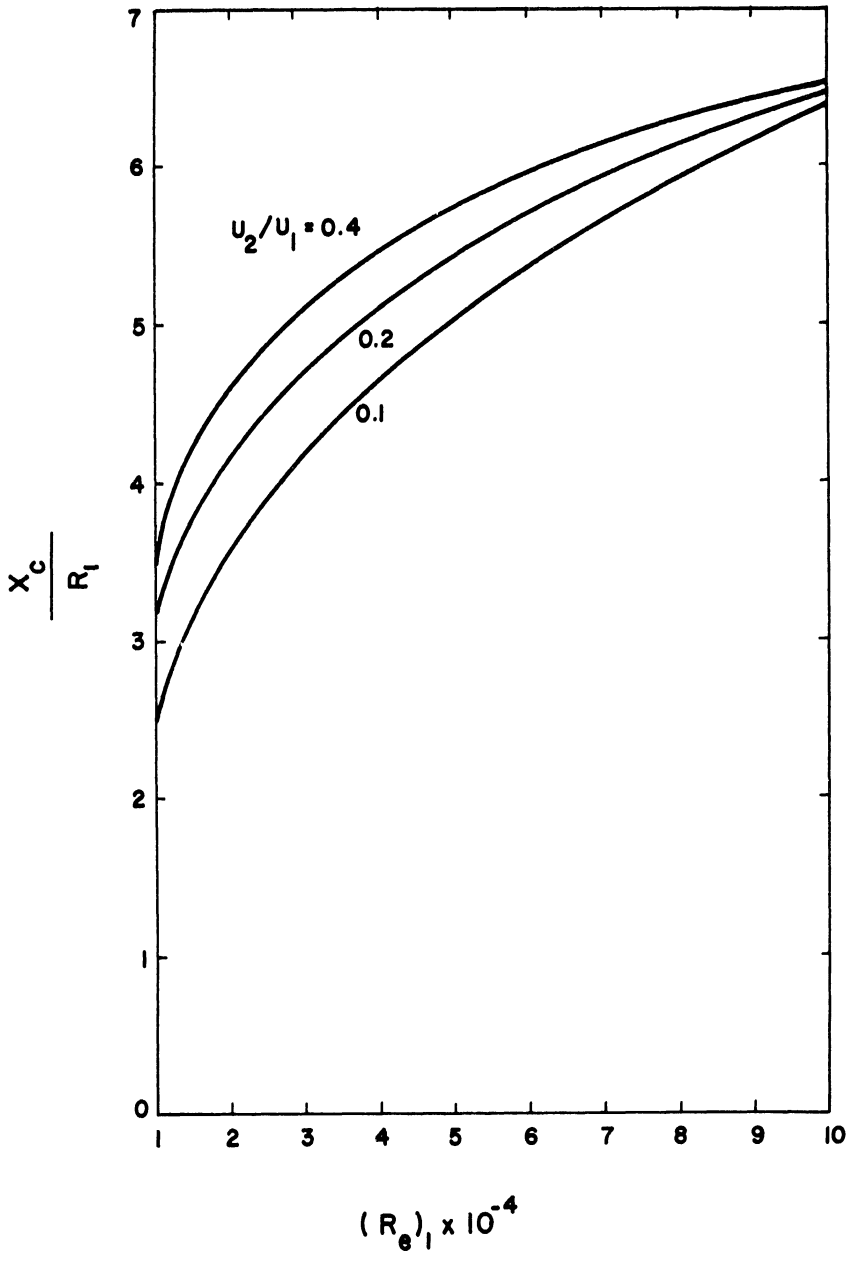

Figure 36. Predicted Length of Turbulent Core for $R_2/R_1 = 2$.

interest to note that the effect of the Reynolds number decreases significantly at high values of this parameter.

B. The Developed Jet

In the case of the smaller jet tube, the data seemed to indicate the possibility that the flow was self-preserving some distance from the source. These results were compared with those computed by means of the analysis of Section 4, Chapter V. For the conditions corresponding to the experimental results shown in Figure 16, the computed velocities are given in Figure 37. The value of the exchange coefficient, k, in the turbulent shear law (Equation (2.12)) which best fit the experimental data was 0.010. This is the same value obtained by Szablewski[51] for the transition region of a free jet with ambient velocity. It would appear, then, that although there occurs, in the case of the small jet tube, an approximate similarity in the velocity profiles downstream of the source, the turbulent structure is not the same as that in a free jet, for which k has been found to be 0.0158.

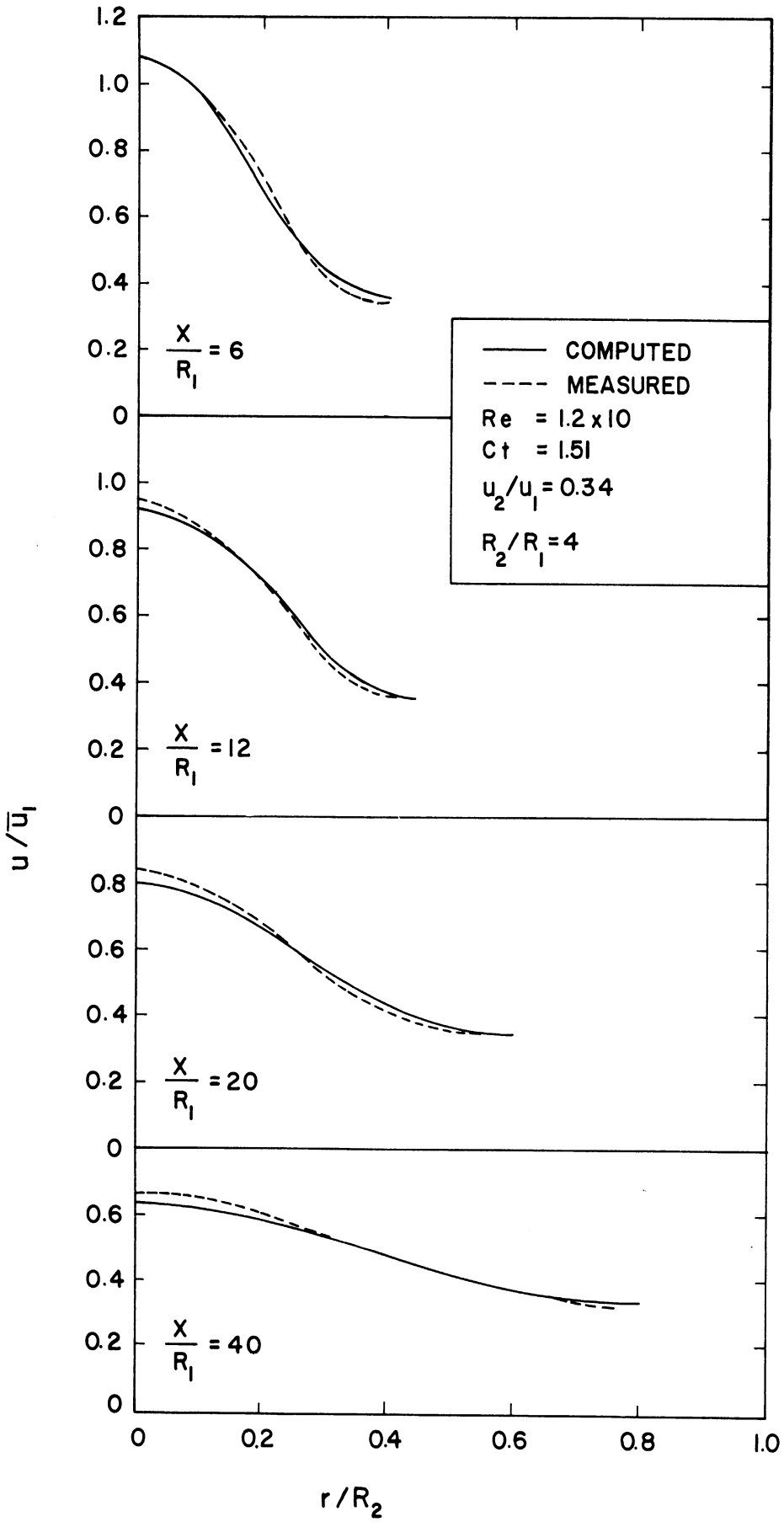

Figure 37. Comparison of Computed and Measured Velocities.

CHAPTER X

CONCLUSIONS

The confined circular jet with turbulent core has been studied by measuring impact tube pressure profiles and wall pressures in a water system. The characteristics of the flow near the jet entrance have been examined in some detail by the application of knowledge of turbulent structure of fully developed tube flow.

It was demonstrated mathematically that the pressure should fall, at first linearly, near the jet entrance. The wall pressure data seem to bear out this result, although hydrodynamic pressure measurement within the jet were not possible. The concept of an "equilibrium core", from which the linear pressure rise was predicted, also indicates that the velocity profile near the axis should not change for a short distance downstream of the entrance, and this result was verified experimentally.

The detailed mathematical analysis is more difficult than in the case of jets with potential core as fewer simplifications of the equations of motion are possible. Over a certain range of conditions, however, an approximate integral theory has been formulated on the basis of the concepts mentioned above. This theory permitted the calculation of several important characteristics of the flow.

As in the case of the jet with potential core, the velocity on the axis remains constant for some distance downstream of the entrance, although this distance was somewhat shorter in the case of the turbulent core, its specific value depending predominantly on the jet tube Reynolds number. The effect of the jet Reynolds number on the overall behavior of

the mixing flow was found to depend on several factors. For small ratios of jet tube to mixing tube diameters, the jet is allowed to develop into the kind of jet flow considered by previous workers. Under these circumstances, the usual assumption that the characteristics of the developed portion of the jet are independent of the nature of the source is approximately valid.

An exception to this independence in this case, however, is found in the boundary layer development at the wall. Thus, the pressure gradient in the first few diameters downstream of the entrance can have an important effect on the growth of the wall boundary layer, and the probability that it will separate or become turbulent. It was not possible to study the detailed development of the boundary layer with the equipment constructed for the jet studies. It may be noted, however, that in the case of the potential core, the pressure gradient is independent of the jet Reynolds number, whereas it is strongly dependent on the latter in the case of the turbulent core.

For larger ratios of jet tube to mixing tube diameters, the mixing region reaches the wall before the flow has an opportunity to develop fully, and there is little similarity to conventional confined jet flows.

It is demonstrated by a simple mathematical treatment, that recirculation can be predicted very simply, if the assumptions made by previous workers in establishing a model for the flow are valid. Under these circumstances, the occurrence of recirculation is shown to be uniquely dependent on the similitude parameter suggested by Curtet on the basis of a detailed analysis of the equations of motion, and later

derived by Becker from a more general development. The development of the wall boundary layer, and the nonsimilarity of the reduced velocity profiles in the mixing region, however, can destroy the uniqueness of this correspondence. Thus, if the boundary layer remains thin, and the jet is permitted to attain its fully developed configuration before recirculation begins, the Curtet criterion for recirculation is nearly an exact one. The deviation of the flow from these restricted conditions, of course, makes it a very complex problem in which the development of the flow at any cross section depends on the history of the fluid as well as on the local turbulence characteristics. Under these circumstances the principles of self-preservation and similarity of structure are not operable. Nonetheless, it may be concluded that the Curtet similitude analysis takes into account the most important features of the momentum exchange, and can supply information of interest even in cases where his model is not strictly valid.

In general, the jet with turbulent core is found to develop more rapidly at first since the turbulent stresses and radial pressure gradient are greater near the entrance. If the mixing tube diameter is sufficiently large the jet develops into a flow similar to that found downstream of a potential core.

The confined jet is of some interest in the design of jet pumps. The jet pump consists of several components, however, which require individual attention. These are: a nozzle, secondary or induced flow entrance chamber, a mixing tube, and a diffuser. The overall design of such a device depends on an optimization of the complete assembly. Thus, the coupling between the performance of the various components is of prime

importance. For example, the mixing tube may be designed for a maximum pressure recovery with a given nozzle and secondary entrance configuration. The resulting velocity distribution at the exit of the mixing tube, however, may be a poor one from the standpoint of diffuser performance. A great deal of fundamental research on the detailed flow in all the components will be necessary before a jet pump may be designed on a rational basis.

CHAPTER XI

SUGGESTIONS FOR FURTHER STUDIES

There are several interesting aspects of the flow in a circular confined jet which should be studied in more detail. One is a possible manifestation of the instability problem and resulting periodic flows found by Curtet in his studies of plane jets. There are several possible modes for such phenomena in circular jets. The jet may sweep around the mixing tube producing a spiral trail of vortices, or it might flip from one side of the tube to the other.

Another important feature of confined jets is the development of the wall boundary layer. This is the unique situation where an axially symmetric internal boundary layer grows in a pressure gradient which may be either positive or negative. The effect of pressure gradient, wall roughness, and entrance shape on the boundary layer growth, separation and transition could be studied visually by means of dye addition in liquids or by means of velocity measurements in larger systems.

A third area of practical interest is the mixing of two different liquids. Both velocity and composition profiles would be necessary for an analysis of the flow. Two distinct Reynolds numbers would be involved.

APPENDIX A

INTEGRATION OF CONVECTION TERMS IN EQUATION (4.1)

For convenience, let $\tau = -\overline{u'v'}\,\rho$. Then Equation (4.1) may be written as follows:

$$u\frac{\partial u}{\partial x} + v\frac{\partial u}{\partial r} = -\frac{1}{\rho}\frac{\partial p}{\partial x} + \frac{1}{r}\frac{\partial}{\partial r}\left(r\,\tau/\rho\right) \tag{A-1}$$

Integrating between two limits, r_1 and r_2 which may be functions of x:

$$\int_{r_1}^{r_2} u\frac{\partial u}{\partial x}\,r\,dr + \int_{r_1}^{r_2} v\frac{\partial u}{\partial r}\,r\,dr = -\frac{1}{\rho}\int_{r_1}^{r_2}\frac{\partial p}{\partial x}\,r\,dr + \int_{r_1}^{r_2}\frac{\partial}{\partial r}\left(r\,\frac{\tau}{\rho}\right)dr \tag{A-2}$$

The last term is obviously:

$$\int_{r_1}^{r_2}\frac{\partial}{\partial r}\left(r\,\frac{\tau}{\rho}\right)dr = \frac{r_2\,\tau(r_2) - r_1\,\tau(r_1)}{\rho} \tag{A-3}$$

The integrals of the convection terms may be put into simpler form which are analagous to the terms appearing in the boundary layer momentum integral equation.

First, from the continuity equation, an expression for v is:

$$v = -\frac{1}{r}\int_0^r \frac{\partial u}{\partial r}\,r\,dr \tag{A-4}$$

Inserting this expression for v in the second integral of Equation (A-2), and integrating by parts:

$$-\int_{r_1}^{r_2}\frac{\partial u}{\partial r}\int_0^r \frac{\partial u}{\partial x}\,r\,dr = \int_{r_1}^{r_2} u\frac{\partial u}{\partial r}\,dr - \left[u\int_0^r \frac{\partial u}{\partial r}\,r\,dr\right]_{r_1}^{r_2}$$

So, the second integral becomes:

$$\int_{r_1}^{r_2} v\frac{\partial u}{\partial r}\,r\,dr = \int_{r_1}^{r_2} u\frac{\partial u}{\partial x}\,r\,dr + u(r_1)\int_0^{r_1}\frac{\partial u}{\partial x}\,r\,dr - u(r_2)\int_0^{r_2}\frac{\partial u}{\partial x}\,r\,dr$$

The first integral may be transformed as follows:

$$\int_{r_1}^{r_2} u\frac{\partial u}{\partial x}\,r\,dr = \frac{1}{2}\int_{r_1}^{r_2}\frac{\partial(u^2)}{\partial x}\,r\,dr$$

A theorem related to Leibnitz' rule for integrals is:

$$\int_{y_1(x)}^{y_2(x)}\frac{\partial u(x,y)}{\partial x}\,dy = \frac{d}{dx}\int_{y_1}^{y_2} u\,dy + u(y_1)\frac{dy_1}{dx} - u(y_2)\frac{dy_2}{dx} \qquad \text{(A-5)}$$

This rule may be applied to the integrals of the convection terms.

Substituting the results into Equation (A-2):

$$\frac{d}{dx}\int_{r_1}^{r_2} u^2 r\,dr + u(r_1)\frac{d}{dx}\int_{0}^{r_1} u\,r\,dr - u(r_2)\frac{d}{dx}\int_{0}^{r_2} u\,r\,dr$$

$$= -\frac{1}{\rho}\int_{r_1}^{r_2}\frac{\partial P}{\partial x} r\,dr + \frac{1}{\rho}\left[r_2\,\tau(r_2) - r_1\,\tau(r_1)\right] \qquad \text{(A-6)}$$

Finally, Equation (A-6) may be rewritten as follows:

$$\frac{d}{dx}\int_{r_1}^{r_2} u^2 r\,dr + \left[u(r_1) - u(r_2)\right]\frac{d}{dx}\int_{0}^{r_1} u\,r\,dr - u(r_2)\frac{d}{dx}\int_{r_1}^{r_2} u\,r\,dr$$

$$= -\frac{1}{\rho}\int_{r_1}^{r_2}\frac{\partial P}{\partial x} r\,dr + \frac{1}{\rho}\left[r_2\,\tau(r_2) - r_1\,\tau(r_1)\right]$$

(A-7)

APPENDIX B

COMPUTER ALGORITHM

On the following pages are listed the parameters which must be supplied for the computations, and the MAD statements of the program.

Input Parameters for MAD Program

Symbol	Parameter
AZ	initial value of a/R_1
BZ	initial value of b/R_1
WRAD	maximum value of b/R_2 for which calculations will proceed
PGRAD	the constant B in Equation (4.13)
PRAD	a/R_1 for which equilibrium core begins to deteriorate
CORAD	a/R_1 for which core is to be assumed completely dissipated
UEZ	minimum value of $U/\bar{u}_1$ for which calculations will proceed
CC	c^2
K	k
H	interval at which numerical solution will be computed, Δx

The following parameters must be specified for each particular flow which is to be analysed

U2	$U_2/\bar{u}_1$
R1	R_1/R_2
RE1	jet tube Reynolds number
INTVAL	frequency of print out

```
MAD PROGRAM

$ COMPILE MAD,PRINT OBJECT,PUNCH OBJECT,EXECUTE,DUMP

R     THIS PROGRAM COMPUTES THE AXIAL VELOCITY AND PRESSURE
R     FIELDS IN A CONFINED CIRCULAR JET WITH FULLY
R     DEVELOPED TURBULENT CORE.  THE RUNGE-KUTTA METHOD
R     IS USED TO SOLVE A SYSTEM OF ORDINALY DIFFERENTIAL
R     EQUATIONS NUMERICALLY.

R....PRELIMINARY DECLARATIONS....

      INTEGER I,J,I1,J1,K1,L1,FLAG, CORE  , COUNT, INTVAL
      DIMENSION Y(5),DF(5),G(20,DIM),F(20,DIM),E(3),N(3),DIM(2)
     2 ,LP(8), LT(8), R(25), U(25), Q(5), LN(8), VN(50), VO(50)
      VECTOR VALUES DIM = 2, 1, 3
      INTERNAL FUNCTION PHI.(I1,J1,K1,L1) = F(I1,J1)/F(K1,J1)-
     2 F(I1,L1)/F(K1,L1)
      EQUIVALENCE (Y(1),B), (Y(2),V), (Y(3),UC)
      EXECUTE SETRKD.(5,Y(1),DF(1),Q,X,H)
      PI = 3.14159
      PISQ = PI*PI
      PI2 = 3./16.-1./PISQ
      PI3 = 0.25 - 1./PISQ
      PI4 = 1./PISQ - 1./8.
      PI8 = 0.25-1./PISQ

R....READ DATA AND COMPUTE BASIC PARAMETERS....

      READ FORMAT BASIC, AZ,BZ,WRAD,PGRAD,PRAD,CORAD,
     2 UEZ, CC, K, H
      VECTOR VALUES BASIC = $7F10.4*$
      PRINT FORMAT FIRSTP
      PRINT RESULTS AZ,BZ,WRAD,H      ,UEZ,PGRAD,PRAD,CORAD,CC,K
READ  READ FORMAT DATA,      U2, R1, RE1, INTVAL
      VECTOR VALUES DATA = $2F10.4, E10.2,I10*$
      DR = 1./20.
      THROUGH CALCR, FOR I=0,1, I.G.20
CALCR R(I) = I*DR
      URAT = 0.69 + 0.013*ELOG.(RE1)
      UZ = 1./URAT
      QQ = R1*R1*(1.-U2) + U2
      FF = 0.079/RE1.P.0.25
      BETA = 1. + 4.*FF
      MCP = R1*R1*(BETA-R1*R1*(1.-U2)*(1.-U2)/2.)/(QQ*QQ)
      CT = 1./SQRT.(MCP)
      SFF = SQRT.(FF)
      M = 5.3*SFF/(R1*R1)
      PRINT COMMENT $1RESULTS FOR$
      PRINT RESULTS M, MCP, UZ
      PRINT FORMAT THESIS, U2, 1./R1, RE1, FF, URAT, BETA, CT
```

MAD PROGRAM CONTINUED

```
          R....INITIALIZE VARIABLES....

          X = 0.
          Y(1) = AZ*R1
          Y(2) = BZ*R1
          Y(3) = U2
          Y(4) = 0.
          Y(5) = 0.
          LP(0) = 1.0
          FLAG = 1
          CORE = 1
          COUNT = 1
          TRANSFER TO COMP

          R....COMPUTE FLOW IN CORE REGION....

RK        S = RKDEQ.(0)
          WHENEVER S .E. 1.0
COMP      L = Y(2)-Y(1)
          DELTA = X/R1*PGRAD
          THROUGH SETL, FOR I = 1,1,I.G.8
          LP(I) = LP(I-1)*L
          LN(I) = -LP(I)/I
SETL      LT(I) = LP(I)*(Y(2)/I-L/(I+1))
          DELU = UZ-Y(3)
          C = (3.*DELU-M*Y(1)*(Y(1)+2.*Y(2)))/LP(2)
          D = 2.*(M*Y(1)*Y(2)-DELU)/LP(3)
          E(1) = (6.*DELU-2.*M*Y(2)*(2.*Y(1)+Y(2)))/LP(3)
          E(2) = (2.*M*Y(1)*(2.*Y(1)+Y(2))-6.*DELU)/LP(3)
          E(3) = -3./LP(2)
          N(1) = -E(1)/L
          N(2) = -E(2)/L
          N(3) = 2./LP(3)
          G(1,1) = 0.
          G(2,1) = Y(3)*(2.*C*LT(2)+3.*D*LT(3))+(3.*LT(4)-4.*LN(5)/3.)
         2 *C*C+(3.*LT(6)-9.*LN(7)/4.)*D*D
          WHENEVER Y(1) .L. PRAD*R1
          G(3,1) = LT(1)*Y(3)+C*(LT(3)-LN(4))+D*(LT(4)-1.5*LN(5))+Y(2)
         2 *(2.*C*LN(3)+3.*D*LN(4))+(1.-Y(2)*Y(2))*(LN(2)*C+1.5*D*
         3 LN(3))-(1.+DELTA)/DELTA*(Y(2)*Y(2)-Y(1)*Y(1))/4.*Y(3)
          OTHERWISE
          G(3,1) = LT(1)*Y(3)+C*(LT(3)-LN(4))+D*(LT(4)-1.5*LN(5))+Y(2)
         2 *(2.*C*LN(3)+3.*D*LN(4))+(1.-Y(2)*Y(2))*(LN(2)*C+1.5*D*
         3 LN(3))
          END OF CONDITIONAL
          G(4,1) = LT(3)*Y(3)+C*(LT(5)-LN(6)/2.)+D*(LT(6)-0.75*LN(7))+
         2 Y(2)*(0.667*C*LN(5)+3*LN(6))
          G(5,1) = Y(3)*LT(4)+C*(LT(6)-0.4*LN(7)+Y(2)*LN(6)/2.) +
         2 D*(LT(7)-0.6*LN(8)+0.75*Y(2)*LN(7))
          G(1,2) = Y(1)*(DELU-M*Y(1)*Y(1)-LP(2)*(L*D+C))
          G(2,2) = Y(3)*L+Y(2)*C*LP(2)+(Y(2)*D-0.667*C)*LP(3)-0.75*
         2 D*LP(4)
          G(3,2) = 0.5 - Y(1)*Y(1)/2.
          G(4,2) = LT(3)
          G(5,2) = LT(4)
          G(6,2) = 0.
```

MAD PROGRAM CONTINUED

```
          THROUGH SETF, FOR VALUES OF J = 1, 2
          THROUGH SETF, FOR I=1,1,I.G.3
SETF      F(I,J) = G(I,J)+G(4,J)*E(I)+G(5,J)*N(I)
          WHENEVER Y(1) .L. PRAD*R1
          WHENEVER CORE .E. 1
          CORE = 2
          PRINT COMMENT $ END OF EQUILIBRIUM CORE AT$
          XR1 = X/R1
          PRINT RESULTS XR1
          END OF CONDITIONAL
          LSQ = CC*LP(2)
          G(6,1) = LSQ*4.*M*M*Y(1)*Y(1)*Y(1)
          DF(3) = (G(6,1)/F(1,1)+DF(2)*PHI.(2,2,1,1))/PHI.(3,1,1,2)
          DF(1) = -(F(2,2)*DF(2)+F(3,2)*DF(3))/F(1,2)
          DF(5) = -Y(3)*DF(3)
          DF(4) = DF(5)/DELTA
          OTHERWISE
          F(4,1) = FF/R1*(Y(1)*Y(1)*(1.-DELTA)+Y(2)*Y(2)+
         2 (1.+DELTA)-4.*DELTA*F(3,1)/Y(3))/4.
          F(4,2) = -FF*F(3,2)/(Y(3)*R1)
          DF(2) = PHI.(4,1,1,2)/PHI.(2,1,1,2)
          DF(1) = (F(4,2)-F(2,2)*DF(2))/F(1,2)
          DF(4) = -FF/R1
          DF(5) = DELTA*DF(4)
          DF(3) = -DF(5)/Y(3)
          END OF CONDITIONAL
          WHENEVER X .L. 0.000001
          X = -(1.-AZ)*R1/DF(1)
          XZRAT = X/R1
          Y(2) = R1+DF(2)*X
          Y(4) = DF(4)*X
          Y(3) = SQRT.(U2*U2-2.*Y(4))
          TRANSFER TO PRINT
          END OF CONDITIONAL
          TRANSFER TO RK
          END OF CONDITIONAL
          WHENEVER X.G.10.*R1
          PRINT COMMENT $ X LIMIT EXCEEDED$
          OR WHENEVER Y(2) .G. WRAD
          PRINT COMMENT $ MIXING REGION REACHES WALL AT$
          PRINT RESULTS X
          OR WHENEVER Y(1).L.CORAD*R1
          PRINT COMMENT $ END OF CORE AT$
          PRINT RESULTS X
          FLAG = 3
          COUNT = 1
          TRANSFER TO PRINT
          OTHERWISE
          WHENEVER COUNT .E. INTVAL
          COUNT = 1
          TRANSFER TO PRINT
          OTHERWISE
          COUNT = COUNT+1
          TRANSFER TO RK
          END OF CONDITIONAL
          END OF CONDITIONAL
```

```
MAD PROGRAM CONTINUED

                FLAG = 2
PRINT           PRINT FORMAT VELHD1, X/R1, Y(1)/R1, Y(2), Y(3), Y(4), Y(5)
                THROUGH CALCU, FOR I=0,1, I.G.20
                WHENEVER R(I) .L. Y(1)
                U(I) = UZ-M*R(I)*R(I)
                OR WHENEVER R(I) .GE. Y(1) .AND. R(I) .L. Y(2)
                U(I) = (Y(3)+(Y(2)-R(I))*(Y(2)-R(I))*(C+D*(Y(2)-R(I))))
                OTHERWISE
                U(I) = Y(3)
                END OF CONDITIONAL
CALCU           PRINT FORMAT VELOC, R(I), U(I)
                WHENEVER FLAG .E. 2
                TRANSFER TO READ
                OR WHENEVER FLAG .E. 1
                TRANSFER TO RK
                END OF CONDITIONAL

               R....COMPUTE FLOW IN DEVELOPED JET....

                V = Y(3)
                UC = UZ
                DELU = UC-V
                B = SQRT.((QQ-V)/(2.*PI3*DELU))
                Y(4) = 0.5*(Y(4)+Y(5))
RK2             S = RKDEQ.(0)
                WHENEVER S.E.1.0
                DELU = UC-V
                F(2,1) = V
                F(3,1) = -UC
                F(4,1) = K*PISQ*DELU*DELU/B
                F(1,2) = 2.*B*(UC*UC*PI2-V*V/16. + UC*V*PI4)
                F(2,2) = B*B*(PI4*UC-5.*V/8.)
                F(3,2) = B*B*(2.*PI2*UC + PI4*V)
                F(4,2) = 0.
                F(1,3) = 2.*DELU*PI8*B
                F(2,3) = 0.5 - PI8*B*B
                F(3,3) = PI8*B*B
                DF(2) = (F(4,1)*PHI.(3,3,1,2)/F(3,1)+F(4,2)/F(1,2))/
               2 (PHI.(2,2,1,3)+F(2,1)*PHI.(3,3,1,2)/F(3,1))
                DF(1) = (F(4,2)-F(2,2)*DF(2)+F(3,2)*(F(2,1)*DF(2)-F(4,1))/
               2 F(3,1))/F(1,2)
                DF(3) = (F(4,1)-F(2,1)*DF(2))/F(3,1)
                DF(4) = -V*DF(2)
                TRANSFER TO RK2
                END OF CONDITIONAL
                WHENEVER X .G. 40.
                PRINT COMMENT $1MAXIMUM X REACHED$
                FLAG = 2
                OR WHENEVER V .LE. U2*UEZ
                PRINT COMMENT $1EDDY OF RECIRCULATION BEGINS$
                FLAG = 2
                OR WHENEVER B .G. WRAD
                PRINT COMMENT $1MIXING REGION HAS REACHED WALL$
                FLAG = 2
                END OF CONDITIONAL
```

MAD PROGRAM CONTINUED

```
            WHENEVER COUNT .E. INTVAL .OR. FLAG .E. 2
            COUNT = 1
            PRINT FORMAT VELHD2, X/R1, Y(1), Y(2), Y(3), Y(4)
            THROUGH PRINTU, FOR I=0,1, I.G.20
            WHENEVER R(I) .L. Y(1)
            U(I) = V+0.5*DELU*(1.+COS.(PI*R(I)/B))
            OTHERWISE
            U(I) = V
            END OF CONDITIONAL
PRINTU      PRINT FORMAT VELOC, R(I), U(I)
            OTHERWISE
            COUNT = COUNT +1
            END OF CONDITIONAL
            WHENEVER FLAG .E. 2, TRANSFER TO READ
            TRANSFER TO RK2
            VECTOR VALUES FIRSTP = $1H1///S15,55HJ. M. DEALY - CONFINED C
           2IRCULAR JET WITH TURBULENT CORE//S10,69HRESULTS OF NUMERICAL
           3APPROXIMATION TO SOLUTION OF EQUATIONS OF MOTION////*$
            VECTOR VALUES THESIS = $1H1///S20,41HCONFINED CIRCULAR JET WI
           2TH TURBULENT CORE      ///S15,57HNUMERICAL APPROXIMATION OF I
           3NTEGRATED EQUATIONS OF MOTION/////S15,24HVELOCITY RATIO, U2/U
           41 = S6,F10.4//S15,22HRADIUS RATIO, R2/R1 = S8,F10.4//S15,27HJ
           5ET TUBE REYNOLDS NUMBER = S3,E10.3//S15,26HFANNING FRICTION F
           6ACTOR = S4,F10.4//S15,25HRATIO OF AVERAGE TO AXIAL/S18,22HJET
           7 TUBE VELOCITIES = S5,F10.4//S15,30HMOMENTUM CORRECTION FACTO
           8R =  F10.4//S15,25HCRAYA-CURTET PARAMETER = S5,F10.4*$
            VECTOR VALUES VELHD1 = $1H1/////S15,10HAT X/R1 = F10.4//S20,
           2 7HA/R1 = F10.4/S20,7HB/R2 = F10.4/S20,20HU(OUTSIDE JET)/U1 =
           3 F10.4/S20,31HDIMENSIONLESS AXIAL PRESSURE = F10.4/S20,30HDIM
           4ENSIONLESS WALL PRESSURE = F10.4////S15,23HTHE VELOCITY PROFI
           5LE IS///S23,4HR/R2,S21,4HU/U1/*$
            VECTOR VALUES VELHD2 = $1H1/////S15,10HAT X/R1 = F10.4//S20,
           2 7HB/R2 = F10.4/S20,20HU(OUTSIDE JET)/U1 = F10.4/S20,13HU(AXI
           3S)/U1 = F10.4/                                    S20,25HDIMEN
           4SIONLESS PRESSURE = F10.4////S15,23HTHE VELOCITY PROFILE IS//
           5/S23,4HR/R2,S21,4HU/U1/*$
            VECTOR VALUES VELOC = $S20,F10.4,S15,F10.4*$
            END OF PROGRAM
```

APPENDIX C

SAMPLE COMPUTER OUTPUT

The computer output for the calculations of flows corresponding to the experimental conditions of Figures 16 and 24 is shown in this appendix.

CONFINED CIRCULAR JET WITH TURBULENT CORE

NUMERICAL APPROXIMATION OF INTEGRATED EQUATIONS OF MOTION

VELOCITY RATIO, U2/U1 =	.3400
RADIUS RATIO, R2/R1 =	4.0000
JET TUBE REYNOLDS NUMBER =	.120E 05
FANNING FRICTION FACTOR =	.0075
RATIO OF AVERAGE TO AXIAL JET TUBE VELOCITIES =	.8121
MOMENTUM CORRECTION FACTOR =	1.0302
CRAYA-CURTET PARAMETER =	1.5125

AT X/R1 = .1120

A/R1 = .9000
B/R2 = .2516
U(OUTSIDE JET)/U1 = .3425
DIMENSIONLESS AXIAL PRESSURE = -.0008
DIMENSIONLESS WALL PRESSURE = .0000

THE VELOCITY PROFILE IS

R/R2	U/U1
.0000	1.2314
.0500	1.2130
.1000	1.1577
.1500	1.0656
.2000	.9367
.2500	.3450
.3000	.3425
.3500	.3425
.4000	.3425
.4500	.3425
.5000	.3425
.5500	.3425
.6000	.3425
.6500	.3425
.7000	.3425
.7500	.3425
.8000	.3425
.8500	.3425
.9000	.3425
.9500	.3425
1.0000	.3425

AT X/R1 = .1520

A/R1 = .8657
B/R2 = .2522
U(OUTSIDE JET)/U1 = .3425
DIMENSIONLESS AXIAL PRESSURE = -.0011
DIMENSIONLESS WALL PRESSURE = -.0000

THE VELOCITY PROFILE IS

R/R2	U/U1
.0000	1.2314
.0500	1.2130
.1000	1.1577
.1500	1.0656
.2000	.9367
.2500	.3479
.3000	.3425
.3500	.3425
.4000	.3425
.4500	.3425
.5000	.3425
.5500	.3425
.6000	.3425
.6500	.3425
.7000	.3425
.7500	.3425
.8000	.3425
.8500	.3425
.9000	.3425
.9500	.3425
1.0000	.3425

END OF EQUILIBRIUM CORE AT

XR1 = .572043

END OF CORE AT

X = .308011

AT X/R1 = 1.2320

A/R1 = -.0254
B/R2 = .2635
U(OUTSIDE JET)/U1 = .3534
DIMENSIONLESS AXIAL PRESSURE = -.0204
DIMENSIONLESS WALL PRESSURE = -.0038

THE VELOCITY PROFILE IS

R/R2	U/U1
.0000	1.2302
.0500	1.1356
.1000	.9333
.1500	.6913
.2000	.4775
.2500	.3599
.3000	.3534
.3500	.3534
.4000	.3534
.4500	.3534
.5000	.3534
.5500	.3534
.6000	.3534
.6500	.3534
.7000	.3534
.7500	.3534
.8000	.3534
.8500	.3534
.9000	.3534
.9500	.3534
1.0000	.3534

AT X/R1 = 5.2320

B/R2 = .3791
U(OUTSIDE JET)/U1 = .3503
U(AXIS)/U1 = 1.0753
DIMENSIONLESS PRESSURE = -.0110

THE VELOCITY PROFILE IS

R/R2	U/U1
.0000	1.0753
.0500	1.0446
.1000	.9578
.1500	.8295
.2000	.6815
.2500	.5387
.3000	.4254
.3500	.3608
.4000	.3503
.4500	.3503
.5000	.3503
.5500	.3503
.6000	.3503
.6500	.3503
.7000	.3503
.7500	.3503
.8000	.3503
.8500	.3503
.9000	.3503
.9500	.3503
1.0000	.3503

AT X/R1 = 9.2320

B/R2 = .4273
U(OUTSIDE JET)/U1 = .3477
U(AXIS)/U1 = .9665
DIMENSIONLESS PRESSURE = -.0101

THE VELOCITY PROFILE IS

R/R2	U/U1
.0000	.9665
.0500	.9458
.1000	.8865
.1500	.7966
.2000	.6880
.2500	.5753
.3000	.4735
.3500	.3963
.4000	.3539
.4500	.3477
.5000	.3477
.5500	.3477
.6000	.3477
.6500	.3477
.7000	.3477
.7500	.3477
.8000	.3477
.8500	.3477
.9000	.3477
.9500	.3477
1.0000	.3477

AT X/R1 = 19.2320

B/R2 = .5327
U(OUTSIDE JET)/U1 = .3428
U(AXIS)/U1 = .7986
DIMENSIONLESS PRESSURE = -.0084

THE VELOCITY PROFILE IS

R/R2	U/U1
.0000	.7986
.0500	.7887
.1000	.7601
.1500	.7151
.2000	.6576
.2500	.5926
.3000	.5258
.3500	.4628
.4000	.4091
.4500	.3694
.5000	.3470
.5500	.3428
.6000	.3428
.6500	.3428
.7000	.3428
.7500	.3428
.8000	.3428
.8500	.3428
.9000	.3428
.9500	.3428
1.0000	.3428

AT X/R1 = 29.2320

B/R2 = .6221
U(OUTSIDE JET)/U1 = .3395
U(AXIS)/U1 = .7024
DIMENSIONLESS PRESSURE = -.0073

THE VELOCITY PROFILE IS

R/R2	U/U1
.0000	.7024
.0500	.6967
.1000	.6798
.1500	.6528
.2000	.6175
.2500	.5760
.3000	.5311
.3500	.4855
.4000	.4422
.4500	.4038
.5000	.3729
.5500	.3514
.6000	.3406
.6500	.3395
.7000	.3395
.7500	.3395
.8000	.3395
.8500	.3395
.9000	.3395
.9500	.3395
1.0000	.3395

AT X/R1 = 39.2320

B/R2 = .7000
U(OUTSIDE JET)/U1 = .3371
U(AXIS)/U1 = .6399
DIMENSIONLESS PRESSURE = -.0065

THE VELOCITY PROFILE IS

R/R2	U/U1
.0000	.6399
.0500	.6361
.1000	.6249
.1500	.6069
.2000	.5829
.2500	.5542
.3000	.5222
.3500	.4885
.4000	.4548
.4500	.4228
.5000	.3941
.5500	.3702
.6000	.3521
.6500	.3409
.7000	.3371
.7500	.3371
.8000	.3371
.8500	.3371
.9000	.3371
.9500	.3371
1.0000	.3371

AT X/R1 = 59.2320

B/R2 = .8316
U(OUTSIDE JET)/U1 = .3341
U(AXIS)/U1 = .5634
DIMENSIONLESS PRESSURE = -.0055

THE VELOCITY PROFILE IS

R/R2	U/U1
.0000	.5634
.0500	.5614
.1000	.5554
.1500	.5455
.2000	.5322
.2500	.5160
.3000	.4973
.3500	.4770
.4000	.4556
.4500	.4340
.5000	.4129
.5500	.3931
.6000	.3752
.6500	.3600
.7000	.3480
.7500	.3395
.8000	.3349
.8500	.3341
.9000	.3341
.9500	.3341
1.0000	.3341

AT X/R1 = 79.2316

B/R2 = .9410
U(OUTSIDE JET)/U1 = .3323
U(AXIS)/U1 = .5163
DIMENSIONLESS PRESSURE = -.0049

THE VELOCITY PROFILE IS

R/R2	U/U1
.0000	.5183
.0500	.5170
.1000	.5131
.1500	.5069
.2000	.4983
.2500	.4877
.3000	.4754
.3500	.4617
.4000	.4470
.4500	.4316
.5000	.4161
.5500	.4009
.6000	.3863
.6500	.3728
.7000	.3608
.7500	.3505
.8000	.3424
.8500	.3365
.9000	.3331
.9500	.3323
1.0000	.3323

MIXING REGION HAS REACHED WALL

CONFINED CIRCULAR JET WITH TURBULENT CORE

NUMERICAL APPROXIMATION OF INTEGRATED EQUATIONS OF MOTION

VELOCITY RATIO, U2/U1 =	.4700
RADIUS RATIO, R2/R1 =	2.0000
JET TUBE REYNOLDS NUMBER =	.144E 05
FANNING FRICTION FACTOR =	.0072
RATIO OF AVERAGE TO AXIAL JET TUBE VELOCITIES =	.8145
MOMENTUM CORRECTION FACTOR =	1.0288
CRAYA-CURTET PARAMETER =	1.2088

AT X/R1 = .4973

A/R1 = .9000
B/R2 = .5058
U(OUTSIDE JET)/U1 = .4776
DIMENSIONLESS AXIAL PRESSURE = -.0036
DIMENSIONLESS WALL PRESSURE = .0000

THE VELOCITY PROFILE IS

R/R2	U/U1
.0000	1.2278
.0500	1.2233
.1000	1.2098
.1500	1.1873
.2000	1.1558
.2500	1.1153
.3000	1.0658
.3500	1.0072
.4000	.9397
.4500	.8632
.5000	.4837
.5500	.4776
.6000	.4776
.6500	.4776
.7000	.4776
.7500	.4776
.8000	.4776
.8500	.4776
.9000	.4776
.9500	.4776
1.0000	.4776

AT X/R1 = .5173

A/R1 = .8961
B/R2 = .5061
U(OUTSIDE JET)/U1 = .4776
DIMENSIONLESS AXIAL PRESSURE = -.0037
DIMENSIONLESS WALL PRESSURE = -.0000

THE VELOCITY PROFILE IS

R/R2	U/U1
.0000	1.2278
.0500	1.2233
.1000	1.2098
.1500	1.1873
.2000	1.1558
.2500	1.1153
.3000	1.0658
.3500	1.0072
.4000	.9397
.4500	.8622
.5000	.4886
.5500	.4776
.6000	.4776
.6500	.4776
.7000	.4776
.7500	.4776
.8000	.4776
.8500	.4776
.9000	.4776
.9500	.4776
1.0000	.4776

AT X/R1 = 1.4973

A/R1 = .6973
B/R2 = .5171
U(OUTSIDE JET)/U1 = .4813
DIMENSIONLESS AXIAL PRESSURE = -.0108
DIMENSIONLESS WALL PRESSURE = -.0018

THE VELOCITY PROFILE IS

R/R2	U/U1
.0000	1.2278
.0500	1.2233
.1000	1.2098
.1500	1.1873
.2000	1.1558
.2500	1.1153
.3000	1.0658
.3500	1.0072
.4000	.8606
.4500	.6455
.5000	.4945
.5500	.4813
.6000	.4813
.6500	.4813
.7000	.4813
.7500	.4813
.8000	.4813
.8500	.4813
.9000	.4813
.9500	.4813
1.0000	.4813

END OF EQUILIBRIUM CORE AT

XR1 = 2.397344

AT X/R1 = 2.4973

A/R1 = .4723
B/R2 = .5266
U(OUTSIDE JET)/U1 = 4896
DIMENSIONLESS AXIAL PRESSURE = -.0187
DIMENSIONLESS WALL PRESSURE = -.0058

THE VELOCITY PROFILE IS

R/R2	U/U1
.0000	1.2278
.0500	1.2233
.1000	1.2098
.1500	1.1873
.2000	1.1558
.2500	1.1125
.3000	1.0154
.3500	.8744
.4000	.7210
.4500	.5866
.5000	.5027
.5500	.4896
.6000	.4896
.6500	.4896
.7000	.4896
.7500	.4896
.8000	.4896
.8500	.4896
.9000	.4896
.9500	.4896
1.0000	.4896

AT X/R1 = 3.4973

A/R1 = .1615
B/R2 = .5357
U(OUTSIDE JET)/U1 = .5080
DIMENSIONLESS AXIAL PRESSURE = -.0310
DIMENSIONLESS WALL PRESSURE = -.0150

THE VELOCITY PROFILE IS

R/R2	U/U1
.0000	1.2278
.0500	1.2233
.1000	1.2072
.1500	1.1573
.2000	1.0767
.2500	.9756
.3000	.8641
.3500	.7526
.4000	.6512
.4500	.5701
.5000	.5197
.5500	.5080
.6000	.5080
.6500	.5080
.7000	.5080
.7500	.5080
.8000	.5080
.8500	.5080
.9000	.5080
.9500	.5080
1.0000	.5080

END OF CORE AT

X = 1.938671

AT X/R1 = 3.8773

A/R1 = .0045
B/R2 = .5392
U(OUTSIDE JET)/U1 = .5159
DIMENSIONLESS AXIAL PRESSURE = -.0354
DIMENSIONLESS WALL PRESSURE = -.0190

THE VELOCITY PROFILE IS

R/R2	U/U1
.0000	1.2278
.0500	1.2116
.1000	1.1650
.1500	1.0951
.2000	1.0086
.2500	.9124
.3000	.8133
.3500	.7184
.4000	.6344
.4500	.5682
.5000	.5267
.5500	.5159
.6000	.5159
.6500	.5159
.7000	.5159
.7500	.5159
.8000	.5159
.8500	.5159
.9000	.5159
.9500	.5159
1.0000	.5159

REFERENCES

1. G. Abramovich, The Theory of Turbulent Jets, M.I.T. Press, 1963.

2. L. G. Alexander, T. Baron and E. W. Comings, Transport of Momentum, Mass and Heat in Turbulent Jets, University of Illinois Eng. Exp. Stat. Bull. Series, No. 413, 1953.

3. T. Baron and L. G. Alexander, "Momentum, Mass and Heat Transfer in Free Jets," CEP, 47, (1951), 181.

4. H. A. Becker, Concentration Fluctuations in Ducted Jet-mixing, Sc. D. Thesis, Chem. Eng., M.I.T., 1961.

5. H. A. Becker, H. C. Hottel, and G. C. Williams, "Mixing and Flow in Ducted Turbulent Jets," Ninth Symposium on Combustion - 1962, 7, Academic Press, 1963.

6. H. Blasius, "Das Ähnlichkeitsgesetz bei Reibungsvorgängen in Flüssigkeiten," VDI, Forschungsarb., 131, (1913), 1.

7. A. J. Chapman and H. H. Korst, "Free Jet Boundary with Consideration of Initial Boundary Layer," Proc. of 2nd US Nat. Cong. of Appl. Mech., ASME, (1956), 723.

8. S. Corrsin,"Investigation of Flow in an Axially Symmetrical Heated Jet of Air," NACA Wartime Report, W-94, 1943.

9. S. Corrsin and M. S. Uberoi, "Further Experiments on the Flow and Heat Transfer in a Heated Turbulent Air Jet," NACA TN 1865, 1949.

10. R. C. Cunningham, "Jet-Pump Theory and Performance with Fluids of High Viscosity," Trans. of ASME, 79, (1957), 1807.

11. Roger Curtet, "Sur L'Ecoulement D'un Jet Entre Parois," Publications Scientifiques et Techniques Du Ministere De L'Air, No. 359, 1960.

12. R. Curtet, "Confined Jets and Recirculation Phenomena with Cold Air," Combustion and Flame, 2, (1958), 383.

13. R. Curtet and R. Ricou, "Effects De Turbulence sur Des Constructions Hydrauliques," 9th Congres De L'A.I.R.H., Dubrovnik, Yugoslavia, Sept. 1961.

14. M. B. Donald and H. Singer, "Entrainment in Turbulent Fluid Jets," Trans. of the Institution of Chemical Engineers, 37, 1959.

15. A. Fage, "On the Static Pressures in Fully Developed Turbulent Flow," Proc. of Royal Soc. of London A, 155, (1936), 576.

16. C. K. Ferguson, "Mixing of Parallel Flowing Streams in a Pressure Gradient," Proceedings of Heat Trans. and Fluid Mech. Inst., Berkeley, 1949.

17. Gustav Flügel, "The Design of Jet Pumps," NACA TM 982, 1941.

18. R. G. Folsom, "Predicting Liquid Jet Pump Performance," Proc.of Nat. Cong. on Ind. Hydraulics, II, (1948), 105.

19. R. G. Folsom and C. K. Ferguson, "Jet Mixing of Two Liquids," Trans. ASME, 71, (1949), 73.

20. W. Forstall and E. W. Gaylord, "Momentum and Mass Transfer in a Submerged Water Jet," Journal of Applied Mechanics, 77, (1955), 161.

21. W. Forstall, Jr., and A. H. Shapiro, "Momentum and Mass Transfer in Coaxial Gas Jets," Journal of Applied Mechanics, 74, (1950), 339.

22. S. Goldstein, "A Note on the Measurement of Total Head and Static Pressures in a Turbulent Stream," Proc. of Roy. Soc. of London, A, 155, (1936),570.

23. H. Görtler, "Berechnung von Aufgaben der freien Turbulenz auf Grund eines neuen Naherungsansatzes," Z.A.M.M., 22, (1942), 244.

24. J. E. Goslein and Marrough P. O'Brien, "The Water Jet Pump," Univ. of Calif. Publ. in Eng., 3, No. 3, (1942), 167.

25. J. O. Hinze, Turbulence, McGraw-Hill Book Co., Inc., 1959.

26. J. O. Hinze, and B. G. van der Hegge Zijnen, "Heat and Mass Transfer in the Turbulent Mixing Zone of an Axially Symmetrical Jet," Proc. of Seventh Int. Cong. for Appl. Mech., London, (1948), 286.

27. G. T. J. Hooper, "Turbulent Momentum Diffusivity Within a Circular Tube," Int. Journ. of Heat and Mass Transfer, 6, (1963), 805.

28. J. G. Knudsen, Heat Transfer, Friction, and Velocity Gradients in Annuli Containing Plain and Transverse Fin Tubes, Ph.D. Thesis, Univ. of Michigan, 1949.

29. J. G. Knudsen and D. L. Katz, "Velocity Profiles in Annuli," Proceedings of the First Midwestern Conference on Fluid Dynamics, (1950), 175.

30. J. G. Knudsen and D. L Katz, Fluid Dynamics and Heat Transfer, McGraw-Hill Book Co., Ind., 1958.

31. M. Z. von Krzywoblocki, "Jets - Review of Literature," Jet Propulsion, 26, (1956), 760.

32. A. M. Kuethe, "Investigations of the Turbulent Mixing Regions Formed by Jets," Journal of Applied Mechanics, 2, A 87, 1935.

33. H. L. Langhaar, "Steady Flow in the Transition Length of a Straight Tube," Journal of Applied Mechanics, 64, A-55, 1942.

34. H. Latzko, "Heat Transfer in a Turbulent Liquid or Gas Stream," NACA TM 1068.

35. John Laufer, "The Structure of Turbulence in Fully Developed Pipe Flow," NACA Report 1174, 1954.

36. J. C. Laurence, "Intensity, Scale, and Spectra of Turbulence in Mixing Region of Free Subsonic Jet," NACA Report 1292, 1956.

37. Fred Locker, "Hydraulic Studies of a Water Jet-Pump for the Keswick Dam Fish-Trap, Central Valley Project, California," US Dept. of Int., Bur. of Recl. Hydraulic Lab. Rep. 154, 1944.

38. H. M. Martin, and S. E. Rice, "Experimental Determination of Design Data for Design of Jet Pumps for Boulder Dam Power Plant," US Dept. of Int., Bur. of Recl., Hydraulic Lab. Rept. 97, 1941.

39. Sami Mikhail, "Mixing of Coaxial Streams Inside a Closed Conduit," Journal of Mechanical Engineering Science, 2, (1960), 59.

40. Shih-I Pai, Fluid Dynamics of Jets, D. Van Nostrand Co., Inc., 1954.

41. Ludwig Prandtl, "Bemerkungen zur Theorie der freien Turbulenz," Z.A.M.M., 22, (1942), 241.

42. L. Prandtl and O. G. Tietjens, Applied Hydro- and Aeromechanics, Dover, 1957.

43. Hans Reichardt, "Gesetzmässigkeiten der freien Turbulenz," VDI-Forschungsheft, 414, 1942.

44. R. S. Rosler and S. G. Bankoff, "Large Scale Turbulence Characteristics of a Submerged Water Jet," A.I.Ch.E. Journ. 9, (1963), 673.

45. Donald Ross, A Study of Incompressible Turbulent Boundary Layers, Ph.D. Thesis, Harvard University, 1953.

46. V. A. Sandborn, "Experimental Evaluation of Momentum Terms in Turbulent Pipe Flow," NACA TN 3266, 1955.

47. Hermann Schlichting, Boundary Layer Theory, 4th Ed., McGraw-Hill Book Co., Inc., 1960.

48. A. H. Shapiro, R. Siegel, and S. J. Kline, "Friction Factor in the Laminar Entry Region of a Smooth Tube," Proc. of 2nd Nat. Cong. of Appl. Mech., ASME, (1954), 733.

49. H. B. Squire and J. O. Trouncer, "Round Jets in a General Stream," ARC - TR, R and M No. 1974, 1944.

50. V. L. Streeter, "The Kinetic Energy and Momentum Correction Factors for Pipes and for Open Channels of Great Width," Civil Engineering, 12, (1942), 212.

51. W. Szablewski, "Contributions to the Theory of a Free Jet Issuing from a Nozzle," NACA TM 1311, 1951.

52. W. Szablewski, "The Diffusion of a Hot Air Jet in Air in Motion," NACA TM 1288, 1950.

53. M. W. Thring and M. P. Newby, "Combustion Length of Enclosed Turbulent Jet Flames," Fourth Internat. Symp. on Comb. - 1952, p. 789, The Williams and Wilkins Co., 1953.

54. Walter Tollmien, "Calculation of Turbulent Expansion Processes," NACA TM 1085, 1945.

55. A. A. Townsend, The Structure of Turbulent Shear Flow, Cambridge, 1956.

56. A. A. Townsend, "Turbulent Flow," Handbook of Fluid Dynamics, V. Streeter, Ed., McGraw-Hill Book Co., Inc., 1961.

57. A. A. Townsend, "The Properties of Equilibrium Boundary Layers," Journal of Fluid Mechanics, 1, (1956), 561.

58. A. A. Townsend, "Equilibrium Layers and Wall Turbulence," Journal of Fluid Mechanics, 11, (1961), 97.

59. E. M. Uram, "The Growth of an Axisymmetric Turbulent Boundary Layer in an Adverse Pressure Gradient," Proc. of 2nd US Nat. Cong. of Appl. Mech., ASME, (1954), 687.

60. K. Viktorin, "Investigation of Turbulent Mixing Processes," NACA TM 1096, 1946.

NOMENCLATURE

Symbols for constants and those defined in the text and used only once are not listed here.

Symbol	Meaning
a	radius of equilibrium or kinematic core region
b	radius of outer limit of mixing region
c	proportionality factor in Prandtl mixing length expression (Equation (2.16))
k	exchange coefficient (Equation (2.12))
ℓ	Prandtl mixing length
m	Curtet parameter of similitude (defined in Equation (2.32))
m_o	initial value of m
M	kinematic momentum flux
p	pressure
P	hydrodynamic pressure
Q_1	volumetric flow rate - source
Q_2	volumetric flow rate - secondary flow
Q_t	total flow rate in mixing tube
R_1	radius of source
R_2	radius of mixing tube
r	radial coordinate
t	time
u	velocity in axial direction

u_a value of u at $r = a$

$\bar{u}$ average velocity over cross section

u_o velocity on axis

U_1 jet source velocity

U_2 secondary flow velocity at $x = 0$

U velocity outside the jet

U_o velocity on axis at source

v radial velocity

w velocity in angular direction

x axial coordinate, measured from source

x_c length of core

y coordinate normal to direction of main flow

$(Re)_1$ jet tube Reynolds number

Ct Craya-Curtet number (defined in Equation (2.34))

β_1 momentum factor for turbulent pipe flow

β_2 momentum factor in mixing tube (defined in Equation (2.39))

γ dimensionless pressure gradient (defined in Equation (4.4))

ϵ turbulent viscosity coefficient

η r/x

λ ratio of pressure gradients (Equation (4.12))

μ viscosity

ρ density

τ shear stress

ϕ angular independent variable